LOW-THRUST SOLID AND HYBRID PROPULSION SYSTEMS (PHASE II)

Final Report

8 February 1968 LMSC-685070

N68-18062

Prepared for National Aeronautics and Space Administration
Headquarters, Washington, D.C.

Contract NAS-7-573

LOCKHEED MISSILES & SPACE COMPANY
A GROUP DIVISION OF LOCKHEED AIRCRAFT CORPORATION
SUNNYVALE, CALIFORNIA

PRECEDING PAGE BLANK NOT FILMED.

FOREWORD

This is the final report under Contract NAS 7-573, Low Thrust Solid and Hybrid Propulsion Systems (Phase II). The program was conducted under the sponsorship of NASA – Office of Advanced Research and Technology. Mr. William Cohen was NASA Program Manager. NASA Technical Managers were Mr. Eugene F. Wyszpolski and Mr. John W. Behm. Program Manager for Lockheed Missiles & Space Company was Dr. H. T. Hahn. Principal contributors were:

Propulsion	Mr. A. B. Anderson
	Mr. P. K. Chung
	Dr. W. H. Cutler
	Dr. H. T. Hahn
	Mr. A. J. Hief
	Mr. K. F. Johanson
	Mr. B. S. Leonard
	Dr. W. L. Owens
	Dr. J. C. Pope
Orbital Mechanics	Mr. H. F. Michielsen
Materials	Mr. D. M. Lorimer
Reliability	Mr. H. K. Burbridge
	Mr. D. H. Wythe
Producibility	Mr. W. F. Miller
	Mr. J. M. Vellinga

The counsel of Drs. E. Miller and H. M. Kindsvater is also gratefully acknowledged.

SUMMARY

In Phase I of this study certain NASA missions (ATS-4, Voyager, ATM, EVA) were selected as bases to establish typical future requirements for low-thrust ($<$ 10 lbf) reaction control systems (LTRCS). Missions were selected primarily for availability of information at the time, with no attempt being made to favor solid or hybrid systems. It was realized that the selected missions would probably not provide an all-inclusive set of functional requirements. For example, they did not include functions such as spin-despin, propellant ullage control, or drag make-up. However, it was anticipated that the selected missions would provide a sufficient breadth of requirements to permit meaningful tradeoff studies between all LTRCS. If solid/hybrid systems were not competitive, then a principal objective was to determine methods of overcoming the deficiencies.

In addition to the Phase I requirements, other potential applications were investigated. Of these, the most interesting arose in conjunction with the final injection of a synchronous satellite into orbit. The payload is normally provided with LTRCS for attitude control and station-keeping (of the order of 10^{-3}g or less) and these devices could be used also for orbit injection in apogee. In each case, the advantages of reduced acceleration and reduced number of systems must be balanced against possible disadvantages, such as increased time into orbit and increased impulse requirement. The impulse penalty was evaluated and found to be relatively small. Another area which offers requirements for LTRCS is that of accurate positioning of navigational satellites which are subjected to continuous low-level disturbances.

Thrust range and specific impulse characteristics are summarized for 4 solid/hybrid and 13 competitive active and passive systems. A comparison of these characteristics with mission requirements eliminated approximately one-third of the systems. The systems remaining in contention after the elimination process were subjected to tradeoff analyses in greater depth.

In selecting criteria for the tradeoff studies, the state of development could not be used in ranking the systems, since many of the LTRCS are underdeveloped. The

present cost of a system was not a valid criterion either, since the study was primarily concerned with the development of solid and hybrid systems in the post-1968 period and future development costs are difficult to estimate. Nor was it possible to obtain an objective comparison of systems on a producibility basis, due to the varying states of system development. Minimum pulse bit capabilities were readily achieved by all systems and so could not furnish a basis for elimination. Weight and reliability were the only selection criteria found satisfactory for rating systems in such extremely divergent states of development. Accordingly, weights of solid, hybrid and competitive LTRCS were estimated and corresponding reliability data were generated. Due to the similarity of parts used in all of the systems, the reliability values are very closely related and, as the systems are provisionally configured, do not by themselves provide a sufficient tool for rating of systems. Originally, Task IV was designed to investigate the feasibility of programming the system rating process. With only two criteria, programming the selection process becomes feasible but unnecessary.

As a result of the tradeoff studies the solid LTRCS were found to be competitive in a few cases. The subliming solid system would be a good choice for the Voyager evasive maneuver. Also, the low thrust solid pulse motor (Repetitive Impulse Generator) is among the leaders in performing ATS-4 North-South station-keeping and station acquisition functions. However, in general, the weights of present solid and hybrid systems are too high for these relatively high-thrust, high-impulse missions. The competitive position of the solid/hybrid systems at lower thrust and impulse levels is illustrated by a hypothetical requirement of 10^{-4} lbf thrust and 100 lbf-sec impulse, for which all but the superheated subliming solid rank among the leaders.

Deficiencies and problem areas of the four solid-hybrid systems presently under development are indicated, and development needs defined. For example, no competitive hybrid LTRCS presently exists. Consideration is also given to materials of construction and producibility. All four systems were found capable of implementation into hardware. In reviewing the deficiencies of solid/hybrid LTRCS relative to the Phase I mission requirements, the high total impulse and thrust levels led to greater weight from propellant and/or power supply. Invasion of this higher impulse/thrust regime may be regarded as both a challenge for the existing solid/hybrid systems to meet and an invitation to develop new systems of greater capability.

Two advanced low-thrust propulsion concepts, a hypergolic high-specific impulse and a very-low thrust system, are described. For the former, a series of inorganic hydride-fluoride reactions are screened by free energy and molecular weight criteria. Combustion parameters are computed for certain of the more promising reactions. Three of the reactions are estimated to provide chamber temperatures in excess of 3500°K and vacuum specific impulse in excess of 315 lbf-sec/lbm ($\epsilon = 100$). Kinetic and thermal flow analyses suggest that a hypergolic reaction is possible. Weight comparison indicates that such a system, if developed, would be competitive weightwise in fulfilling eight of the nine mission requirements. The second advanced system, a vaporizing metal such as zinc, is proposed for countering very small forces, essentially continuously, while operating in the 10^{-9} to 10^{-6} lbf range.

As a result of this study it is recommended that additional development be undertaken for

- low thrust solid pulse motor (Repetive Impulse Generator),
- the advanced high specific impulse hybrid system, and
- the vaporizing metal system.

It appears that the development of these systems will provide solid/hybrid systems which can be competitive or superior to any of the other LTRCS systems used in space missions.

CONTENTS

Section | Page

APPENDIXES | Page

ILLUSTRATIONS

TABLES

Section 1
SYSTEM SELECTION

1.1 LOW-THRUST SYSTEM CHARACTERISTICS

In the Phase I report (Ref. 1) the characteristics of 17 low-thrust reaction control systems (LTRCS) were qualitatively described. Because of limits defined in Phase I, the analysis was concerned only with systems delivering less than 10 lb of force. Typical values of thrust level range and specific impulse are listed in Table 1-1 for both minimum pulse bit and steady-state operation of all active systems considered. The characteristics and applicability to the selected missions of passive attitude control systems were also considered. Presentation of the passive system comparison is deferred to Section 1.3, where it is included in the overall characteristics-requirements comparison.

The systems in Table 1-1 embrace a variety of useful thrust ranges from 10^{-6} lb to greater than 10 lb. Steady-state specific impulse varies from the 60 lbf-sec/lbm of a pressurized cold-gas system to the 7000 lbf-sec/lbm of electrostatic systems. Under minimum bit operational conditions, the performance of many of the systems is reduced by failure to reach full thrust during the brief pulse period. The bases for selection of the values in Table 1-1 are given in Appendix A.

1.2 MISSION REQUIREMENTS

1.2.1 Existent

Certain NASA missions were selected in Phase I to form a basis for determining requirements for low-thrust systems in the period beyond 1968. The selection of typical

Table 1-1

SUMMARY OF ACTIVE LTRCS CHARACTERISTICS

	Max. Thrust (lbf)	Min. Thrust (lbf)	Steady State Spec. Impulse lbf-sec/ lbm	Minimum Pulse	
				Impulse Bit (lbf-sec.)	Assoc. Spec. Impulse lbf-sec/ lbm
Subliming Solid	≈0.1	2×10^{-6}	80	12×10^{-9}	80
Subliming Solid (Heated)	≈0.1	4×10^{-6}	205	12×10^{-9}	150
Hybrid Hydrogen Monoprop.	1	0.1×10^{-3}	225	0.5×10^{-6}	225
Solid Propellant Impulse Bit	>10	1×10^{-3}	190	10×10^{-3}	190
Pressurized Cold Gas	>10	1×10^{-3}	60	7.5×10^{-6}	60
Vaporized Liquid (NH_3)	>10	1×10^{-3}	85	7.5×10^{-6}	85
Monopropellant Hydrazine	>10	50×10^{-3}	190	1×10^{-4}	140
Cold Gas Monoprop. Hydrazine	>10	0.5×10^{-3}	110	0.3×10^{-3}	110
Bipropellant Vapor	>10	10^{-3}	350	10×10^{-6}	230
Bipropellant Liquid	>10	0.1	300	1×10^{-3}	150
Water Electrolysis	>10	0.01	360	0.1×10^{-3}	260
Resistojet & Radioisotope (NH_3)	50×10^{-3}	7.5×10^{-6}	220	0.5×10^{-3}	200
Electrostatic	10×10^{-3}	10×10^{-6}	7000*	0.1×10^{-6}	7000*
Pulsed Plasma	60×10^{-6}	1×10^{-6}	2000	1×10^{-6}	2000
Penning Discharge	1×10^{-3}	1×10^{-6}	1500	10×10^{-9}	1500

*The colloid ion engine has I_{sp} = 1000 – 1500 lbf-sec/lbm

NASA missions (in September 1966) was based on:

- A potential requirement for several low-thrust applications
- Ready availability of reference material
- Possibility of eventual funding of the mission

On the basis of these criteria and the national space objectives, the missions selected were ATS-4, Voyager, Apollo Telescope Mount (ATM) and the Extra Vehicular Activities (EVA) on a manned interplanetary probe.

It was realized that these missions would probably not provide an all-inclusive set of functional requirements. For example, they did not include functions such as spin-despin, propellant ullage control, or drag make-up. Since all missions but EVA involved relatively heavy vehicles, there was no expressed need for thrusts below 30×10^{-6} lb, such as might be required on smaller satellites to counter continuous disturbances. However, it was anticipated that the selected missions would provide sufficient requirements to permit meaningful tradeoff studies between all the competitive low-thrust systems. These studies would then serve to identify the principal contending systems, against which the performance of the solid and hybrid systems can be measured.

A summary of existent or derived mission requirements is given in Table 1-2. Calculations and other considerations in support of Table 1-2 are given in Appendix B.

1.2.2 Potential

The number of existent or derived requirements for low-thrust systems is, perhaps, less than anticipated due to several factors. Among these the following may be cited:

- A tendency to combine the effects of smaller external forces with that of the largest force to reduce the number of thrusters.
- A possibly incomplete definition of requirements due to the advanced nature of the missions selected; i.e., additional requirements may develop as additional space experiments are proposed.

Table 1-2

SUMMARY OF SELECTED MISSION REQUIREMENTS

	ATS-4	VOYAGER	ATM	EVA
Weight, Vehicle, lb	1800	>5500	14,000	~200
FUNCTION				
Attitude Control & Slewing				
Duration	2 yr	1 yr	14-28 d	-
Thrust range	30 μlb-0.7 lb	0.02-2 lb	16 mlb-4.2 lb	-
I, lbf-sec/thruster	833	111	5800	
Operations/thruster	84,500-204,000	4250 (transit) 22100 (orbit)	232,000	-
Power, w.	~ 450		~ 650	-
Station-Keeping	E-W / N-S			
Duration, yr	2 / 1	-	-	-
Thrust range	>232μlb / >1.3 mlb	-	-	-
I, lbf-sec/thruster	3060 / 2708	-	-	-
Operations/thruster	730 / 365	-	-	-
Station Acquisition				
Thrust range	>(3-20) mlb	-	-	-
I_T, lbf-sec	5800-10,300	-	-	-
Evasive Manuever				
Thrust range	-	>0.2 mlb	-	-
I_T, lbf-sec	-	34.2	-	-
Momentum Dumping				
Thrust range	-	-	>173 μlb	-
I_T, lbf-sec	-	-	34800	-
Power, w.	-	-	~100	-
Translation & Att. Cont.				
Thrust range	-	-	-	>1 lb
I_T, lbf-sec	-	-	-	2500

To extend the utility of low-thrust systems, other potential applications were considered. Of these, the most encouraging appeared to arise in conjunction with the final injection of a satellite, such as ATS-4, into synchronous orbit and the essentially continuous countering of small forces acting upon navigational satellites over long periods.

Low-Thrust Injection into Synchronous Orbit. Injection into synchronous orbit is customarily achieved through a Hohmann transfer from a low parking orbit, both impulses being of high-thrust (more than 10^{-1} g or 180 lbf for ATS-4) and relatively instantaneous (Fig. 1-1). The payload is provided, however, with low-thrust devices for the purpose of attitude control and station keeping (of the order of 10^{-3} g or less), and the question arises whether these devices could be used also for orbit injection in apogee, thereby avoiding the acceleration of a high-thrust engine from the intermediate orbit into the final synchronous orbit. The advantages of reduced acceleration and reduced number of systems must be balanced against possible disadvantages, such as increased time into orbit and increased impulse requirement. The impulse penalty is evaluated in the following paragraphs.

Table 1-3 shows velocity requirements for a Hohmann transfer from parking orbits in various altitudes (h_1) to a synchronous orbit with a non-dimensional radius ρ = 6.61072 (where $\rho = r/r_e$ and r_e is Earth's mean equatorial radius), hence an altitude of 19,323 nm. (Other symbols are defined in Table 1-3). The circular velocity in the parking orbit and the perigee velocity of the intermediate one are indicated by V_1 and V_2 in ft/sec. Similarly, V_3 and V_4 are the apogee velocity of the intermediate orbit and the circular synchronous velocity, the latter obviously independent of the altitude of the parking orbit. The velocity increments ΔV_p and ΔV_a in perigee and apogee are shown next, together with the total velocity increment ΔV. Also shown is the limit value $\Delta \bar{v} = V_1 - V_4$ of the velocity increment which would be required for an infinitely low thrust, spiralling, transfer between the parking orbit and the synchronous orbit. A comparison between $\Delta \bar{v}$ and ΔV shows that, even in this limiting case, low thrust consumes less than 20 percent more impulse $(m\Delta V)$ than a Hohmann transfer. This suggests that a finite low thrust, in apogee only, is likely to cause a loss of 5 percent or less.

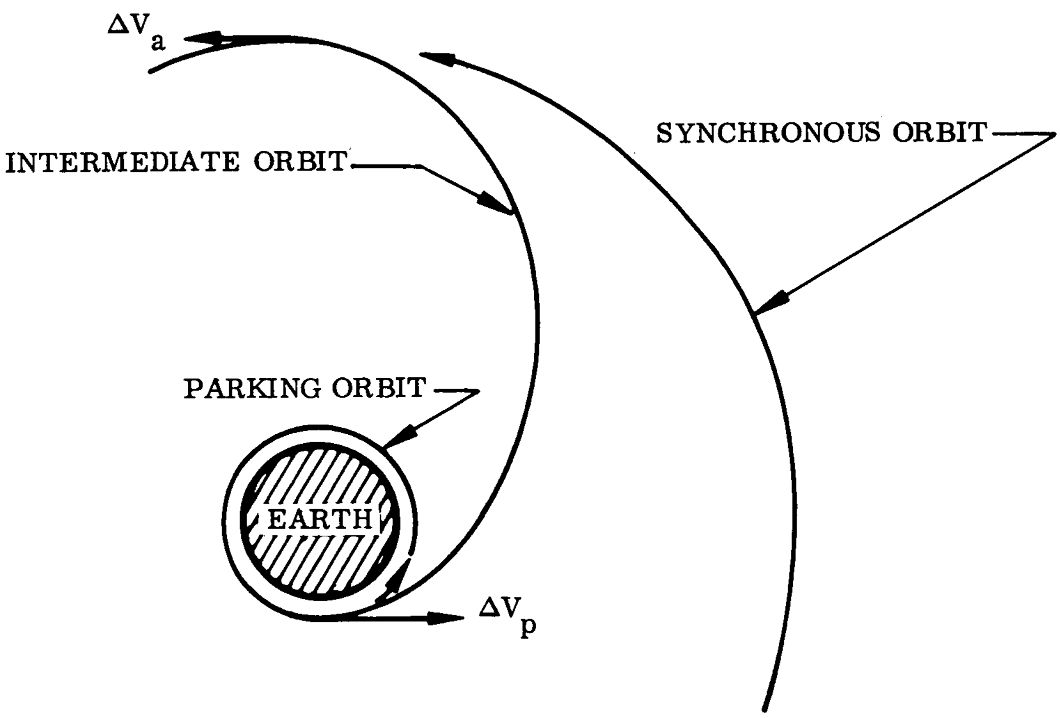

Fig. 1-1 Hohmann-Transfer to Synchronous Orbit

Table 1-3

VELOCITY REQUIREMENTS FOR A HOHMANN-TRANSFER TO SYNCHRONOUS ORBIT

$\rho_p =$ r_p/r_e	h_1 nm	V_1 (circ. park.)	V_2 (per. transf)	V_3 (apog. transf)	V_4 (synchr)	$\Delta V_p = V_2 - V_1$	$\Delta V_a = V_4 - V_3$	$\Delta V = \Delta V_a + \Delta V_p$	$\Delta \bar{v}$ $V_1 - V_4$	$\frac{\Delta \bar{v} - \Delta V}{\Delta V / 100}$
1.025	86	25618	33710	5226	10087	8092	4861	12953	15531	19.90
1.05	172	25311	33252	5281	10087	7941	4806	12747	15224	19.43
1.075	258	25015	32810	5335	10087	7795	4752	12547	14928	18.98
1.1	344	24729	32382	5388	10087	7653	4699	12352	14642	18.54
1.125	430	24453	31968	5440	10087	7515	4647	12162	14366	18.12
1.15	516	24186	31568	5491	10087	7382	4596	11978	14099	17.71

Symbols

r_p = parking orbit radius, nm
r_e = Earth's mean equatorial radius, nm
ρ_p = r_p/r_e = dimensionless orbital radius
h_1 = parking orbit altitude. nm
V_1 = circular velocity in parking orbit, ft/sec
V_2 = perigee velocity of transfer orbit, ft/sec
V_3 = apogee velocity of transfer orbit, ft/sec
V_4 = circular velocity in synchronous orbit, ft/sec
ΔV = velocity increment for Hohmann transfer, ft/sec
$\Delta \bar{v}$ = velocity increment for infinitely low thrust transfer from parking to synchronous orbit. ft/sec

From the ΔV_a of about 4800 ft/sec, it follows that the burning time at apogee is anywhere from 150 to 1500 sec for an acceleration of 1 g to 10^{-1} g. However, for an acceleration of 10^{-3} g the burning time becomes 150,000 sec, or close to two days. Obviously, this implies that orbit injection then must be performed in a sequence of apogee pulses, each of a few hr duration and each time raising the perigee until, after many such pulses, the perigee reaches synchronous altitude. The total operation will readily require three or four times the actual burning time, that is, close to one week. This total elapsed time will be inversely proportional to the acceleration level, hence about 10 weeks for 10^{-4} g, etc.

Since transfer from the intermediate orbit to the synchronous orbit is primarily a matter of energy increase, it can be assumed that optimum conditions are closely represented by accelerations tangential to the instantaneous orbit. A tangential force, applied anywhere outside the perigee and the apogee will raise not only the perigee but also, to some extent, the apogee. Therefore, if low thrust is to be used in the apogee area, the initial transfer must be one to a point lower than the final apogee, in order to allow for a simultaneous raising of both the perigee and the apogee to synchronous altitude (Fig. 1-2, not to scale). This means that the perigee pulse ΔV_p is then bound to be less than the values shown in Table 1-3, and since ΔV is expected to be higher there must be a relatively larger increase in the apogee pulse ΔV_a .

So far, the total velocity increment ΔV has been considered as a measure for efficiency. This is justified only as far as specific impulses (I_{sp}) are equal for the high-thrust and the low-thrust engines. If the low-thrust engines can be made to have a slightly higher I_{sp} than the high-thrust engines, a break-even point is soon reached, beyond which the low thrust apogee impulse would be more efficient than the all-high-thrust orbit injection.

This qualitative summary of velocity and impulse conditions is offered to comprehend the physical meaning of the following numerical results.

The effect of tangential thrust along a limited part around the apogee of an elliptical orbit was integrated in closed form. With these results the gradual acquisition of a

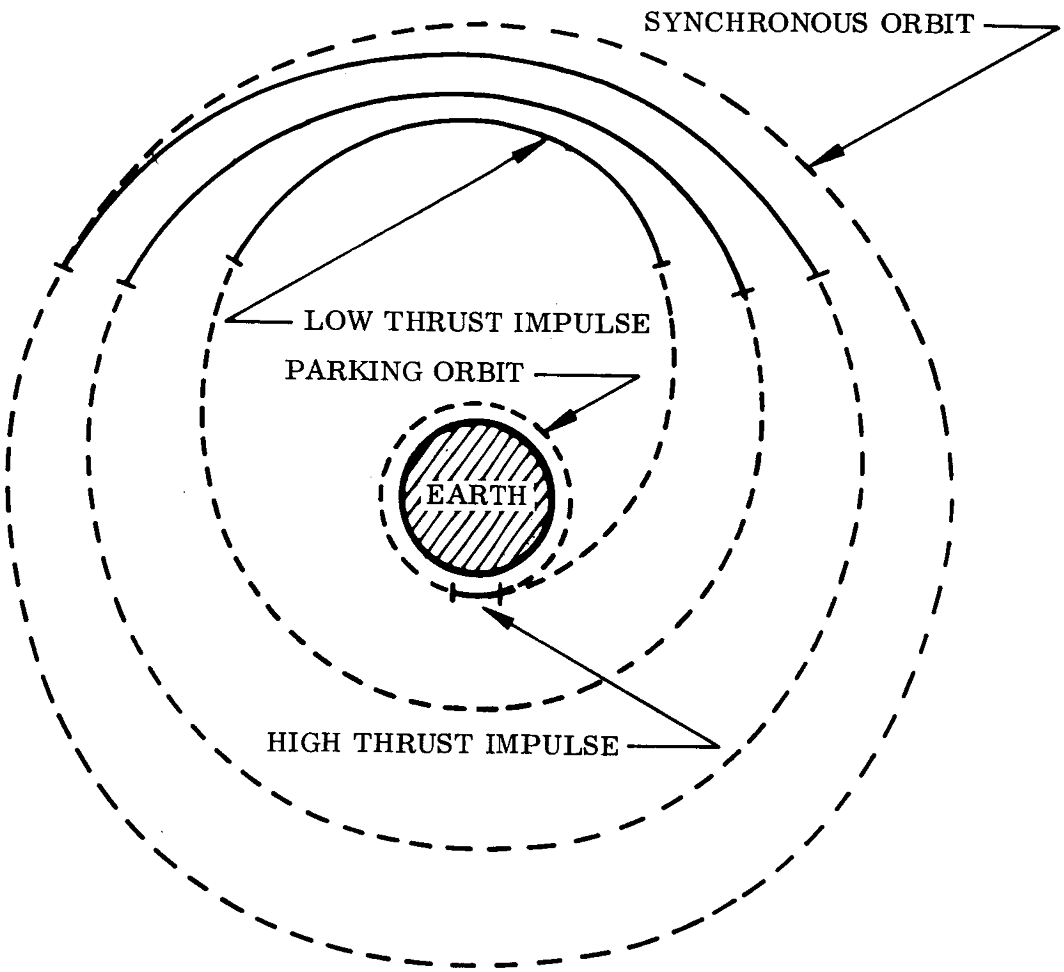

Fig. 1-2 Low-Thrust Orbit Injection Into Synchronous Orbit From Transfer Apogee

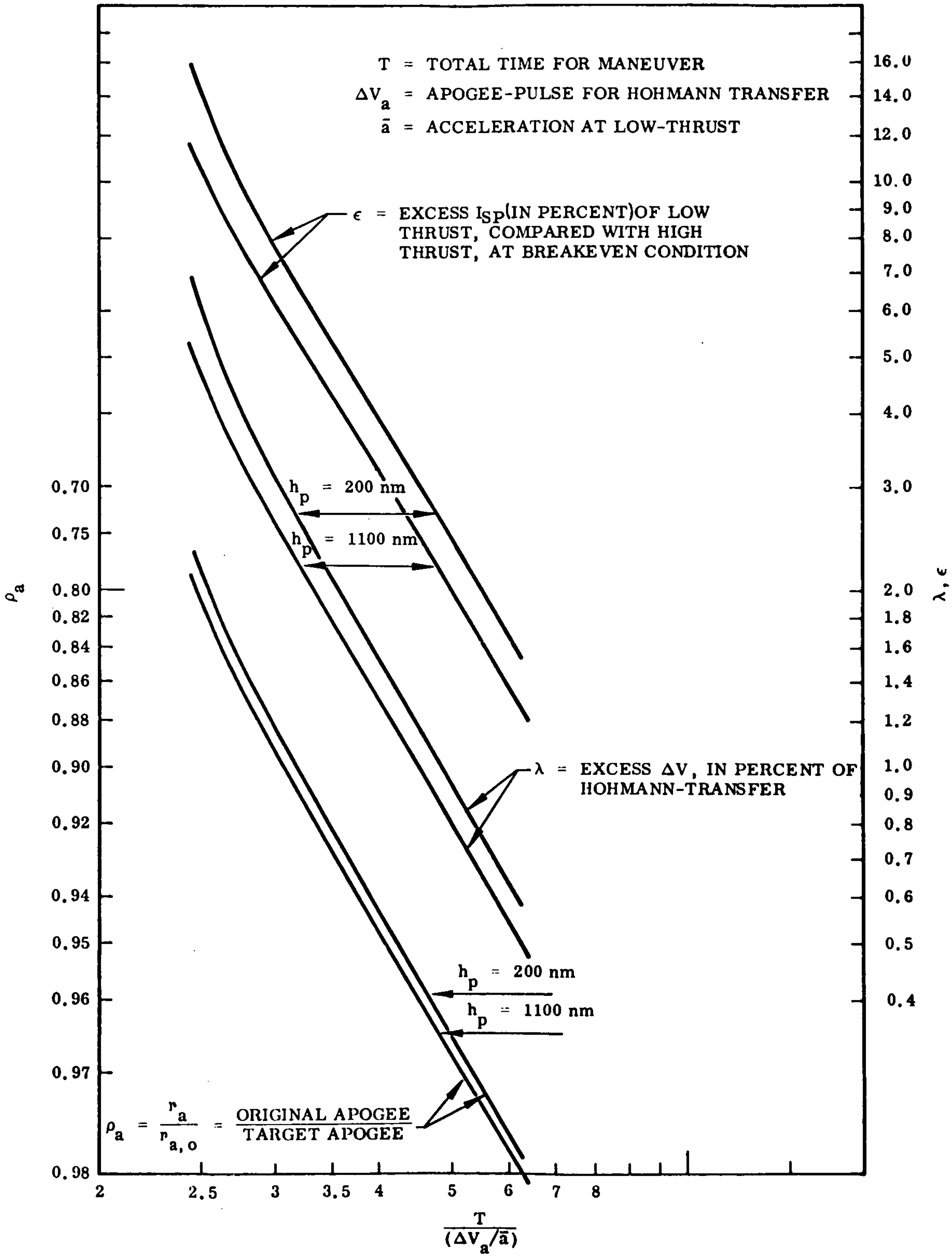

Fig. 1-3 Low-Thrust Orbit Injection From Elliptical Transfer Orbit to Synchronous Orbit

synchronous orbit by a low tangential thrust was integrated numerically with steps of one revolution. The integration was performed from synchronous orbit backward to an orbit the perigee of which was located on the assumed parking orbit. The characteristics of such an extended maneuver are primarily determined by the fraction of time during which the low thrust is operating. As this fraction becomes lower, the longer the elapsed time for the whole maneuver, the smaller the loss as compared with a Hohmann transfer, and the higher the original apogee to be reached from the high-thrust perigee impulse.

Figure 1-3 graphically shows the results with the elapsed time as an independent parameter. All parameters are shown in a non-dimensional form. The elapsed time T is expressed as a multiple of a fictitious time $T_o = \Delta V_a / \bar{a}$, where $\bar{a}$ is the low-thrust acceleration. For instance, with $\bar{a} = 10^{-3}$ g = 0.032172 ft/sec, it is found that for a parking orbit of 258 nm altitude and hence ΔV_a = 4752 ft/sec (from Table 1-3) that T_o = 147,700 sec = 1.71 days. A value of 4 for $T/(\Delta v_a/\bar{a})$ would therefore correspond to a total elapsed time of about one week.

Three parameters are shown in Fig. 1-3. All three are given for parking orbit altitudes of 200 nm and 1100 nm. The selection of the latter was made because only an excessive spread in altitude would show up adequately in the graph. Linear interpolation can be used for other orbit altitudes.

The parameter λ indicates the excess ΔV required over the Hohmann transfer ΔV as shown in Table 1-3. For instance, λ = 1.5 percent means that a total ΔV of 1.5 × 127 ft/sec = 190 ft/sec is required over and above the ΔV of approximately 12,680 ft/sec of a Hohmann transfer from a 200 nm orbit. This total ΔV of 12,680 + 190 = 12,870 ft/sec applies to high thrust perigee and low thrust apogee together and is based on the assumption that the I_{sp} for both are equal. As pointed out earlier, ΔV_p is less than and ΔV_a is more than the values in Table 1-3.

The parameter ϵ is concerned with a possible inequality between the two specific impulses. It shows the percentage by which the specific impulse of low-thrust systems must surpass that of high thrust systems to eliminate the loss associated with the parameter λ, described above. Again, as an example, if the high thrust has an I_{sp} of 280 sec and ϵ is found to be 4 percent, then the I_{sp} for the low thrust device must be $1.04 \times 280 = 291$ sec, in order for the better efficiency of low thrust to balance the loss associated with low thrust from flight mechanics considerations.

Finally, a parameter $\rho_a = r_a / r_{a.0}$ is plotted, where r_a is the initial apogee altitude of the intermediate orbit after the high thrust perigee pulse has been applied, and $r_{a.0}$ is the synchronous radius as shown earlier $(6.61072\ r_e)$.

To summarize, it appears possible to justify the use of thrusts corresponding to 10^{-3} g (1.8 lbf) or less if sufficient time is available. The impulse penalty can be relatively small and may be outweighed by advantages gained by lower acceleration and reduced number of propulsion systems. The impulse penalty may be overcome by increasing the specific impulse of the low thrust system (Section 3.4.1).

Very-Low-Thrust, High-Duty-Cycle Requirements. Another area which promises to afford requirements for LTRCS is that of accurately positioning navigational satellites. Satellites of this type are subject to diurnal and relatively steady forces, such as magnetic fields or drag forces, which require thrust levels in the 10^{-9} to 10^{-6} lbf range for correction. The ability to predict satellite position with a high degree of accuracy is essential to satisfactory operation. While higher thrust levels applied briefly to counter cumulative effects are possible, the very low thrust levels, utilized at high duty cycle, permit a vernier-like adjustment of trajectory.

Advanced systems for this type application are proposed and discussed in Section 3.4.2.

1.3 COMPARISON AND SELECTION OF CONTENDING SYSTEMS

As a result of a comparison of system characteristics with each mission requirement, certain systems can be eliminated from further consideration. Such an elimination may be the result of too high or too low a thrust range, an excessive power requirement, or the requirement for a very large number of operations. It might reflect the absence of a sufficient gravitational or magnetic field. Some systems are applicable to rotational functions only, not translational functions. Or the system accuracy may be judged insufficient.

A summary of the item-by-item comparison is given in Table 1-4, together with the bases for elimination where applicable. Certain systems can be eliminated for more than one reason, although only one reason may be indicated. The comparison reduces the number of potential applications by approximately one-third.

The remaining contenders were then subjected to the trade-off studies described in Section 2.

Table 1-4

COMPARISON OF MISSION REQUIREMENTS AND SYSTEM CHARACTERISTICS

Requirement	Subliming Solid	Heated Subliming Solid	Hybrid Hydrogen Monopropellant	Solid Propellant Impulse Bit	Pressurized Cold Gas	Vaporizing Liquid (NH_3)	Monopropellant Hydrazine	Monopropellant N_2H_4 Cold Gas	Bipropellant Vapor	Bipropellant Liquid	Water Electrolysis	Resistojet (NH_3)	Electrostatic	Pulsed Plasma	Penning Discharge	Gravity Gradient	Gyrostabilizers	Magnetic Torques
ATS-4																		
Attitude Control and Slewing	+	+	+	0(1)	+	+	+	+	+	+	+	+	+	+	+	0(11)	+	0(12)
Station-Keeping (E-W)	+	+	+	+	+	+	+	+	+	+	+	+	+	0(2)	+	0(3)	0(3)	0(3)
Station-Keeping (N-S)	+	+	+	+	+	+	+	+	+	+	+	+	+	0(4)	0(2)	0(3)	0(3)	0(3)
Station Acquisition	+	+	+	+	+	+	+	+	+	+	+	+	?	0(4)	0(4)	0(3)	0(3)	0(3)
Voyager																		
Evasive Maneuver	+	+	0(13)	0(7)	+	+	+	+	+	+	0(13)	0(13)	0(13)	0(4)	0(13)	0(3)	0(3)	0(3)
Attitude Control	+	+	+	0(1)	+	+	+	+	+	+	+	+	0(4)	0(4)	0(4)	0(5)	+	0(6)
ATM																		
Attitude Control and Slewing	+	+	+	0(1)	+	+	+	+	+	+	+	+	0(4)	0(4)	0(4)	0(8)	+	0(9)
Momentum Dumping	+	+	+	+	+	+	+	+	+	+	+	+	+	0(4)	+	0(14)	0(7)	+
EVA																		
Attitude Control and Translation	0(4)	0(4)	?	+	+	0(10)	+	+	+	+	0(10)	0(4)	0(4)	0(4)	0(4)	0(3)	0(3)	0(3)

\+ Capable of meeting requirement
0 Incapable of meeting requirement for reason shown:

(1) Number of required operations too great
(2) Max. thrust too low without paying I_t penalty
(3) Not applicable to translational functions
(4) Max. thrust too low
(5) Negligible gravity field in transit: highly elliptical orbit
(6) Negligible or unknown magnetic field
(7) Not applicable
(8) Inaccurate, not local vertical
(9) Inaccurate
(10) Power requirement too high
(11) Stabilization within ±0.3 degrees impossible
(12) Two-axis control only
(13) High degree of sophistication is unnecessary
(14) **Not applicable without reorientation**

? Marginal

Section 2
TRADEOFF STUDIES

The systems remaining in contention after the previously described elimination process were subjected to analysis in greater depth. The objective of the resulting tradeoff studies was to define a level of excellence for the solid and hybrid low-thrust systems to reach or exceed, in order to contend seriously for future NASA missions. The purpose was not to select a single optimum system for a given application.

Each functional requirement is treated separately to illustrate as many relative capabilities as possible. In some cases, a combination of functions may be made in order to reduce complexity of the overall propulsion system. However, such combination would be disadvantageous to low specific impulse solid systems, since the total impulse would be increased. Descriptions of all systems are given in Ref. 1 and schematic diagrams are shown in Section 2.2.

2.1 WEIGHT ANALYSES

For uniformity, and lacking a final design, the attitude control systems were assumed to have six nozzles, the ATS-4 North-South stationkeeping and EVA systems to have two nozzles, and all others one nozzle. In those systems requiring electric power, it was assumed that only one nozzle functioned at a time.

2.1.1 Solid and Hybrid Systems

The weights of subliming solid systems operating with ammonium carbamate as propellant are estimated to be as shown in Table 2-1. This propellant was selected as a result of its use in the LMSC "B" motor. A specific impulse of 80 lbf-sec/lbm at 110°F is assumed (85 percent of theoretical). The total impulse and thrust were selected from the requirements determined for the individual missions.

Table 2-1

SUBLIMING SOLID SYSTEM WEIGHTS

Mission	ATS-4				Voyager		ATM	
Function	Attitude Control	N-S Sta. Keeping	E-W Sta. Keeping	Station Acquis.	Attitude Control	Evasive Maneuver	Attitude Control	Momentum Discharge
I_T (lb-sec)	5000	5420	3060	10,300	666	34.2	34,800	34,800
Thrust (lbf)	3×10^{-5}	1.3×10^{-3}	2.3×10^{-4}	3×10^{-3}	2×10^{-2}	2×10^{-4}	1.6×10^{-2}	1.7×10^{-4}
Power Available (w)		~450					~650	~100
Power Required, (w)	8.0	30.5	11.6	60.6	361.5	11.0	290.5	10.6
Total Weights (lbm)	87.8	99.8	51.7	210.0	116.9	5.4	955.0	879.4
Container, etc.	20.1	22.8	9.8	64.1	8.0	1.5	438.5	438.5
Valves, nozzles and lines	3.0	1.0	0.5	0.5	3.0	0.5	3.0	3.0
Propellant	62.5	67.8	38.3	129.	8.3	0.4	435.	435.
Solar Cells	2.2	8.2	3.1	16.4	97.6	3.0	78.5	2.9

Assumptions:

Propellant – Ammonium carbamate
Control – Temperature
Nozzles – Only one thrusting at a time

Misc. Power:

Valve – 3 w each
Temp. Controller – 0.5 w
Heat Loss – 2.5 w
Nozzle Heater – 1.5 w
Conversion Factor – 0.27 lbm/w
Power for Sublimation – 100 percent duty cycle basis

Similarly, weights were determined for the superheated subliming solid system. In this, the propellant was the same, but the specific impulse was assumed to be 205 lbf-sec/ lbm at 2000°F (85 percent of theoretical). The computed weights are given in Table 2-2.

The weights of both systems are a function of both total impulse and thrust level. These relationships are shown in Fig. 2-1 (a and b) for thrust levels of 10^{-2}, 10^{-3}, 10^{-4} lbf at total impulses up to 11,000 and 33,000 lbf-sec, respectively. Considerable weight saving can result from the superheated system at total impulses of 500 lbf-sec or more. The saving increases markedly with the total impulse at all three thrust levels.

The system weight of the only hybrid system known to have been previously proposed for low-thrust application is the hybrid-hydrogen monopropellant system. Estimated weights of this system are indicated in Fig. 2-2.

The fourth solid and hybrid system examined is the Repetitive Impulse Generator (RIG). The system weights are estimated to be as shown in Fig. 2-3 for impulse bits numbering 4,000, 1,000, and 500. Propellants which can be used in this system have specific impulses in the 120 – 190 lbf-sec/ lbm range. The weights are based on the assumption that the product gases, at impulse bits less than 1 lb-sec, lose heat to the reaction chamber. Above this value, the full value of specific impulse can be attained. This is actually a conservative assumption if the gases are exhausted to vacuum from individual nozzles. For the latter design, the "knees" at 1 lb-sec/bit disappear and the curves can be extrapolated from the zero-impulse intercept with a slope corresponding to the reciprocal of specific impulse.

2.1.2 Competitive Vapor and Liquid Systems

Six vapor and liquid systems,

- Pressurized cold gas
- Vaporizing liquid (NH_3)

Table 2-2

SUPERHEATED SUBLIMING SOLID WEIGHTS

Mission	ATS-4				Voyager		ATM	
Function	Attitude Control	N-S Sta. Keeping	E-W Sta. Keeping	Sta. Acquis.	Attitude Control	Evasive Maneuver	Attitude Control	Momentum Discharge
I_T (lb-sec)	5000	5420	3060	10,300	666	34.2	34,800	34,800
Thrust (lbf)	3×10^{-5}	1.3×10^{-3}	2.3×10^{-4}	3×10^{-3}	2×10^{-2}	2×10^{-4}	1.6×10^{-2}	1.7×10^{-4}
Power Available (w)			~450				~650	~100
Power Required (w)	22.4	40.8	25.4	65.5	312	24.9	254	24.5
Total Weights (lbm)	39.5	44.8	24.7	83.3	92.8	9.1	342.7	280.7
Superheater	0.6	0.4	0.2	0.2	0.6	0.2	0.6	0.6
Container, etc.	5.4	5.9	2.2	14.6	1.6	1.5	100.5	100.5
Valves, nozzles, and lines	3.0	1.0	0.5	0.5	3.0	0.5	3.0	3.0
Propellant	24.4	26.5	14.9	50.3	3.3	0.2	170.0	170.0
Solar Cells	6.1	11.0	6.9	17.7	84.3	6.7	68.6	6.6

Assumptions: As in Table 2-1.

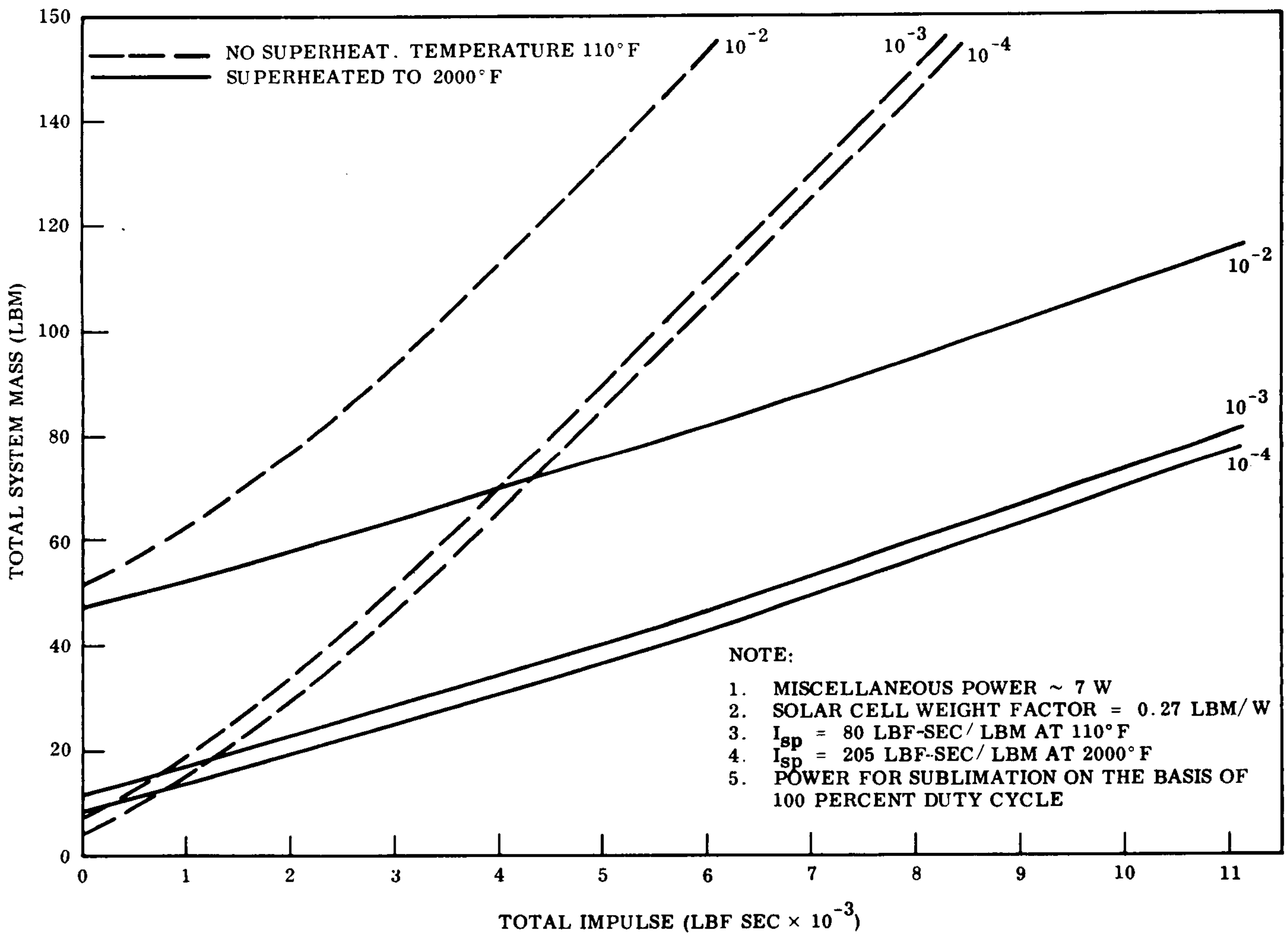

Fig. 2-1a Total System Mass for Ammonium Carbamate Subliming Solid Motors Vs. Total Impulse With Thrust as a Parameter

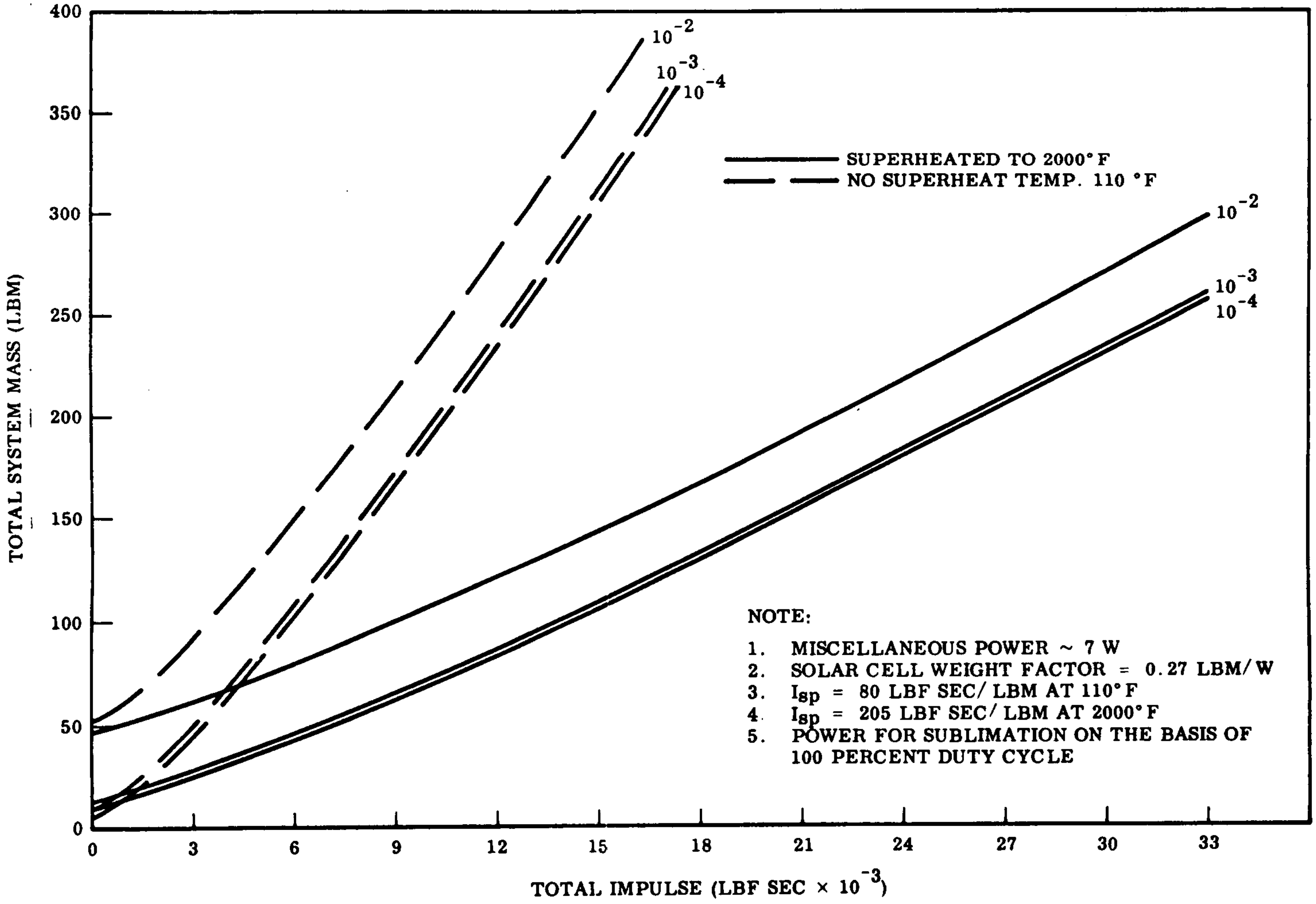

Fig. 2-1b Total System Mass For Ammonium Carbamate Subliming Solid Motors Vs. Total Impulse With Thrust as a Parameter

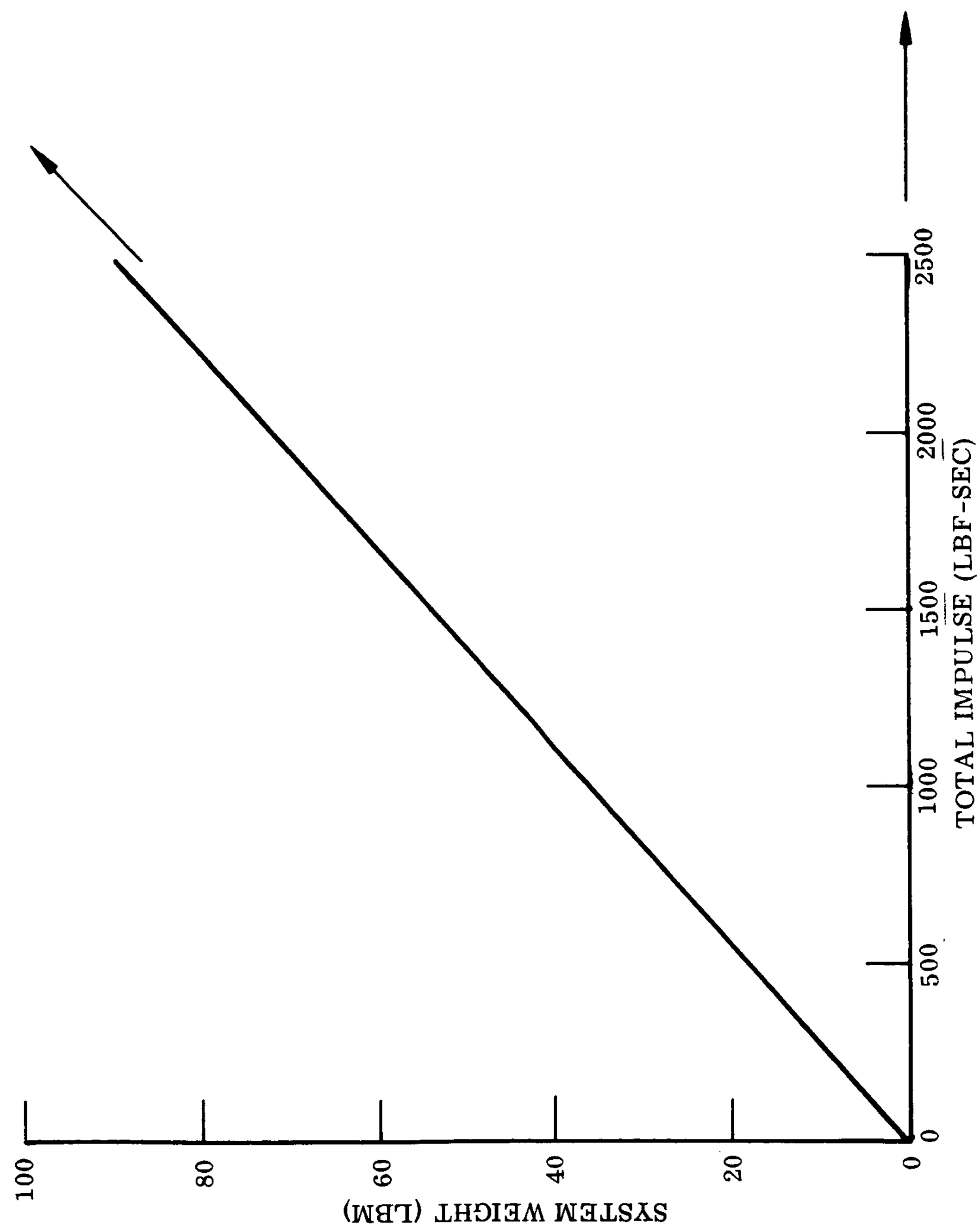

Fig. 2-2 Hydrogen Monopropellant System Weight as a Function of Total Impulse

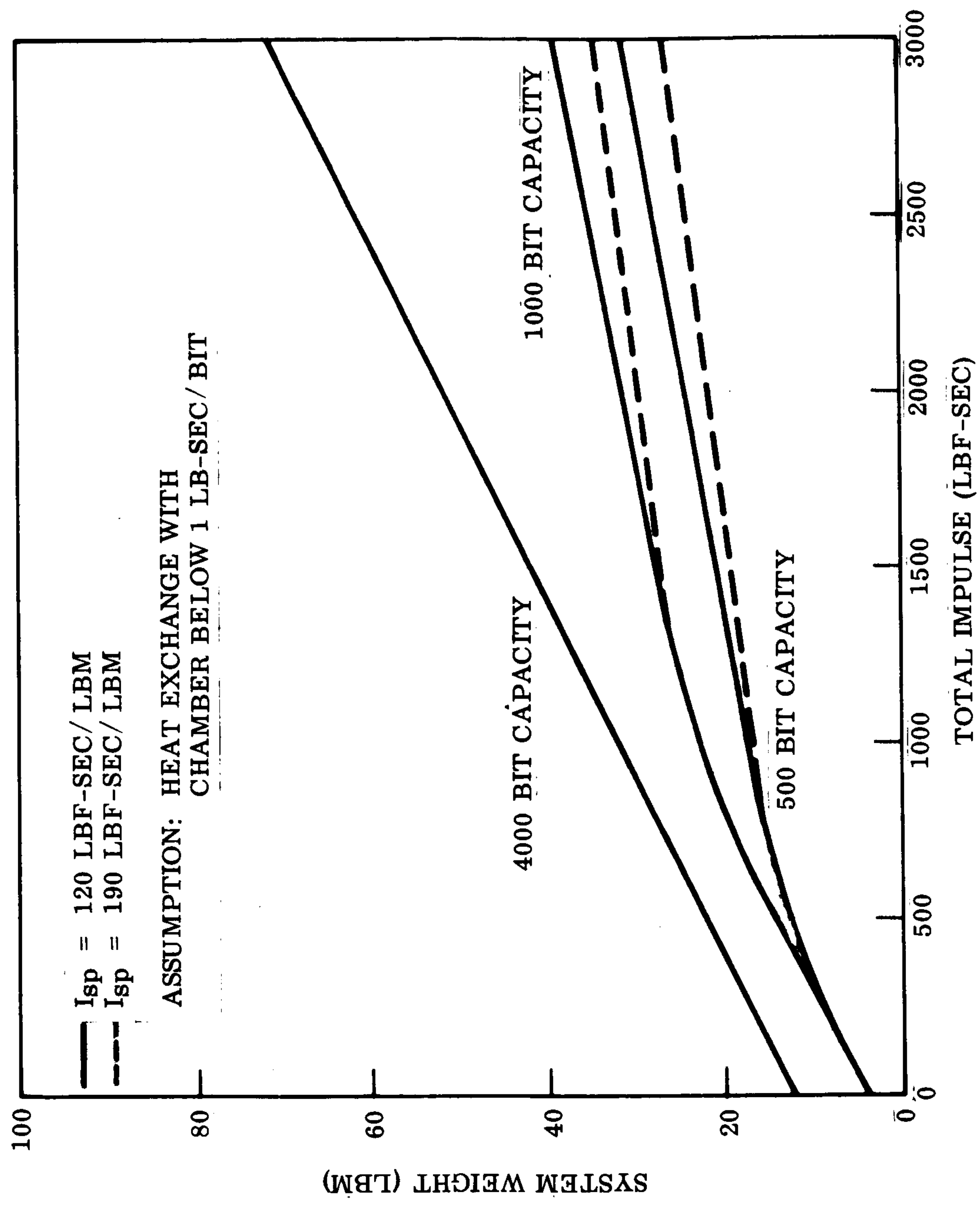

Fig. 2-3 Repetitive Impulse Generator System Weight as a Function of Total Impulse for Various Total Impulse Bit Capacities

- Monopropellant hydrazine
- Monopropellant hydrazine cold gas
- Bipropellant vapor
- Bipropellant liquid

were analyzed to determine the weight involved in fulfilling the specific mission requirements of Section 1.2. Each system weight was estimated in two configurations – the lightest and the most reliable – and two modes of operation – minimum pulse bit and steady state (ref. Table 1-1). The configurations are sketched in Appendix C. The computed weights are given in Table 2-3 for the minimum thrust level indicated in Table 1-1. Attitude control is taken to require a short pulse, while other functions require the steady-state value.

To generalize the weight computations for other unspecified missions, curves in Appendix C depict the relationship of weight and total impulse at impulses in the 0–1,400 and 0–14,000 lbf-sec ranges. These were derived for use at the minimum thrust levels of Table 1-1 and a maximum level of 10 lbf.

2.1.3 Electrical Systems

The weights of six electrical systems

- Water electrolysis rocket
- Ammonia resistojet
- Ion engine
- Colloid engine
- Pulsed plasma, and
- Penning discharge

needed to fulfill the mission requirements were also determined. The system weights are tabulated, together with power supply weights, in Table 2-4, at thrust levels which were optimized for the particular system involved. Information supporting the weight assignments is given in Appendix D.

Table 2-3

COMPETITIVE VAPOR AND LIQUID SYSTEM WEIGHTS IN THE LIGHTEST CONFIGURATIONS

Mission	ATS-4				Voyager		ATM		EVA
Function	Attitude Control	E-W Station Keeping	N-S Station Keeping	Station Acquis.	Attitude Control	Evasive Maneuver	Attitude Control	Momentum Discharge	
System (wt, lb)									
Pressurized Cold Gas	170	105	180	340	25	3.3	1150	1150	85
Vaporizing Liq. NH_3	75	50	80	155	14.5	6.5	530	530	40
Monopropellant N_2H_4	45	25	35	65	8.5	4.0	295	295	16
Monopropellant N_2H_4 Cold Gas	60	35	65	115	14.5	10.3	375	375	30
Bipropellant Liquid	40	15	20	40	10.5	7.3	275	275	13
Bipropellant Vapor	30	20	35	65	10.5	8.5	225	225	12

Table 2-4

ELECTRICAL SYSTEM WEIGHTS

MISSION	ATS-4				VOYAGER		ATM	
Function I_T, lb-sec	Attitude Control 5000	E-W Stat. Keeping 3060	N-S Stat. Keeping 5420	Station Acquis. 10,300	Attitude Control 666	Eva. Maneuver 34	Attitude Control 34800	Momentum Discharge 34800
WATER ELECTROLYSIS								
Thrust, lbf	0.1	0.1	0.1	0.01	0.1	–	0.1	0.1
Power, w	0.5	0.87	1.2	250	0.11	–	125	125
System Wt, lb	51.0	19.5	32.0	50.5	29.6	–	214	214
Power, Wt, lb	0.2	0.2	0.3	67.4	0.03	–	33.7	33.7
Total, lb	51.2	19.7	32.3	117.9	29.6	–	247.7	247.7
AMMONIA RESISTOJET								
Thrust, lbf	3×10^{-4}	3×10^{-4}	1.5×10^{-3}	3×10^{-3}	3×10^{-4}	–	0.1	3×10^{-4}
Power, w	16	16	22	33	16	–	180	16
System Wt, lb	45.3	22.0	44.7	62.0	13.0	–	229	198.0
Power Wt, lb	4.3	4.3	5.7	8.9	4.3	–	48.6	4.3
Total, lb	49.6	26.3	50.4	70.9	17.3	–	277.6	202.3
ION ENGINE								
Thrust, lbf	3×10^{-5}	2.3×10^{-4}	1.3×10^{-6}	3×10^{-3}	–	–	–	1.75×10^{-4}
Power, w	25	62	232	410	–	–	–	49
System Wt, lb	9.2	5.2	14.6	19.4	–	–	–	18.9
Power Wt, lb	6.8	17.0	63.0	110.0	–	–	–	13.3
Total, lb	16.2	22.2	77.6	129.4	–	–	–	32.2
COLLOID ENGINE								
Thrust, lbf	3×10^{-5}	2.3×10^{-4}	1.3×10^{-6}	3×10^{-3}	–	–	–	1.75×10^{-4}
Power, w	3.3	11.9	32	62	–	–	–	9.6
System Wt, lb	15.5	5.5	23.0	41.0	–	–	–	37.3
Power Wt, lb	0.8	3.3	8.7	17.0	–	–	–	2.6
Total, lb	16.3	8.8	31.7	58.0	–	–	–	39.9
PULSED PLASMA								
Thrust, lbf	3×10^{-5}	–	–	–	–	–	–	–
Power, w	15	–	–	–	–	–	–	–
System Wt, lb	80.0	–	–	–	–	–	–	–
Power Wt, lb	4.0	–	–	–	–	–	–	–
Total, lb	84.0	–	–	–	–	–	–	–
PENNING DISCHARGE								
Thrust, lbf	3×10^{-5}	2.3×10^{-4}	–	–	–	–	–	1.75×10^{-4}
Power, w	4.5	39	–	–	–	–	–	28
System Wt, lb	41.1	15.5	–	–	–	–	–	99.3
Power, lb	1.3	10.5	–	–	–	–	–	7.6
Total, lb	42.4	26.0	–	–	–	–	–	106.9

ASSUMPTIONS

Conversion Factor: 0.27 lbm/w

I_{sp}: Ion Engine – 5000 lbf-sec/lbm

Colloid engine – 540 - 1500 lbf-sec/lbm, optimized for each mission on a weight basis

Pulsed plasma – 2000 lbf-sec/lbm

Penning discharge – 1300 lbf-sec/lbm

* – Thermal – storage resistojet, operating 30 seconds maximum per thrusting period. 1% duty cycle. 30 w/thruster

2.1.4 Passive Systems

The passive systems – including gravity gradient, gyrostabilizer, magnetic torque systems, and combinations of these- are applicable only to the attitude control requirements. The passive systems fulfill no translational functions.

A summary of passive system weights is given in Table 2-5. Only active control moment gyrostabilizers (CMG) can be considered for the ATS-4, Voyager and ATM attitude control missions. Details of the estimates are given in Appendix E.

Table 2-5

PASSIVE SYSTEM WEIGHTS

Mission Function	ATS-4 Attitude Control and Slewing	Voyager Attitude Control	ATM Attitude Control and Slewing	ATM Momentum Discharge
GRAVITY GRADIENT	–	–	–	–
(With or without passive cont. mom. gyro)				
CONTROL MOMENT GYRO. (ACTIVE)				
Power, (w)	31	7	38	–
System Wt., (lb)	18.6	15.5	43.0	–
Power Wt., (lb)	8.4	1.9	10.3	–
Unit Weight (lb)	27.0	17.4	53.3	–
Total Weight, (lb)	108.0	52.2	159.9	–
MAGNETIC TORQUE SYSTEM	–	–	–	22
(With or without momentum wheel)				

Conversion Factor: 0.27 lbm/w.

To place the CMG's on a comparable basis with the active systems, the weight of any associated momentum discharge device(s) must be added to the CMG weight. From Figure 2-11 the lightest ATM momentum discharge device is the magnetic torque system. A weight of 22 lb was therefore added to each CMG system weight in the overall comparisons (Section 2.4).

2.2 RELIABILITY ESTIMATES

2.2.1 General

Reliability data were generated for all the low-thrust systems previously considered. The goal was to establish reliability levels characteristic of the best systems available in the near future, and not to single out any particular system as outstanding. It was recognized that the assignment of reliability values by those directly concerned with development or production of a given system may be unintentionally biased. All estimates were therefore generated by analysts who were familiar with reliability techniques, but who were unrelated to any low-thrust development programs.

Functional flow diagrams were drawn for basic configurations in each of the systems. These are illustrated in Figure 2-4(a-q). The basic method used was to assign a failure rate to each part of the particular system under study and by summing these failure rates, applying the mission times involved, and solving the classic reliability equations involved, to calculate a reliability figure of merit. Where redundancy was included in the design as a design decision, the redundancy expressions were employed in the usual fashion to compute the partial reliability of those system elements involved. Common components were assigned identical values to assure a satisfactory basis of comparison. An exception to this policy, due to lack of information, is noted in F.2-2.

2.2.2 Failure Rates

One of the difficulties involved in analysis of systems of these types is the assignment of valid failure rate data, especially since many of the system elements do not have a mechanical action type of function. For instance propellants are complex chemical

Fig. 2-4 Functional Flow Diagrams

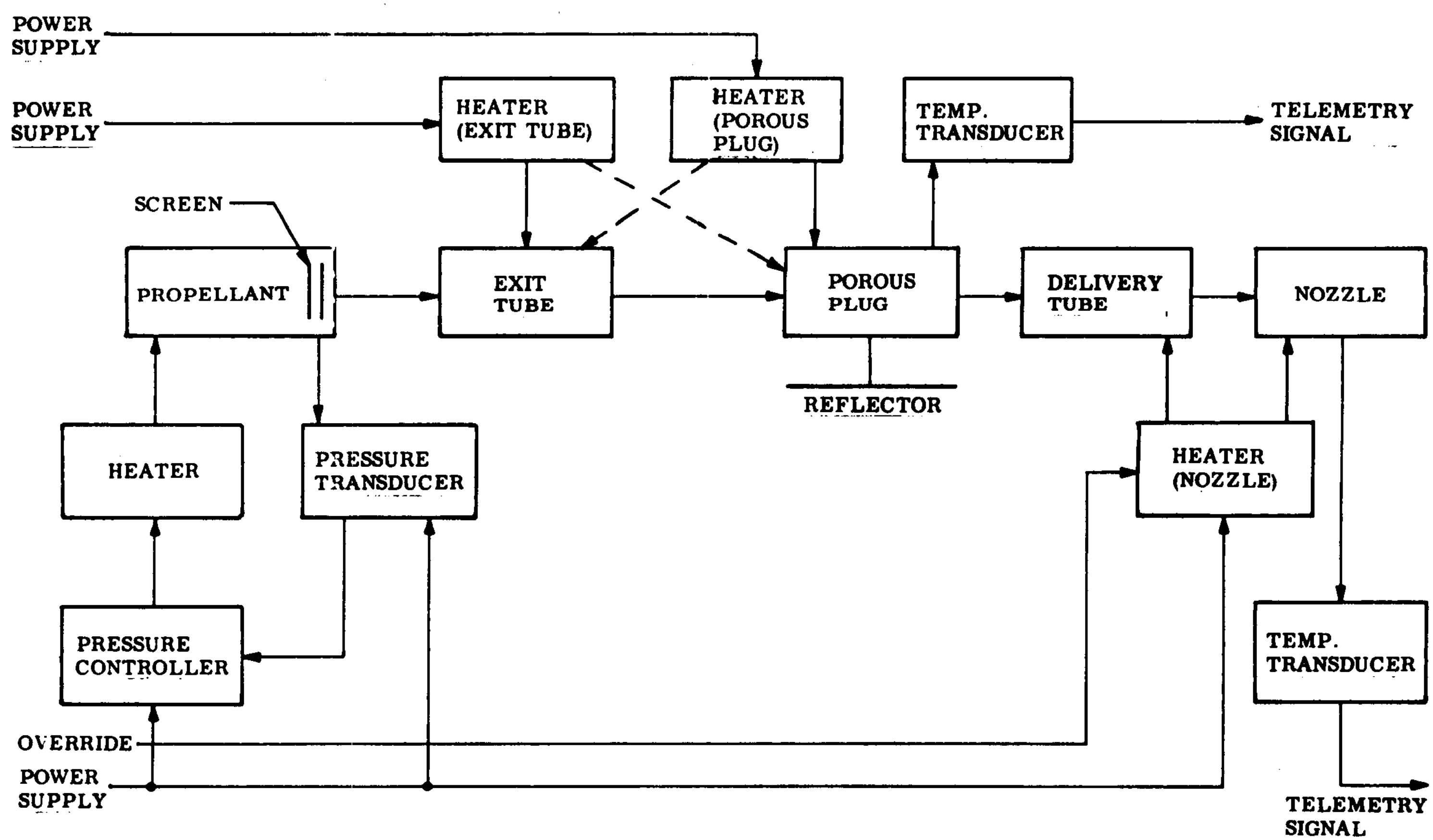

Fig. 2-4a Subliming Solid System

AS IN FIG. 2-4a EXCEPT THAT NOZZLE HEATER IS REPLACED BY ONE OPERATING AT TEMPERATURES UP TO 2000°F.

Fig. 2-4b Superheated Subliming Solid System

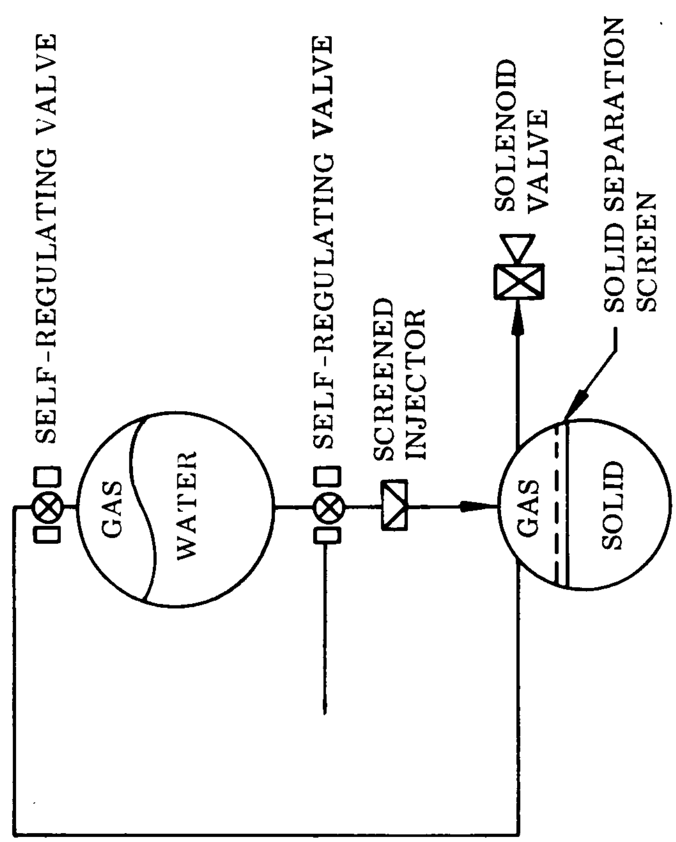

Fig. 2-4c Hybrid Hydrogen Monopropellant System

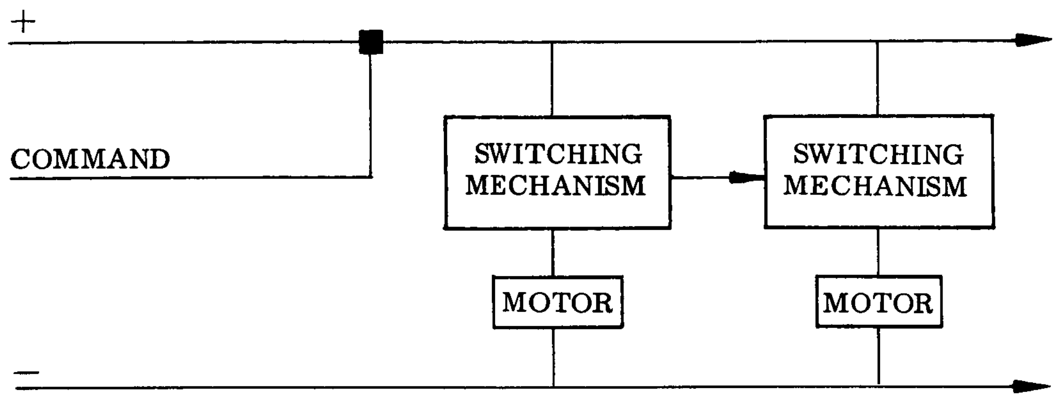

Fig. 2-4d Repetitive Impulse Generator

Schematic diagrams for the pressurized cold gas [e], vaporizing liquid (NH_3)[f], mono-propellant hydrazine[g], cold gas monopropellant hydrazine[h], bipropellant vapor[i], and bipropellant liquid[j] systems are substantially the same as those given in Appendix C.

Fig. 2-4e–j

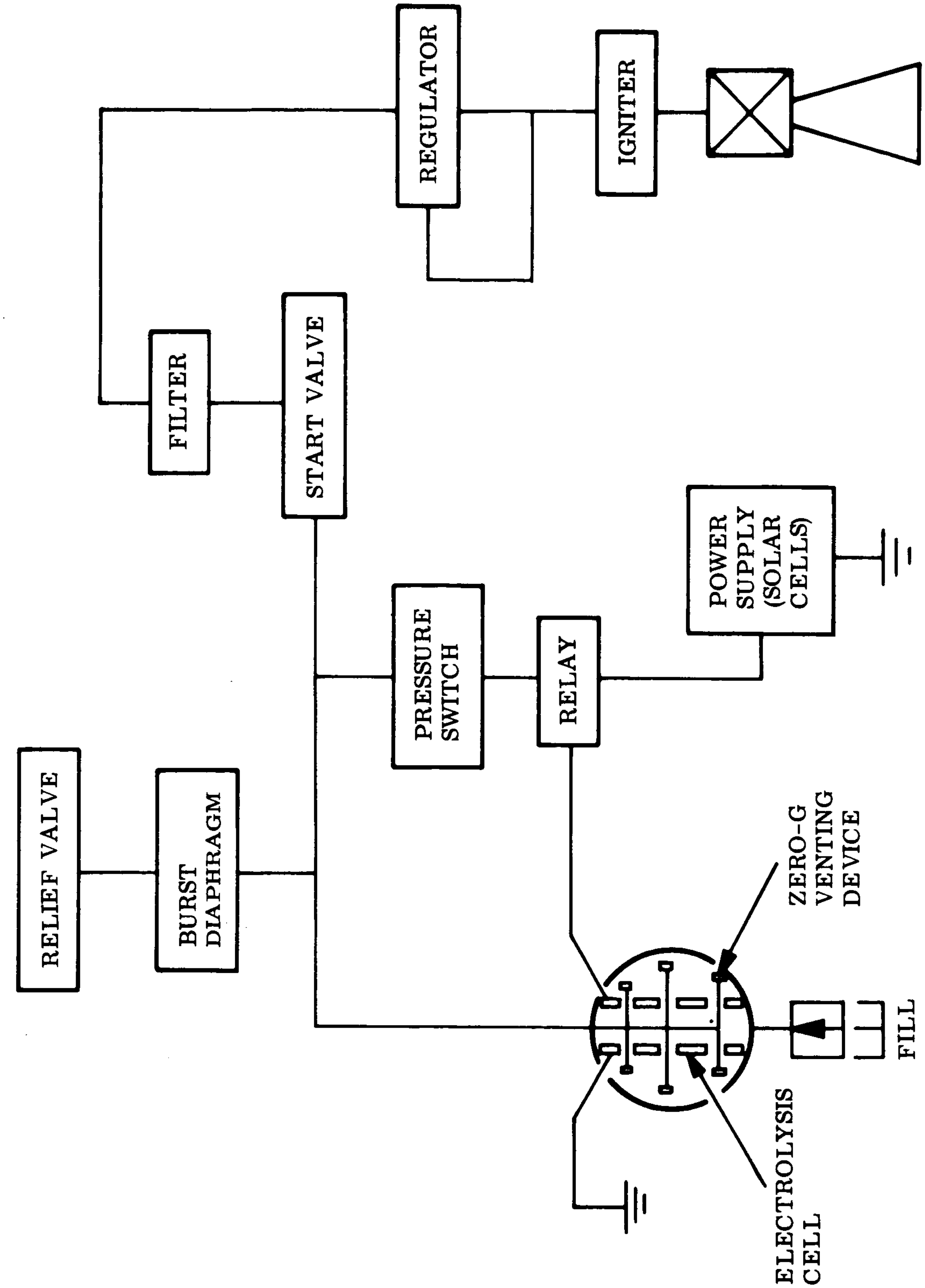

Fig. 2-4k Water Electrolysis System

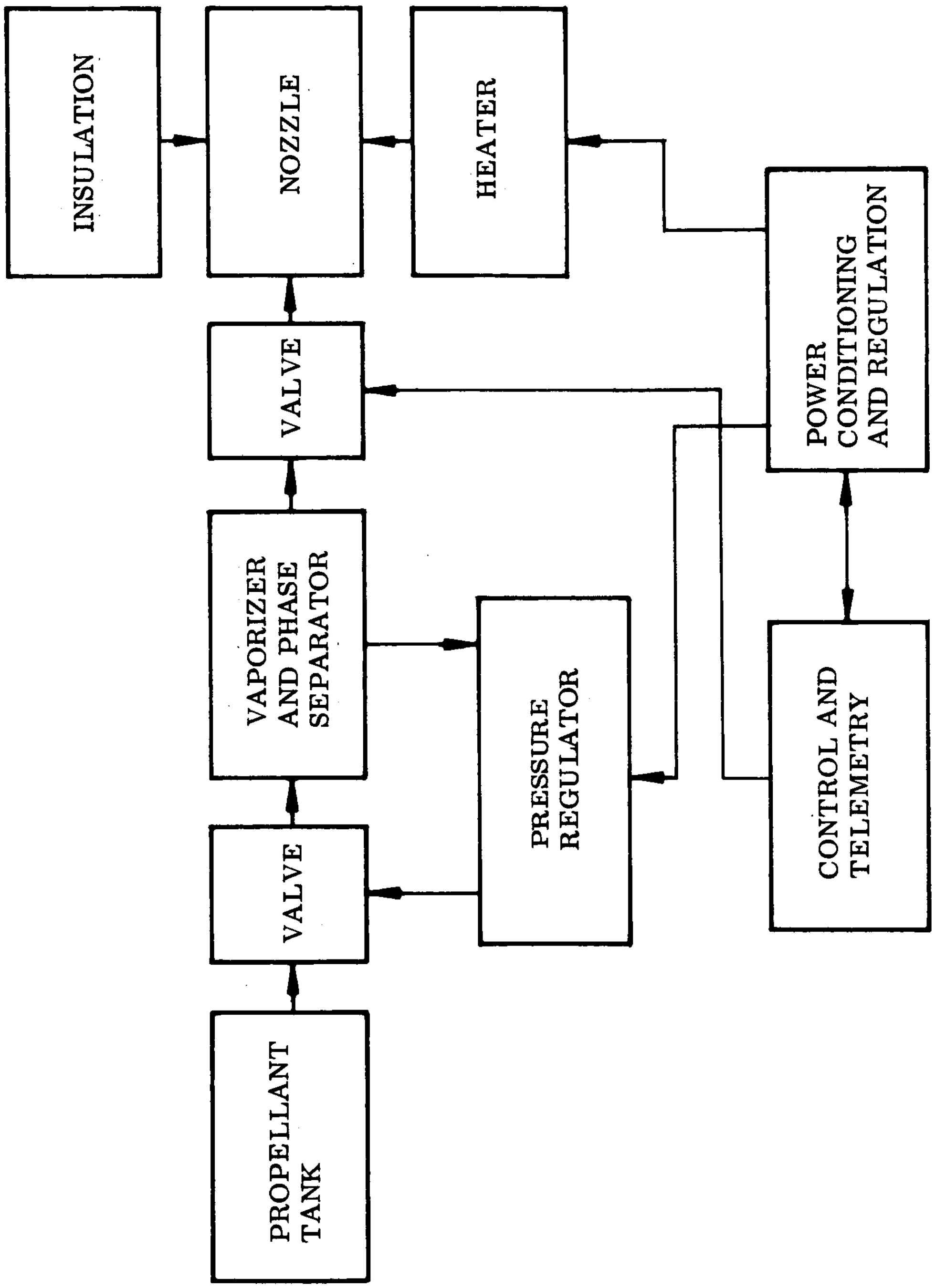

Fig. 2-41 Ammonia Resistojet

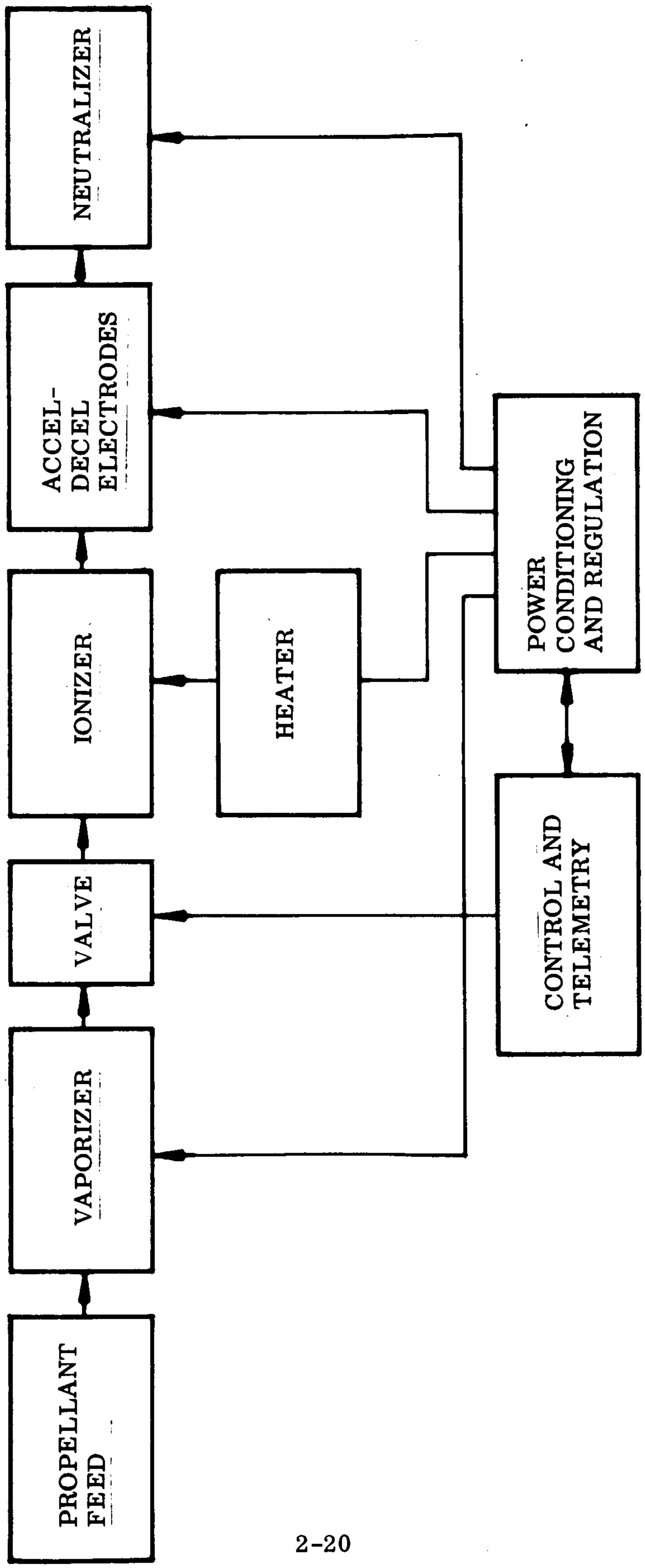

Fig. 2-4m Cesium Contact Ion Engine

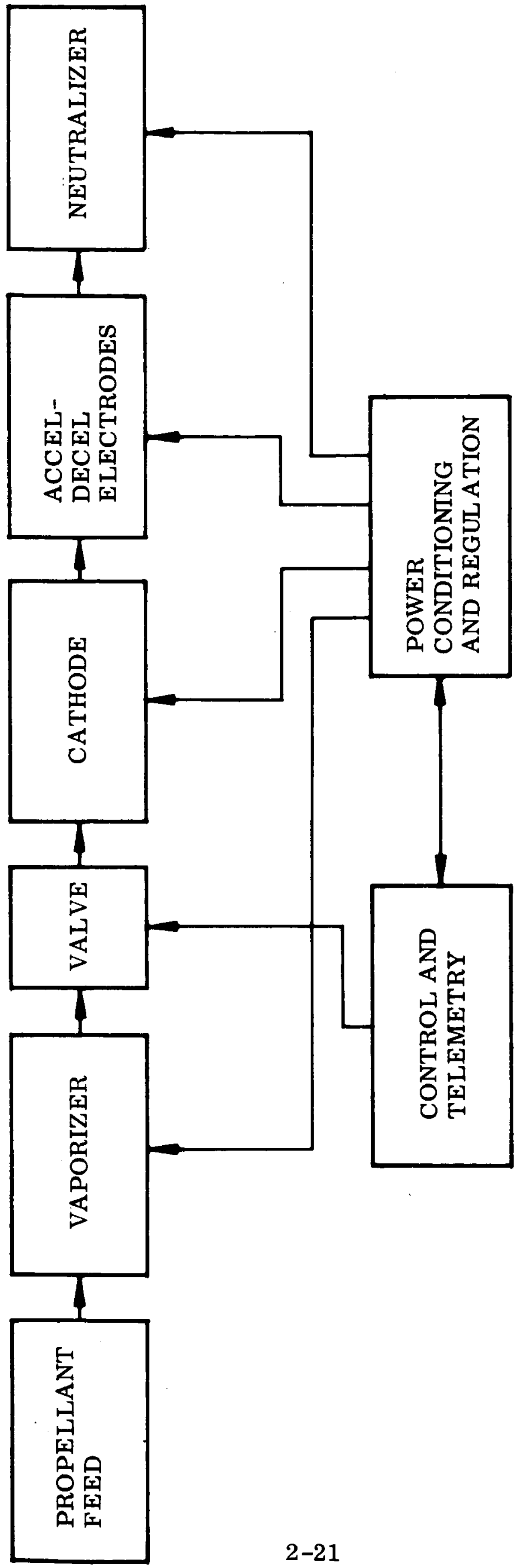

Fig. 2-4n Electron Bombardment Ion Engine

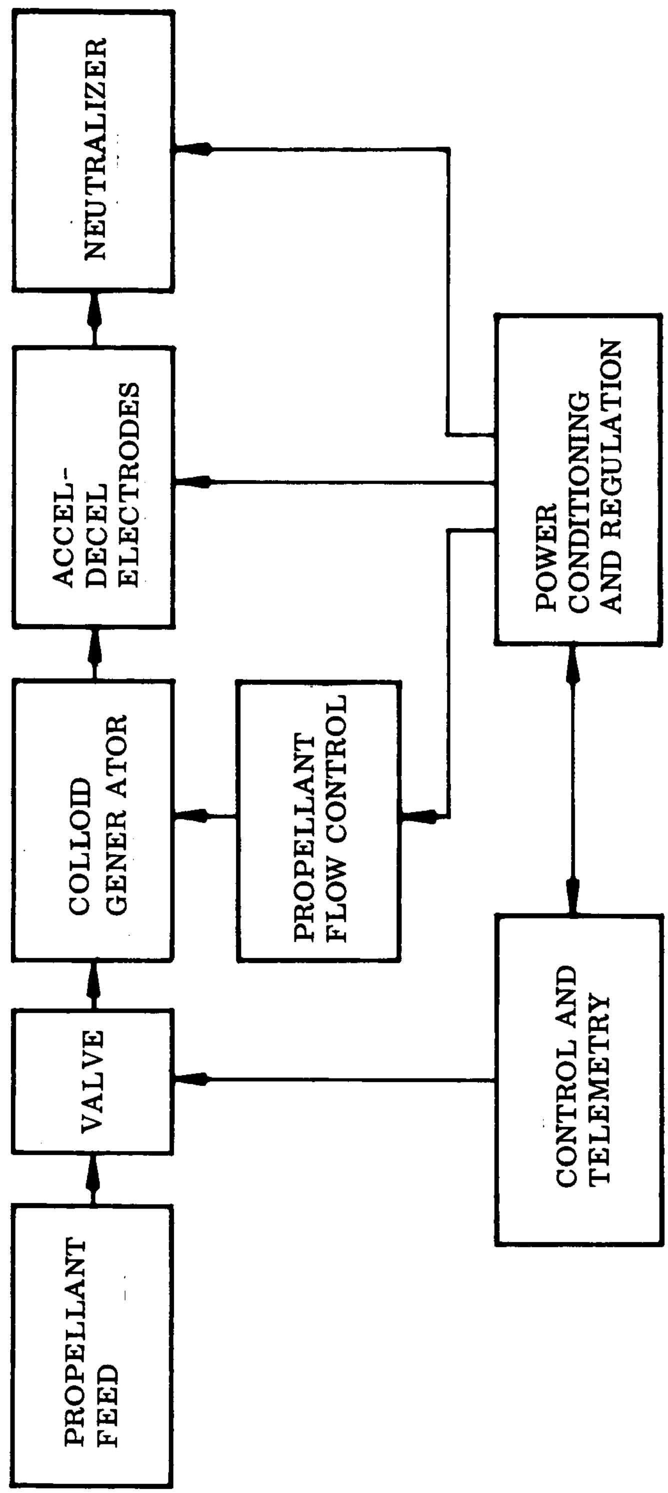

Fig. 2-40 Colloidal Ion Engine

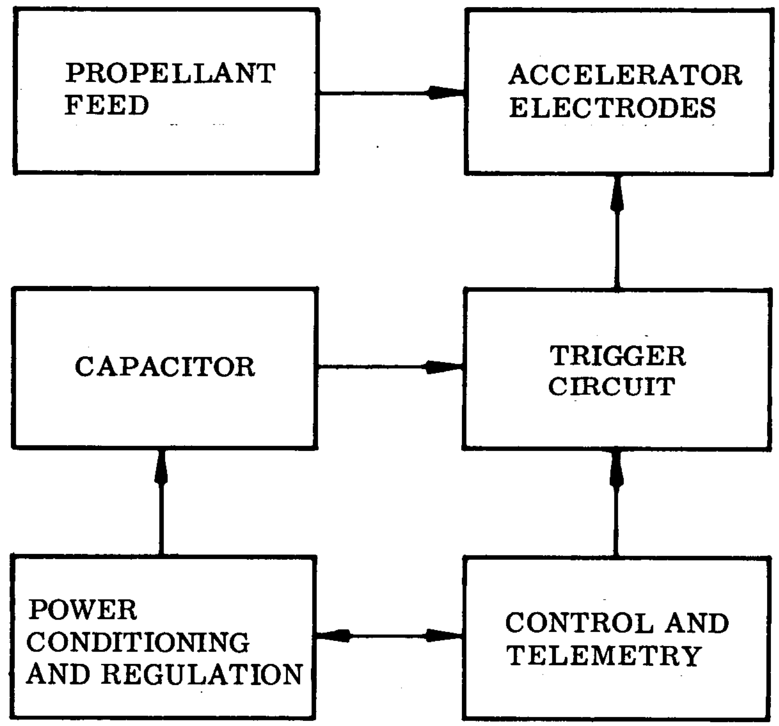

Fig. 2-4p Pulsed Plasma

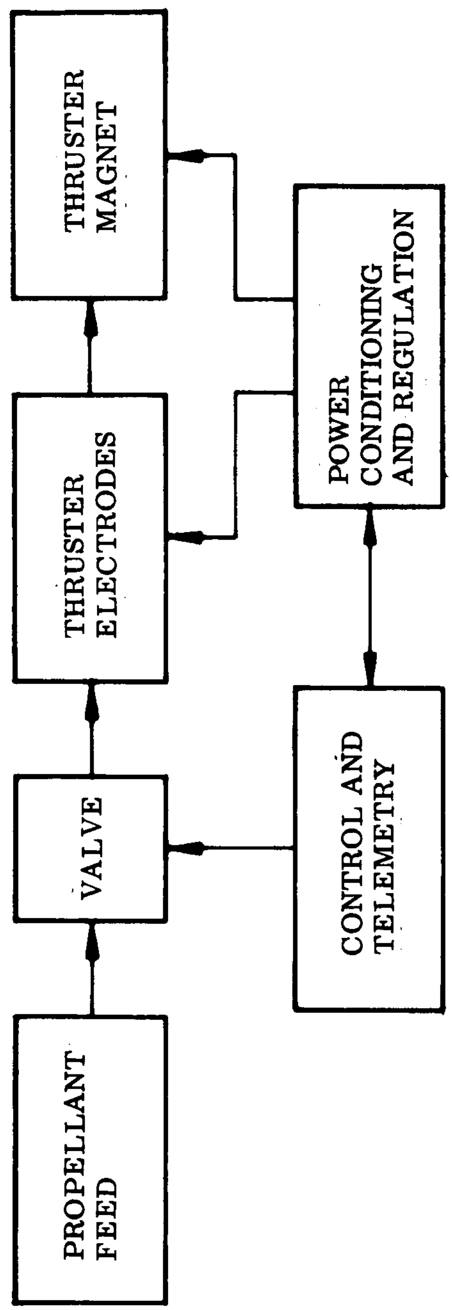

Fig. 2-4q Penning Discharge Thruster

compounds, in solid, liquid, or gaseous states. As such, no failure rate can be assigned to these in the accepted sense for the following reasons:

- Given the correct environmental conditions the probability that the desired chemical changes will not take place is almost zero.
- The usual failure rate format of "failures per million hours" does not apply since the propellant state is amorphous, and can only be judged by the performance of one or more batches.
- About the only weakness for propellants is that of trace impurities contamination, which presumably will be controlled rigorously during processing, and filling of the engine involved.

In the light of these statements the only recourse which is available during reliability analyses, is to assume that the propellant will be properly prepared, and assign to it a reliability percentage value very close to 100%, such as R = 99.999+ %. During the actual manufacture of a motor batch, testing should be performed to ensure that the test data acquired are valid for the several batches, and statistical manipulation of these data will confirm the validity of the percentage assumed, at some confidence level.

Plumbing lines are highly reliable devices, and the same technique of pre-assumption is applied to these devices. The assumption is made that these system elements will be properly tested by overpressure techniques, and maintained in the required state of cleanliness. Thus a reliability figure of merit may be similarly assigned to these system elements, and it is somewhat assured by the fact that plumbing lines have performed satisfactorily on many other programs.

Tanks are treated in a similar manner, with the exception that overpressure and burst pressure tests supply the required reliability data during the actual test and development programs. The assumption is made that tanks for these motors will be fabricated by techniques similar to those used for other tanks which have demonstrated adequate performance when designed to proper safety factors. Thus, the reliability figures of merit assigned are those to be expected of such devices.

For the several types of valves designed into the systems, definite generic data exist. The sources of these data are as follows:

- FARADA Manuals, U.S. Naval Labs, Corona, California
- Jet Propulsion Labs: Space Qualified valves reports (Sterer Publication)
- Sterer Valve Corp.: Test and Reliability data, precision valves.
- Moog Corp: Polaris A3 valve tests.
- Cadillac Gage: Polaris A3 valve tests.

Data for the valves envisioned for use by the design have been applied from these sources, dependent upon the class of valve, such as solenoid-operated, pyro-operated, pressure-operated, etc.

Where electronic components have been used as provisional choices for the design of the controllers in those motors requiring such, failure rates have been assigned from such sources as the Minuteman Program, since this joint Boeing/Autonetics listing accommodates only high reliability parts of proved performance, and is the most comprehensive list available in the USA at this time.

In order to apply the product rule to calculate the reliabilities of the several candidate systems, it was necessary to assume that the exponential law applied; that is to say that the failure of any one system element would be catastrophic in nature, and totally disable the system to the extent that the operation would cease. Such an assumption is not completely valid since the failure characteristics of many of the system components are of an attritive nature due to wear, and thus not exponential. Application of the Weibul mortality equations to devices whose failure characteristic is wear-out was not possible due to the insufficiency of data available. However the exponential method is valid for reliability estimates, if it is assumed that the valves for instance will operate at a cycle rate far less in total cycles than their design permits.

For purpose of calculation a mission time of one year on orbit was employed, and the values obtained for all systems using this period were then extrapolated to assess the reliability where two- and three-year missions might be involved. Extrapolations were made also for the years 1975 and 1980, to estimate the reliability growth of the systems. The assumption in this case was that failure rate of space and defense hardware has halved every 4-5 years. This is a warranted assumption based on the actual failure rate improvement of the total spectrum during the ten years since reliability was first inaugurated as a design discipline. Component reliabilities are listed in Appendix F.

2.2.3 Reliability Assignments

Table 2-6 sets forth the results of all the computations made. The results are expressed as Probability of Survival, P_S. Several conclusions become apparent immediately:

- Due to the similarity of the parts used in all of the systems the reliability values are very closely related.
- Based on the parts count, the systems having electronic controllers are somewhat lower in reliability value than those which do not.
- Computing the reliability values for the systems as they are presently provisionally configured does not by itself provide a valid tool for rating of systems.

2.3 OTHER CRITERIA

2.3.1 State of Development

The principal goal of the present program is to define development needs for solid and hybrid low-thrust systems in the post-1968 period. While most of the competitive systems may be in well-established states of development at present, this is not the case for many of the solid and hybrid systems. In effect then, the state of development could not be used as a criterion in ranking the systems, since by definition these solid and hybrid systems are under-developed.

Table 2-6

SYSTEMS RELIABILITY ESTIMATES

	Estimated P_S 1970 On Orbit for			Estimated P_S 1975 On Orbit for			Estimated P_S 1980 On Orbit for		
	1 Yr	2 Yrs	3 Yrs	1 Yr	2 Yrs	3 Yrs	1 Yr	2 Yrs	3 Yrs
Subliming Solid Reaction Control System	99.84	99.68	99.52	99.91	99.82	99.74	99.96	99.91	99.87
Superheated Subliming Solid System	99.64	99.28	98.92	99.82	99.65	99.48	99.90	99.81	99.73
Hybrid Hydrogen Monopropellant System	99.93	99.86	99.79	99.96	99.93	99.89	99.98	99.96	99.95
Repetitive Impulse Generator	99.95	99.90	99.85	99.95	99.91	99.86	99.98	99.95	99.93
Competitive Systems									
Cold Gas System[a]	99.87	99.74	99.61	99.91	99.82	99.74	99.95	99.91	99.87
Cold Gas System[b]	99.91	99.82	99.73	99.95	99.90	99.85	99.97	99.95	99.93
Vaporized Liquid Ammonia[a]	99.87	99.74	99.61	99.93	99.87	99.80	99.97	99.93	99.90
Vaporized Liquid Ammonia[b]	99.95	99.90	99.86	99.97	99.95	99.93	99.99	99.97	99.96
Monopropellant Hydrazine[a]	99.87	99.74	99.61	99.93	99.87	99.80	99.97	99.93	99.90
Monopropellant Hydrazine[b]	99.91	99.82	99.73	99.95	99.91	99.86	99.98	99.95	99.93
Monopropellant Cold Gas Generator[a]	99.82	99.64	99.46	99.91	99.82	99.73	99.95	99.91	99.86
Monopropellant Cold Gas Generator[b]	99.90	99.80	99.70	99.95	99.90	99.85	99.97	99.95	99.92
Bipropellant Vapor	99.75	99.49	99.24	99.87	99.74	99.62	99.94	99.87	99.81
Bipropellant Liquid[a]	99.67	99.34	99.01	99.83	99.67	99.50	99.92	99.83	99.75
Bipropellant Liquid[b]	99.79	99.58	99.37	99.89	99.79	99.68	99.95	99.89	99.84
Water Electrolysis System	99.90	99.80	99.70	99.95	99.90	99.85	99.97	99.95	99.92
Ammonia Resistojet	99.82	99.64	99.46	99.91	99.82	99.73	99.95	99.91	99.86
Cesium Contact Ion Engine	99.83	99.65	99.48	99.91	99.82	99.74	99.96	99.91	99.87
Electron Bombardment Ion Engine	99.82	99.65	99.47	99.91	99.82	99.73	99.95	99.91	99.87
Colloidal Ion Engine	99.82	99.63	99.45	99.91	99.81	99.73	99.95	99.91	99.86
Pulsed Plasma	99.86	99.71	99.57	99.93	99.85	99.78	99.96	99.93	99.89
Penning Discharge	99.63	99.27	98.90						
Gravity Gradient	>99.99	>99.99	>99.99						
Gyrostabilizers	98.07	96.17	–						
Magnetic Torques	>99.99	>99.99	>99.99						

(a) Lighter configuration
(b) More reliable configuration

Rationale: Appendix F.1.

2.3.2 Cost

The present cost of a system is not a valid criterion either, since this study is primarily concerned with the development of solid and hybrid systems in the post-1968 period. Production costs are not yet available for the advanced systems and future development costs are difficult to estimate. For those systems which are already well-established, previous experience has shown that unit costs are not directly comparable since the cost bases vary in an unknown way from company to company.

2.3.3 Producibility

It is also difficult to assign a quantitative value to the producibility of a system. Hence an objective comparison of systems on this basis is essentially impossible. The only facet of producibility which might permit comparison is production cost and, as stated in the previous paragraph, there is no way of defining these costs yet for the advanced solid and hybrid systems.

However, in the latter cases, producibility studies can serve a useful function by identifying potential production problems during development. Producibility of present solid and hybrid systems is discussed further in Section 3.3.4.

2.3.4 Minimum Pulse Bit

The lowest derived requirement for minimum pulse bit was approximately 0.01 lb-sec for the ATS-4 attitude control function. From Table 1-1, all systems meet this requirement.

It has been previously shown that propellant usage is directly related to minimum pulse bit in disturbed or undisturbed limit cycle operation (Ref. 1, Appendix C). However, in the present cases with fixed total impulse requirements, a system with smaller pulse bit must fire a greater number of times. There is therefore no advantage in selecting the system with minimum impulse bit unless a minimum pulse bit is required for some other reason, such as the minimization of disturbances.

2.4 LEADING CONTENDERS

Based on a comparison of the weight and reliability data described in Sections 2.1 and 2.2, charts were prepared to indicate the leading contenders for fulfillment of each mission requirement. The identification of these low-thrust systems is described in the following subsections. As stated earlier, no attempt is made to pinpoint a single system, but rather to select weight and reliability levels which the low-thrust systems must achieve in order to be competitive.

2.4.1 ATS-4

A diagram of system weight vs. "unreliability", i.e. one minus reliability, for the ATS-4 attitude control and slewing function is shown in Fig. 2-5. The lower left-hand portion of the diagram represents minimum weight and maximum reliability.

Three major groupings are evident. The outermost includes pressurized cold gas, gyros* and the hybrid hydrogen system. A central band includes the majority of the systems. The leading contenders are ion engines and bipropellant vapor.

A similar situation prevails for ATS-4 east-west station-keeping (Fig. 2-6). The outer band contains pressurized cold gas, Penning discharge and the hybrid hydrogen monopropellant systems among others. Two systems can be identified as leaders – the colloid ion engine, and water electrolysis.

The ATS-4 north-south station-keeping function diagram is given in Fig. 2-7. Three groupings are again evident. Three systems – water electrolysis, monopropellant hydrazine and the Repetitive Impulse Generator – appear in leading roles.

System weights and reliabilities for final acquisition of the synchronous orbit by ATS-4 are shown in Figure 2-8. Due to the relatively short mission period of one

*Four gyros are equivalent to 6 other system motors in this application.

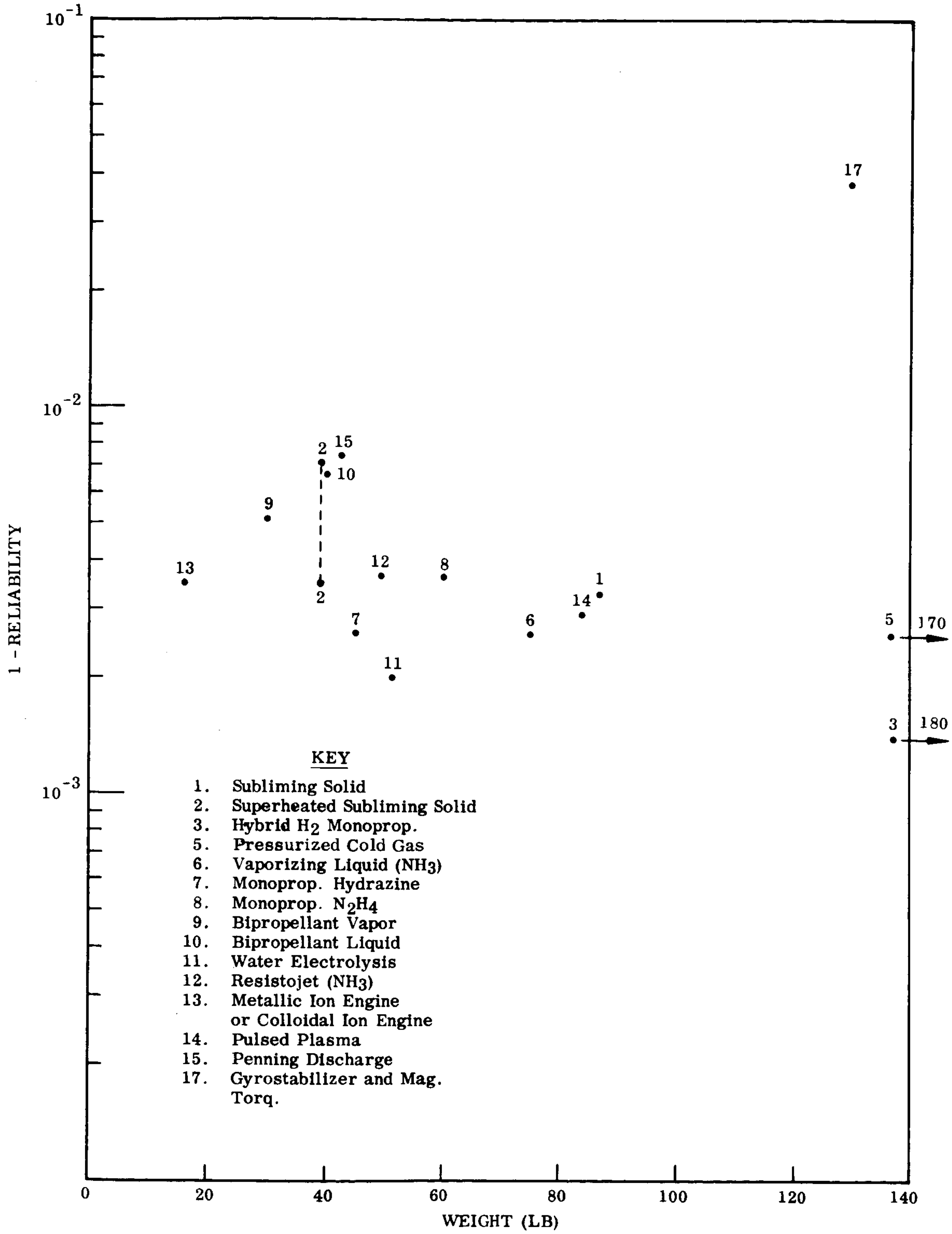

Fig. 2-5 ATS-4 Attitude Control and Slewing Weight Reliability Diagram

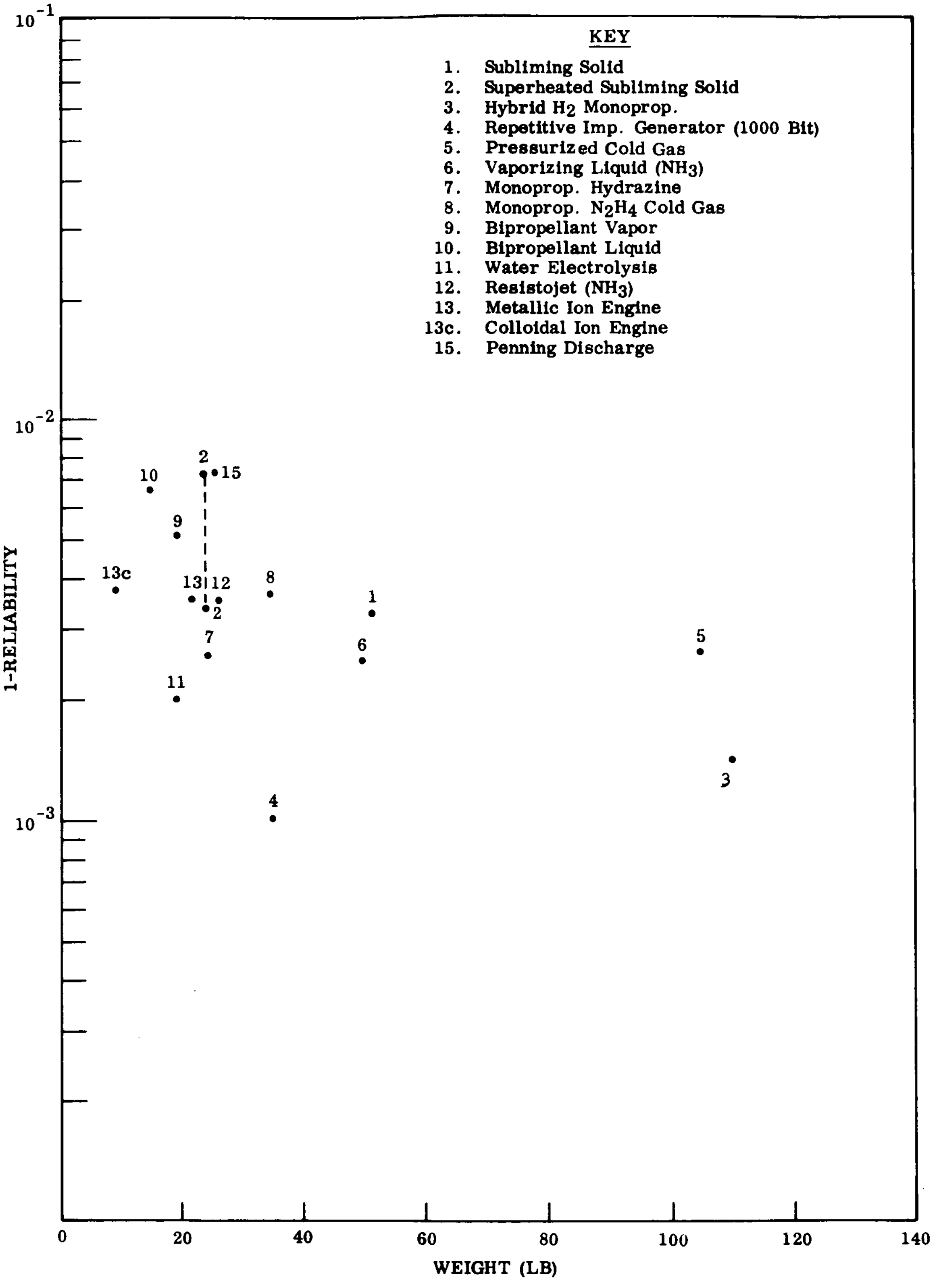

Fig. 2-6 ATS-4 East-West Station Keeping Weight Reliability Diagram

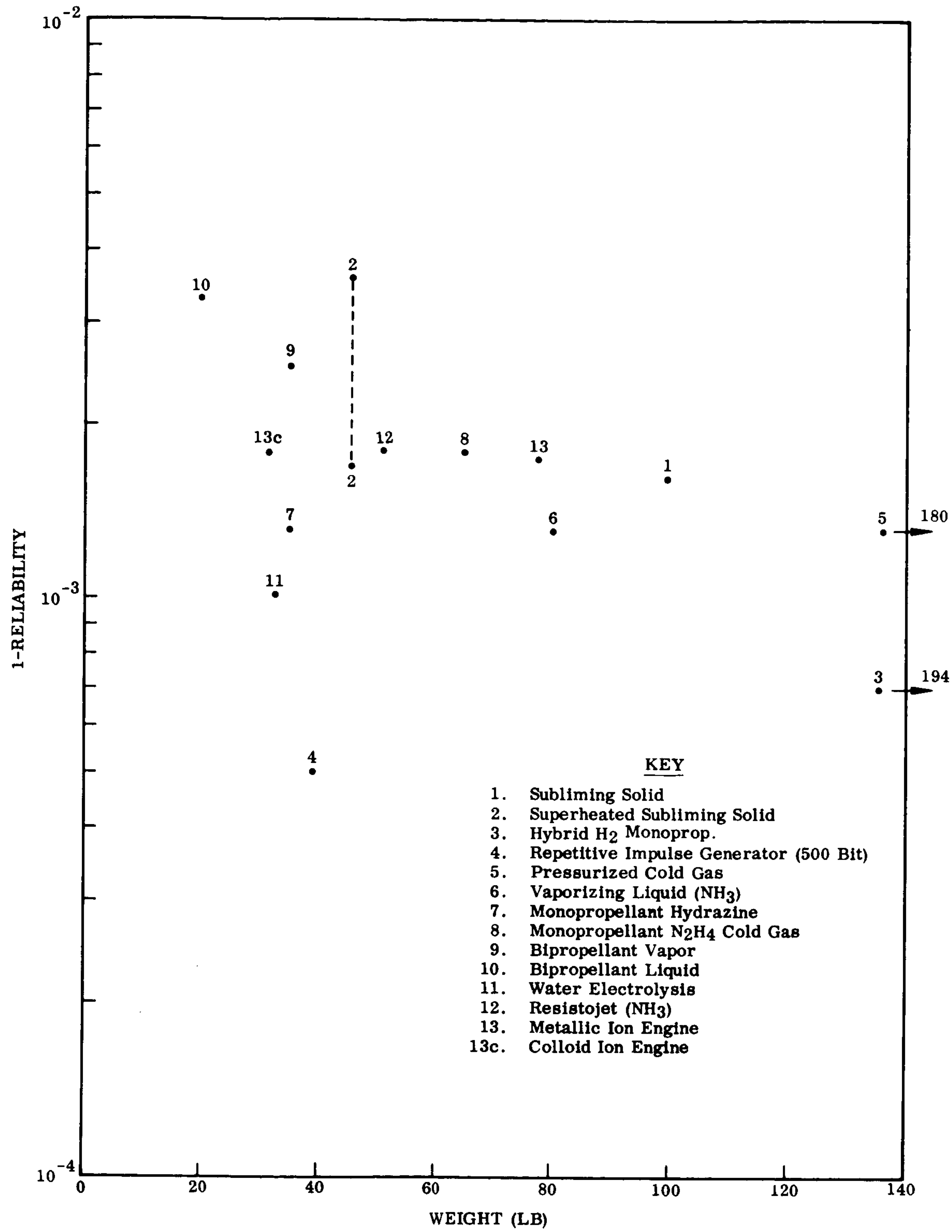

Fig. 2-7 ATS-4 North-South Station Keeping Weight-Reliability Diagram

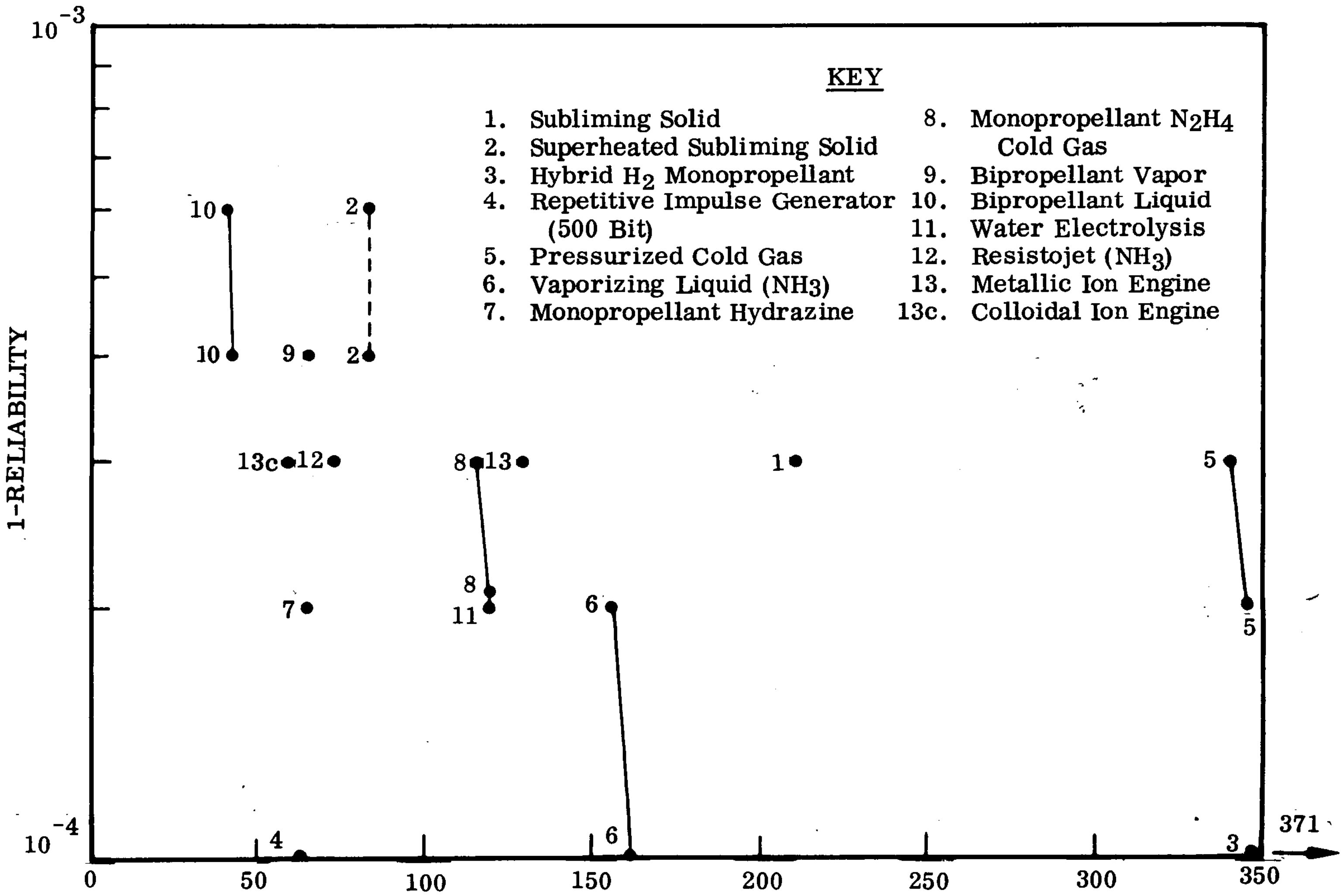

Fig. 2-8 ATS-4 Station Acquisition Weight-Reliability Diagram

week, most of the reliabilities are closely clustered. Greater emphasis must therefore be placed on the weights, and the bipropellant liquid system is clearly ahead in this respect. Several systems, including the colloid ion engine and Repetitive Impulse Generator, are closely grouped at higher weight and reliability. (Tie lines connect the lightest and more reliable configurations of certain systems).

2.4.2 Voyager

The Voyager attitude control weight-reliability relationships are shown in Fig. 2-9. For this application the gyro* and subliming solid systems are much too heavy, due to the relatively high thrust level (0.02 lbf). The remaining systems weigh less than 30 lb. The 20–30 lb range includes the hybrid, pressurized cold gas, and water electrolysis systems. Others are grouped closely in a central band, except for the leaders – monopropellant hydrazine and the bipropellant systems.

For relatively short periods of operation, as in the Voyager evasive maneuver, reliability values could not provide useful comparisons between systems. A basic assumption in the reliability estimate was that all motors fire initially. After firing, the reliability figure decreases exponentially with lengthening period of operation. Values in Table 2-6 are sufficiently close even after one year to indicate insignificant differences for periods of a few days. The weights cited in Tables 2-1 through 2-4 indicate that the closely-grouped leading contenders for the Voyager evasive maneuver are the pressurized cold gas, monopropellant hydrazine and subliming solid systems.

2.4.3 ATM

Contenders for the ATM attitude control and slewing function are shown in Fig. 2-10. The hybrid, pressurized cold gas and subliming solid systems form an outer band. The remaining systems are relatively closely grouped. The lightest system, on an equivalent number of units basis*, is the gyro-stabilizer plus the magnetic torque

*Three gyros are equivalent to 6 other system motors in this application.

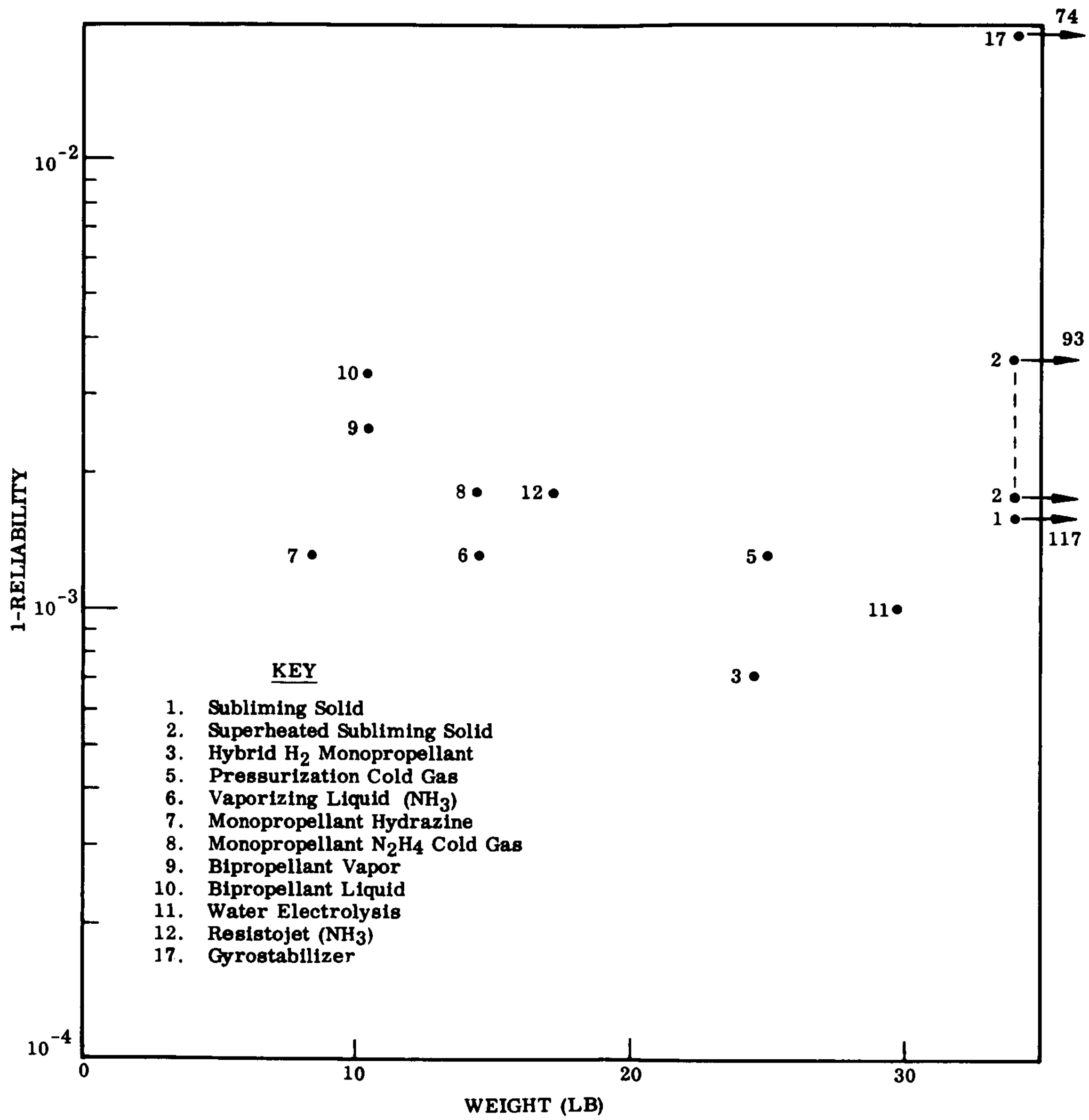

Fig. 2-9 Voyager Attitude Control and Slewing Weight-Reliability Diagram

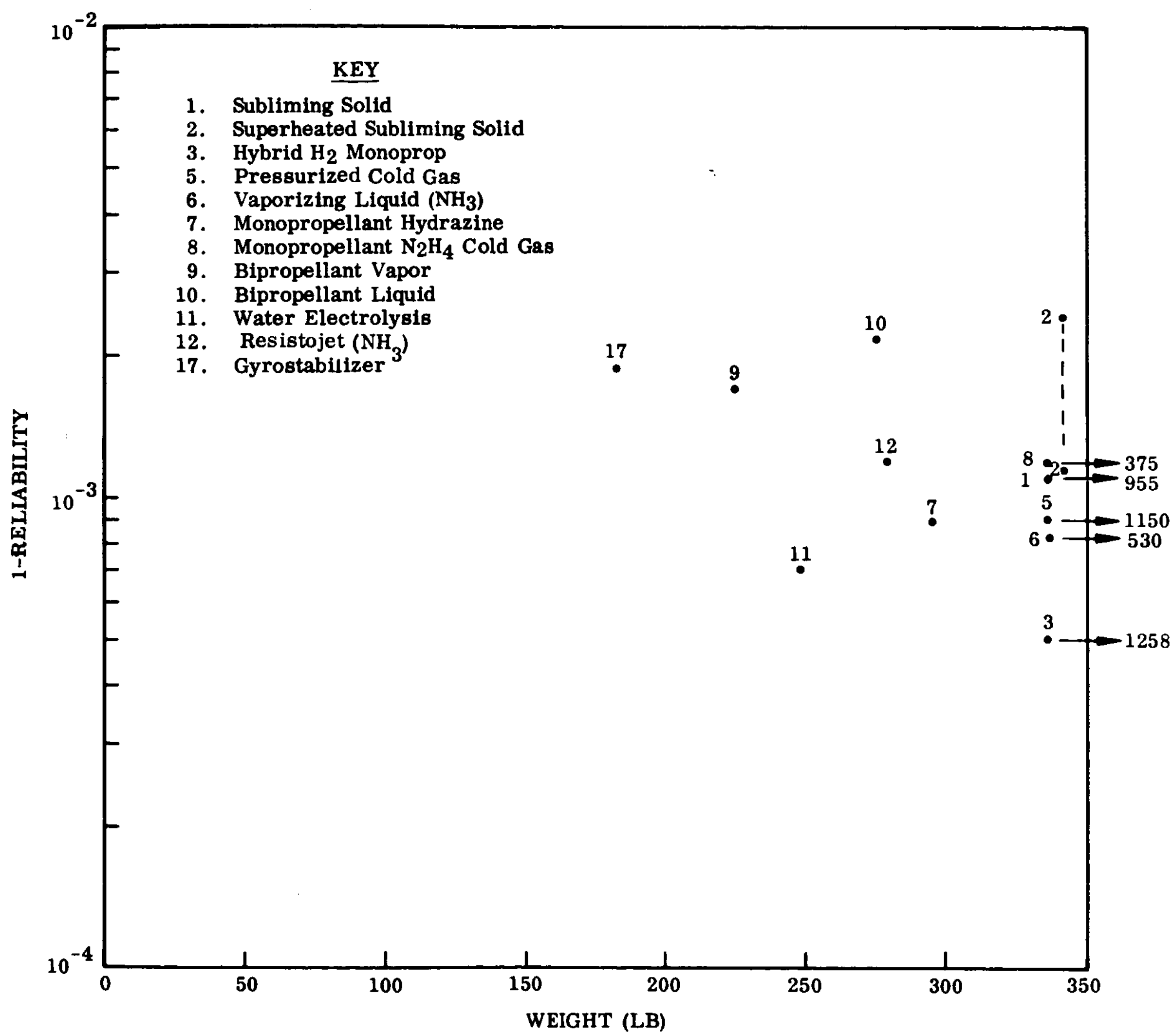

Fig. 2-10 ATM Attitude Control and Slewing Weight-Reliability Diagram

system for discharging momentum. The bipropellant vapor and water electrolysis systems are somewhat heavier, but more reliable.

If gyrostabilizers are used, excess momentum must be removed. The contending momentum discharge systems are displayed in Fig. 2-11. The outermost band contains the hybrid, pressurized cold gas, and subliming solid systems. The remaining systems, except for the magnetic torque systems and ion engines, are grouped closely. The magnetic torque system, with a considerable reliability edge, is in the lead.

2.4.4 EVA

Because of the brief period of operation for extravehicular activities (EVA)*, significant reliability differences between systems were not apparent. From the data in Figs. 2-2 and 2-3 and Table 2-3, the lightest systems were bipropellant vapor and liquid, and monopropellant hydrazine.

2.4.5 Summary of Weight-Reliability Data

A summary of weight and reliability data for the leading contenders and for the solid and hybrid systems is given in Table 2-7. This comparison is discussed further in Section 3.

---

*Assumption: 1000 impulse bits delivered over 2500 seconds.

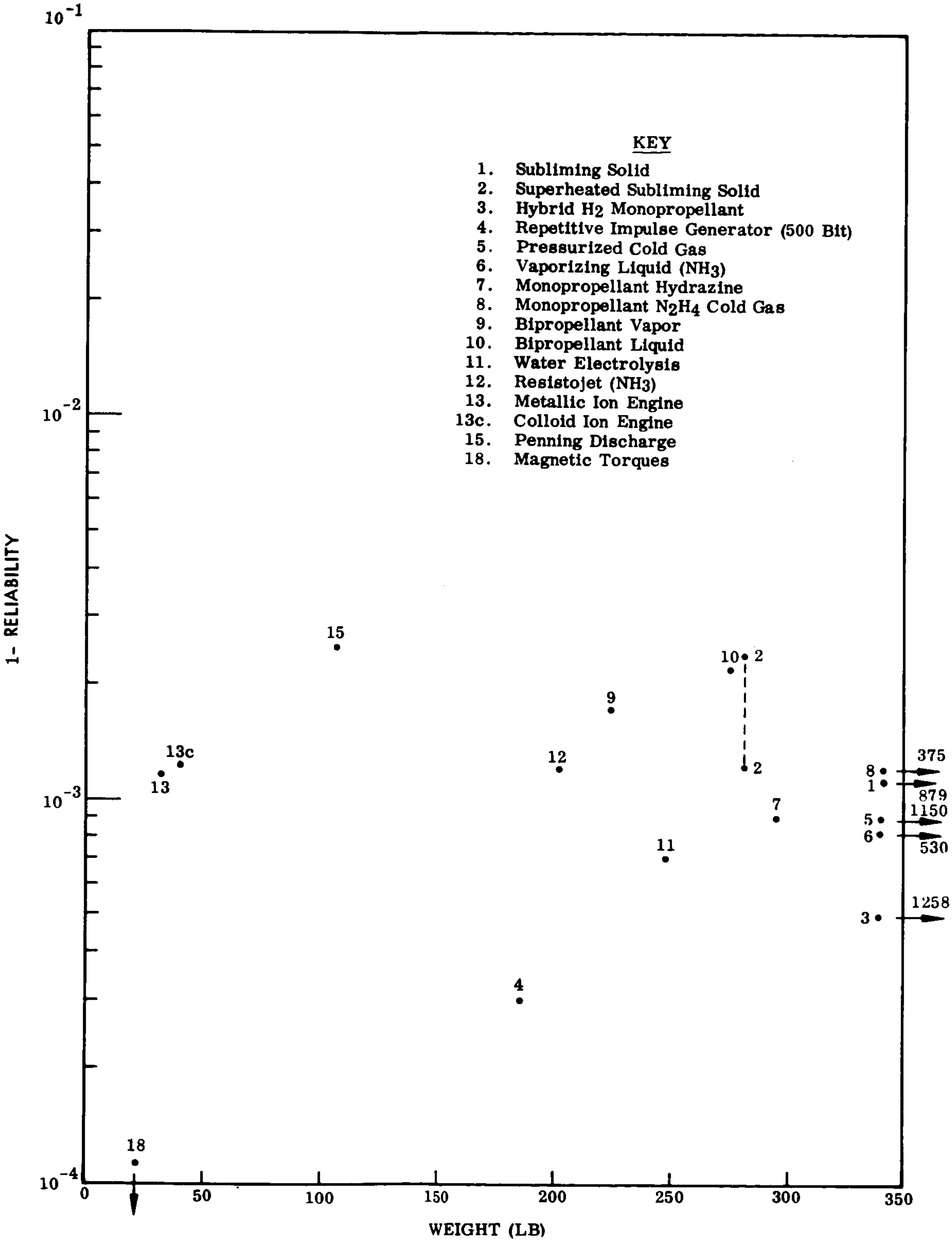

Fig. 2-11 ATM Momentum Discharge Weight-Reliability Diagram

Table 2-7

RELIABILITY AND WEIGHT DATA

Mission Requirements	Criterion	Leading Contenders			Solid and Hybrid Systems: Subliming Solid	Solid and Hybrid Systems: ∅ Superheated Subl. Solid	Solid and Hybrid Systems: Hybrid H_2 Monoprop.	Solid and Hybrid Systems: Repetitive Imp. Gen.
ATS-4 Attitude Control and Slewing		Ion Engines	Bipropellant Vapor					
	Reliability Weight (lb)	.9963 – .9965 16.3 - 16.2	.9949 30		.9968 87.8	.9928 - .9967 39.5	.9986 180	**
ATS-4 E-W Station-Keeping		Colloidal Ion Engine	Water Electrolysis					
	Reliability Weight (lb)	.9963 8.8	.9980 19.7		.9968 51.7	.9928 - .9967 24.7	.9986 109	.999 35
ATS-4 N-S Station-Keeping		Water Electrolysis	Monopropellant Hydrazine	Rep. Impulse Generator				
	Reliability Weight (lb)	.9990 32.3	.9987 35	.9995 39	.9984 99.8	.9964 - .9983 44.8	.9993 194	.9995 39
ATS-4 Station Acquisition		Bipropellant Liquid	Colloidal Ion Engine	Rep. Impulse Generator				
	Reliability Weight (lb)	.9994 - .9996 40 - 42*	.9997 58	.9999 63	.9997 210	.9994 - .9996 83.3	.9999 371	.9999 63
Voyager Attitude Control and Slewing		Monopropellant Hydrazine	Bipropellant Vapor	Bipropellant Liquid				
	Reliability Weight (lb)	.9987 8.5	.9975 10.5	.9967 10.5	.9984 117	.9964 - .9983 92.8	.9993 24.5	**
Voyager Evasive Maneuver***		Press. Cold Gas	Monopropellant Hydrazine	Subliming Solid				
	Weight (lb)	3.3	4	5.4	5.4	9.1	**	**
ATM Attitude Control and Slewing		Gyro + Mag. Torque	Bipropellant Vapor	Water Electrolysis				
	Reliability Weight (lb)	.9981 182****	.9983 225	.9993 248	.9989 955	.9976 - .9988 343	.9995 1258	**
ATM Momentum Discharge		Magnetic Torque	Ion Engine	Colloidal Ion Engine				
	Reliability Weight (lb)	.9999 22	.9989 32.3	.9988 39.9	.9989 879	.9976 - .9988 281	.9995 1258	.9997 187
EVA***		Bipropellant Vapor	Bipropellant Liquid	Monopropellant Hydrazine				
	Weight (lb)	12	13	16	**	**	90	32

* Lightest and most reliable configurations. ∅ Range due to uncertainty in undeveloped superheater reliability. See F.2.2
**System eliminated earlier.
***Mission too brief for significant reliability differences.
****Basis: Equivalent weight based on 3 gyros = 6 motors.

Section 3
DEFINITION OF DEVELOPMENT NEEDS

3.1 SOLID-HYBRID DEFICIENCIES AND PROBLEM AREAS

The solid and hybrid systems presently available are known to be capable of fulfilling functions such as satellite inversion and spin rate correction. However, many of the mission requirements selected in this study involve somewhat higher total impulses or thrust levels, and for these requirements the solid systems are relatively heavy due to propellant and/or power supply weight. The only hybrid, the hydrogen monopropellant system, was proposed for a different application, and suffers from a low mass fraction.

Examination of Figs. 2-5 through 2-11 reveals that, at present, the solid LTRCS systems are competitive in a few cases. The subliming solid system would be a good choice for the Voyager evasive maneuver. Also, the Repetitive Impulse Generator is among the leaders in performing ATS-4 North-South station-keeping and station acquisition functions. However, in general, a satisfactory combination of weight and reliability is not achieved, and considerable improvement in these parameters is desirable. For example, the superheated subliming solid system is relatively low in weight and reliability, while the hybrid hydrogen monopropellant system is relatively high in reliability and weight. The subliming solid system occupies a position intermediate between these extremes.

An analysis, based on Table 2-7, of individual deficiencies and problem areas follows.

3.1.1 ATS-4

To reach a competitive level for ATS-4 attitude control and slewing, the weight of the subliming solid system must be reduced from 88 to about 16 lb., at the same reliability value. From Table 2-1, this weight reduction is more than the entire present propellant weight. Therefore the propellant specific impulse must be increased and the system fixed weight reduced. Since this is a "cold" system, the best opportunity for increasing specific impulse centers on reducing molecular weight of the effluent gas. The container and hardware weight can be reduced roughly in 1:1 correspondence to propellant weight. The specific impulse would have to rise to 580 lbf-sec/lbm to provide a 72-lb weight reduction. This precludes further consideration.

The superheated system would have to be reduced 23 lb in weight with some increase in reliability to compete with the colloid ion engine, or reduced 9.5 lb in weight at about the same reliability to match bipropellant vapor. A third alternative would be to increase the reliability 0.006 at the same weight. The first alternative is impossible since a specific impulse of 1000 lbf-sec/lbm would be required. The second alternative requires a specific impulse of 294 lbf-sec/lbm, a value which would require a temperature of 4100° F in the present system. If weight is not critical, the increase in reliability of 0.006 would require considerable improvement in the Control/Electrical Subsystem.

A weight reduction to at least 30 lb would be required of the hybrid hydrogen monopropellant system. This system has a very low fixed weight, as shown in Fig. 2-2. Therefore, reduction of hardware weight holds little promise. The effective specific impulse is quite low (28 lbf-sec/lbm from Fig. 2-2), so there may be room for improvement here. To attain a weight of 30 lb, an effective specific impulse of 167 lbf-sec/lbm is needed. Since this is primarily a cold gas system, this could not be accomplished by increasing the temperature. The only alternative is to substitute a hydrogen-producing reaction with a higher mass fraction of gaseous products. The present reaction:

$$LiBH_4 + 2H_2O \rightarrow LiBO_2 + 4H_2$$

has a gaseous mass-fraction of 13.85 percent. But other conceivable hybrid-type reactions, e.g.

$$LiH + H_2O \rightarrow LiOH + H_2 \qquad (H_2/\text{total} = 7.7\%)$$

have even lower values. Unless a suitable alternate reaction can be uncovered, there seems little chance for this system to be competitive.

To contend for the ATS-4 East-West station-keeping function, the weight of the subliming solid system must be reduced from 52 to at least 19 lb, with a small reliability increase. To obtain the weight decrease of 33 lb in propellant, container, and hardware would require an increase in specific impulse to 215 lbf-sec/lbm. This must be accomplished primarily by reduction of molecular weight of effluent gas, and not by temperature increase, since the effective operating temperature of this system is low. The molecular weight must be 3.6 or less. Only hydrogen meets this requirement and cryogenic storage does not appear feasible for a 2-yr mission.

The superheated system must be reduced 16 lb in weight and increased 0.003 in reliability to compete with the colloid ion engine, or reduced 5 lb in weight and increased 0.005 in reliability to compare well with water electrolysis. The first alternate is impossible since the fixed weight is greater than this. The second alternative requires a specific impulse of 315 lbf-sec/lbm and is also discarded.

The hybrid hydrogen monopropellant system requires reduction from 109 to 20 lb. This would require a new reaction as stated earlier.

The Repetitive Impulse Generator is sufficiently reliable at present, but would require reduction of weight from 35 to 20 lb. Since the assumed propellant specific impulse of 190 lbf-sec/lbm is already pushing the state-of-the-art for this type propellant, the weight reduction must come from system design. One modification mentioned in Section 2.1.1 would exhaust each tiny motor from individual nozzles and thereby save up to 14 lb.

The ATS-4 North-South station-keeping function requires a reduction in subliming solid weight from 100 to about 35 lb, with an increase in reliability of 0.001. While the reliability increase might be readily achieved, the weight reduction would require a specific impulse of 255 lbf-sec/lbm, and is not feasible for previously stated reasons.

The superheated subliming solid system requires a reliability increase of about 0.0035 and weight reduction of about 9 lb. The former requires improvement in the control and electric subsystem, but the specific impulse would have to be almost 280 lbf-sec/lbm. The system cannot be considered for this application.

The hybrid hydrogen system has more than sufficient reliability for ATS-4 North-South station-keeping, but weight reduction from 194 to about 35 lb would be needed. This appears formidable, and would require a new hydrogen-generating reaction with an effective specific impulse of 155 lbf-sec/lbm.

The Repetitive Impulse Generator is competitive for the North-South station-keeping function. Although reliability is superior to the other leaders, some further weight reduction appears desirable. In this case, individual motor exhausts may save up to 7 lb.

For ATS-4 station acquisition, subliming solid weight would have to be reduced from 210 to about 45 lb. The latter corresponds to a specific impulse of 445 lbf-sec/lbm, and the system therefore holds no promise for this application.

The superheated system requires a weight reduction from 83 to 45 lb, at slightly improved reliability. While the latter may be potentially accomplished by improvement of the thermal, electrical and control sub-systems, the weight reduction requires a specific impulse of 475 lbf-sec/lbm.

The hybrid hydrogen generator weight of 371 lb is prohibitively high and would require reduction to at least 65 lb. As stated earlier, no reaction is known to provide hydrogen at higher mass fraction.

Already competitive with the colloidal ion engine for ATS-4 station acquisition, the Repetitive Impulse Generator has a considerable edge over bipropellant systems in reliability. The weight of the Repetitive Impulse Generator must be reduced 21 lb, however, to match the bipropellant liquid system in weight.

3.1.2 Voyager

Voyager attitude control and slewing function must be performed at a minimum thrust level of 0.02 lbf. This thrust level is above the normal operating range of the subliming solid systems, and places prohibitive demands on the power supplies for both the low-temperature and superheated subliming solid systems. The weights of the solar cells alone exceed the competitive system weights in each case. The only way to overcome this disadvantage is to substitute a propellant with appreciably lower heat of vaporization. In general, however, the molecular weight of the gas increases as the heat of vaporization decreases.

The required total impulse is sufficiently low that the hybrid hydrogen system could be considered if a hydrogen-generating reaction of high mass fraction can be found. Until then, the weight penalty (24.5 lb vs 9 lb) is too great.

For the Voyager evasive maneuver, the subliming solid system is already among the leading contenders. The superheated system is not, nor can it be since the solar cells alone weigh twice as much as the total weight of the leaders.

3.1.3 ATM

The subliming solid system is considerably overweight in meeting the requirements for ATM attitude control and slewing. The weight must be reduced from 955 to 200 lb, or a reduction of 755 lb. This is almost as much as the system weight exclusive of solar cells (Table 2-1), and therefore the system cannot be made competitive unless a new propellant is found with higher specific impulse and lower heat of vaporization.

The weight of the superheated system is more favorable, but, even here, the weight reductions required are relatively large. For example, to be competitive with the gyrostabilizer the weight must be lowered by 161 lb and the reliability increased by 0.001. To be competitive with bipropellant vapor, the weight must be reduced by 118 lb and the reliability increased by 0.001. The first alternative requires a specific impulse of 445 lbf-sec/lbm; the second requires 330 lbf-sec/lbm. Again, it is necessary to both reduce the power requirements as well as to increase the specific impulse.

The hybrid system must be reduced from 1258 to about 200 lb. As indicated earlier, a new reaction of high mass fraction is required before this system could compete effectively.

The ATM momentum discharge function is performed quite effectively by the magnetic torque system. The indicated reliability is so high and the weight so low that neither the subliming solid nor the hybrid systems can be competitive. The Repetitive Impulse Generator requires a decrease from 187 to 22 lb, with a reliability increase from 0.9997 to > 0.9999. This weight saving would require a specific impulse of 4160 lbf-sec/lbm, an impossibly high requirement.

3.1.4 EVA

Only one solid and one hybrid system remains in contention for Extra-Vehicular Activities after the preliminary screening. The hybrid hydrogen generator required a weight reduction from 90 lb to approximately 13 lb. As previously, this in turn required a new hydrogen-producing reaction of high mass fraction.

The Repetitive Impulse Generator weight must be reduced from 32 to about 13 lb. As indicated earlier, the use of individual nozzles instead of exhausting through a common chamber could eliminate the "knee" in the curve and reduce weight up to 14 lb.

3.2 DEVELOPMENT NEEDS

As described in Section 3.1, many of the mission requirements developed in Phase I involve higher total impulses or thrust levels than those which are optimum for present solid and hybrid systems. This may be regarded as both a challenge for the existing systems to meet and an invitation to develop new systems of greater capability.

3.2.1 Phase I Mission Requirements

The low-temperature subliming solid system is basically limited in weight reduction by characteristically low specific impulses and relatively high heats of vaporization. Low specific impulse leads to high propellant weight for a given mission, while high vaporization heat requires large power supply weights. For a given impulse requirement, small weight reductions can be made by selection of a propellant operating at higher temperature or lower specific heat ratio. However, the specific impulse varies only as the square root of absolute temperature, and relatively high temperatures are required to make significant gains in specific impulse. (This is the basis for the superheated system discussed below and one of the advanced concepts discussed in Section 3.4). The only variables left to the system designer are molecular weight and heat of vaporization, which tend to offset each other. With respect to the Phase I mission requirements, no improvements on present propellants will make the low-temperature subliming solid system competitive, except for the Voyager evasive maneuver.

The superheated subliming solid system makes use of high temperature (~ 2000° F) to increase the specific impulse. This temperature is limited by the properties of presently available heater materials. Hence the parameters available to the system designer for weight reduction are again molecular weight and heat of vaporization. Reliability estimates are relatively uncertain at present, due to the superheater. If equivalence to the resistojet can be claimed, competitive position is considerably improved. The superheated system is not presently competitive for any of the Phase I requirements. It can only be made competitive by discovery of a new propellant with lower molecular weight and lower heat of vaporization, and by some reliability improvement.

The only hybrid system (hydrogen monopropellant) is not competitive in any of the applications. In general, its reliability is quite favorable, but the weight is prohibitive. The latter objection can be overcome by substitution of a hydrogen-producing reaction with considerably higher mass fraction.

The Repetitive Impulse Generator is presently competitive for performing ATS-4 north-south station-keeping and station acquisition functions. Some weight reduction would be desirable. Since the specific impulse of 190 lbf-sec/lbm is pushing the foreseeable state-of-the-art, little improvement is likely from this source. Gains will have to be made by improved motor designs, which reduce heat loss and thereby raise the effective specific impulse.

3.2.2 Generalized Requirements

Solid/hybrid LTRCS can be competitive in reliability but suffer a weight disadvantage. The disadvantage to solid and hybrid low-thrust systems of high total impulse and high thrust levels is obvious from the preceding section. That solid and hybrid systems are not always at such a competitive disadvantage is evident from a consideration of lower thrust level — lower total impulse missions.

A hypothetical mission was considered which required only 100 lb-sec of impulse to be delivered at 10^{-4} lbf. The results of a weight comparison are shown in Table 3-1. Many systems are closely clustered at the low end of the scale. Five systems, including the hybrid hydrogen monopropellant system, are in the 4–5 lb group, while three more systems, including the Repetitive Impulse Generator and subliming solid systems, are in the 5–6 lb group. Hence, all the solid and hybrid systems, except the superheated subliming solid system are competitive for this type of mission.

Table 3-1

HYPOTHETICAL LOW-THRUST LOW-IMPULSE MISSION

Basis: $F = 1 \times 10^{-4}$ lbf

$I_T = 1 \times 10^{2}$ lbf-sec

One Nozzle

System	wt, lb
Subliming Solid	5.8
Superheated Subliming Solid	9.1
Hybrid H_2 Monopropellant	4.2
Repetitive Impulse Generator (500 bit)	5.5
Pressurized Cold Gas	5.5
Vaporizing Liquid (NH_3)	7.3
Monopropellent Hydrazine	4.3
Monopropellant N_2H_4 Cold Gas	10.5
Bipropellant Liquid	7.3
Bipropellant Vapor	8.5
Water Electrolysis	4.2
Resistojet (NH_3)	4.0
Metallic Ion Engine	11.2
Colloid Ion Engine	4.4
Pulsed Plasma	12.2
Penning Discharge	17.8

3.3 MATERIALS AND PRODUCIBILITY CONSIDERATIONS

The selection of materials for various components of LTRCS follows conventional rules for selection of materials for aerospace vehicles with the addition of some special requirements. The principal criteria are:

- Performance Requirements
- Environmental Requirements
- Producibility Requirements

In the interest of design optimization, there must be some tradeoffs between the three areas, although performance requirements are usually considered most important.

With respect to the latter, structural materials are defined as those vehicular materials which have a design requirement to carry the loads induced by the vehicle's total mission requirements. In general, failure of a structural material is either a tension (strength) failure, or an instability (buckling caused by axial compression, or bending, or a combination of these) failure. Pressure vessels usually exhibit a tensile (biaxial stress) failure; shells, thrust structure, struts, etc., usually exhibit an instability failure. In aerospace vehicles, the great power needed to overcome gravity puts a premium on lightness. In addition to strength and stiffness requirements for general design, different fuels may create corrosion problems requiring consideration. If there is a combustion chamber, or other high temperature component, the attendant problems must be considered in materials choices.

An aerospace assembly has several environments to survive. These are ground handling, storage atmosphere, launch and ascent, and the space environment. Ground handling includes transport to and within manufacturing facilities and the launch facility, and insurance of cleanliness and test requirements. Thin gage materials and sensitive thermal control surfaces may create the most rigorous design requirements. Atmospheric environmental effects consist mostly of the corrosion potential in seacoast atmospheres. During launch and ascent, inertial loading, vibrations, and heating may occur. In space (hard vacuum) cyclic variations in temperature and various electromagnetic and particle radiations must be considered.

In the producibility category, materials need to be shaped and joined to the desired geometry. The relative ease of doing this, and the cost and availability of the material, constitute its producibility. For pressure vessels, the material needs to be formed into a leakproof cylinder which will withstand biaxial stress. For metals, the simplest fabrication method is welding. Welds usually have lower fracture toughness than base metal, so good welding techniques are required. The other manufacturing processes, such as forming and machining are well in hand except that the small size and light gauge of many parts call for special techniques. For nonmetals, the chief problem again is the small size and thin gauge of the parts. These considerations, together with stringent cleanliness requirements, make it imperative that conceptual designs be modified somewhat to improve producibility and ease of assembly.

3.3.1 Subliming Solid Systems

Superheated Subliming Solid Systems. Many material choices will be similiar to those made for the conventional subliming solid reaction control system. However, some changes will be made to improve fabricability and reliability. This section discusses material choices for both systems where they are similiar, and will include a special subsection on superheater materials and concepts. Table 3-2 lists preliminary material candidates.

The use of stainless steel for the propellant container, tubing, and fittings is dictated by general reliability conditions and the desire to protect products against general corrosion and handling. The particular grades of stainless steel, i.e., 321 and/or 347 are chosen because of their resistance to sensitization by exposure in the 800 – 1500°F range. Adequate in other respects, the 302/304 grades of stainless steel will precipitate chromium carbides in grain boundaries when slowly cooled through the 800 to 1500°F temperature range, a situation which decreases the alloys' corrosion resistance.

Table 3-2

TENTATIVE MATERIALS-SUPERHEATED SUBLIMING SOLID SYSTEM

Part	Material
Fuel Tank	Stainless Steel 321/347
Outer Shield	Glass Reinforced Plastic Laminate
Standoffs	Glass Reinforced Plastic Laminate
Tubing	Stainless Steel 321/347
Tubing Insulation	Pre-impregnated "B" stage epoxy-glass roving cured in place with heater wire
Heater Blanket	Low Temp Curing Epoxy Resin
Heater Wire	"Karma" – 75% Ni-20Cr-2.5Al-2.5Cu
Brazing Alloys	Nickel-Gold or Gold-Nickel-Palladium
Thermal Coatings	Gold Plate or Spray
Nozzle	Hastelloy X Tungsten Cermet
Superheater	(1) Aluminum Oxide with Pt or Pt-Rh Plated on Outside Diameter (2) Cermet of selected electrical conductivity, to be integral with nozzle (3) Ceramic of low thermal conductivity with heater element on I. D. made of Tantalum or Tungsten tube (metallized)

The addition of titanium or columbium to the basic 18-8 composition, to make the 321 and 347 grades respectively, prevents this precipitation. The requirements for welding and brazing in assembly assures that the metal will see these temperatures. Good production design and tungsten inert gas welding will dispense with the need for weld filler wire. For brazing these stainless steels, copper-free brazing alloys are indicated. In addition, carbamate fuels corrode copper alloys. Successful alloys are gold-nickel, and gold-nickel-palladium alloys. Either furnace or induction brazing may be used.

Outer heat shields are provided to control heat losses. Essentially, what is needed is a support for low emittance surfaces. Glass reinforced epoxy or phenolic resin laminates provide a support which is lightweight, strong and space-resistant. Whereas polymers are not as resistant to the space environment as metals or glass, if a proper selection of hardener and/or catalyst is made, the resistance is adequate. Lockspray, a method of gold-coating plastic surfaces, provides a convenient method of applying the necessary low emittance surface to both sides of the shield. Standoffs for the heat shields can also be made of glass fiber reinforced plastic resin to minimize conductive heat losses.

The conceptual design for the propellant heater is a plastic blanket with the heater wires embedded in the plastic, bonded to the outer surface of the propellant container. An epoxy resin will be adequate for the blanket. Heater wire will be of the 75 Ni-20Cr-2.5Al-2.5Cu type (Trade name "Karma"). This composition has a low change in resistivity over the service temperature range so that temperature control is simplified. Sections of the blanket can be made up and bonded to the propellant container with a suitable epoxy adhesive or sections can be made up and partially cured and then fully cured in place on the container.

Insulation and heating for propellant feed line tubing can be a layer of "B" stage epoxy glass roving or tape wound around tubing, then the heater wire (again "Karma") winding and then more layers of roving. The entire subassembly can then be cured as a unit provided that the details are designed with this objective.

The initial design concept for the superheater at the end of the propellant feed line is a tube of alumina with a thin film of platinum or platinum-rhodium plated on the outside surface. One end of the heater is brazed into the stainless steel propellant line and the other end into the nozzle. For these high temperatures Hastelloy X is a suitable and available nozzle material. 50 percent Au, 25 percent Pd and 25 percent Ni or 30 percent Au, 34 percent Pd and 36 percent Ni would be suitable brazing alloys as they all have melting points over 2000° F. The discrepancies in coefficients of thermal expansion must be given careful consideration by actual tests. The coefficients of expansion of the materials previously mentioned are as follows for a temperature range of 32 to 212° F:

Stainless Steel 321/347	9.3×10^{-6} in/in/°F
Hastelloy X	7.6×10^{-6} in/in/°F
Alumina	2.15×10^{-6} in/in/°F

An alternate conception is an integral heater and nozzle made from a cermet with a specified electrical resistivity, such as titanium carbide with a nickel or nickel-molybdenum binder suitable for direct resistance heating. Use of a cermet of this type would require some additional development effort. Another concept is a non-conducting ceramic with a tubular insert of tungsten for a heater. The tungsten heater may need an oxidation and/or corrosion resistant protective coating.

3.3.2 Hydrogen Monopropellant System

The heart of this system is the container for the lithium borohydride, in which the water and $LiBH_4$ react. Since borates can corrode aluminum alloys, stainless steel again is a good choice for this fuel-reaction container. Welding is favored for leak-proof joining of the 321/347 grades of stainless steel. For ease in fabrication, then, it would be logical to make the water and hydrogen container of stainless steel also, and to make all tubing and valves of stainless steel, thus avoiding dissimilar joint problems and simplifying assembly. However, since stainless steel is heavier than aluminum and titanium, weight requirements may dictate the substitution of these metals for some of the parts. The water-hydrogen container could be made of aluminum, such as 6061-T6, if desired.

This, of course, introduces a joining problem with the stainless steel portions of the assembly. Titanium may be used, since hydrogen embrittlement is not a likely problem at low temperatures. However, data is virtually non-existant on the effects of $LiBH_4$ or $LiBO_2$ on titanium. If these compounds or the reactions do not affect titanium, the low-strength grade of commercially pure titanium would be suitable for both containers and propellant lines. This would result in a lighter motor than one of stainless steel. Whereas commercially pure titanium is capable of being welded, formed and otherwise fabricated, to do so is not as simple as with stainless steel, and it is not so easily available in a variety of shapes and sizes. Titanium is somewhat more expensive than stainless steel or aluminum alloys.

The membrane between the water and the hydrogen in the container must be relatively impermeable to hydrogen and water and not reactive to either. Butyl rubber is a candidate for this membrane. Since it will be sealed in the container, it will not be exposed to environments other than space radiation. Any filters and/or wire screening should be of the same material as the containers they are in. Brazing alloys must be compatible with the container and preferably close to the container in the galvanic series. Insulation for the canisters, if necessary, can be handled by the blanket concept of alternate layers of aluminized Mylar and fiberglass spacers. Experience with aluminized Mylar in cryogenic tankage and the Echo satellites shows its suitability in the space environment. Propellant lines can be insulated by ribbons of reflective tape. A heat shield, if necessary, can be constructed of gold-coated glass-reinforced plastic laminate, as described for the subliming solid systems. Stainless steel, again, is a strong choice for the nozzle. The list of materials choices is shown in Table 3-3.

3.3.3 Repetitive Impulse Generator

This system is radically different than those previously discussed. It envisages a large number of propellant charges placed in small cans which have a hole at a specified location which serves as a nozzle. These charges would be fired electrically. The small propellant container requires a material that is formable and corrosion

Table 3-3

TENTATIVE MATERIALS-HYDROGEN MONOPROPELLANT SYSTEM

Part	Material
Lithium Borohydride Reaction Canister	(1) 321/347 Stainless Steel (2) Comm. Pure Titanium
Water – Hydrogen Canister	(1) 321/347 Stainless Steel (2) 6061 Aluminum (3) Comm. Pure Titanium
Tubing	(1) 321/347 Stainless Steel (2) Comm. Pure Titanium
Nozzle	(1) 321/347 Stainless Steel (2) Comm. Pure Titanium
Valves	Stainless Steel
Seals	Hydrogen Resi stant Elastomer
Bladder	Butyl Rubber
Filters-Meshes	Stainless Steel Wire
Insulation	Blanket of aluminized Mylar and woven fiberglass spacers
Heat Shield	Glass-reinforced plastic with gold coating

Table 3-4

TENTATIVE MATERIALS-REPETITIVE IMPULSE GENERATOR

Part	Material
Propellant Can	Aluminum (1100) Alloy
Mounting Frame	Aluminum 6061-T6 Extrusion Magnesium ZK 60 Extrusion
Main Conducting Flat Cable	Mylar with embedded copper wire
Potting Compund for Electronic Components	Epoxy

resistant. Aluminum Alloy 1100 is acceptable. This material can be anodized and colored if desired. The electronic-electrical components should be potted in an epoxy resin. It seems feasible to mount all the electronic circuits together with the propellant container, on a flexible flat Mylar cable, with integral power connections, the flat cable could be bonded to a mounting frame (configured to the particular satellite). The mounting frame can be made from an aluminum or magnesium extrusion, the choice of alloy is not important. The metals would have to be protected against storage environment and the seacoast environment of a launching site. Table 3-4 gives a list of structural materials.

The Repetitive Impulse Generator contains small solid propellant motors, one version of which generates a total impulse of 0.01 lb-sec in a total burning time of 0.05 second. If a heterogeneous (composite) propellant is used, rigid particle size control is necessary to assure reproducibility of the extremely small impulse. Both extrudable and cast double-base propellants may also be considered. Currently, three double-base propellants are available off-the-shelf at the Naval Propellant Plant, Indian Head, Maryland. These propellants – JPN, N-5, and high energy X-12 – have been chosen as a basis for design study. Both N-5 and high energy X-12 are mesa burning, which denotes a negative pressure exponent over a certain pressure range.

The first consideration was to choose a chamber pressure and burning rate combination so that the web thickness is sufficient for ease of handling and the nozzle diameter is large enough for accurate dimensional control.

It is advantageous to operate at a chamber pressure on or near the mesa of the pressure-burning rate curve in order to minimize the effects of grain manufacturing and inhibiting tolerances. At pressures on or near the mesa, a change in burning surface does not change the chamber pressure as rapidly as in a non-mesa propellant. JPN is not a mesa propellant. It is included because it contains no metal additives. Both N-5 and X-12 contain lead salts which may be objectionable in view of the minute nozzle throat diameter. However, all the known lead oxides, either melt or decompose below 1000° so the threat of plugging the nozzle with solid particles may not be a real one. Consequently it is felt that the advantages of the mesa propellants are more significant than the disadvantages derived from the lead it contains.

The mesa of N-5 propellant occurs around 800 psi to 1200 psi; the burning rate in this pressure range is about 0.5 in/sec. The mesa of the high energy X-12 propellant occurs at much higher pressures (2400 to 3100 psi). The burning rate at the mesa is about 1.2 in/sec. The following table lists the web thickness (W) and nozzle throat diameter (D_t) when operating at 500 psia, 1000 psia and 2500 psia. (Assume an orifice coefficient = 0.6).

Pc, psia	JPN		N-5		HE X-12	
	D_t	W	D_t	W	D_t	W
500	0.0196	0.0185	0.0189	0.0155	0.0194	0.0320
1000	0.0139	0.0300	0.0133	0.0230	0.0137	0.0450
2500	-	-	-	-	0.0085	0.0602

Two designs appear feasible; one with N-5 propellant operating at a chamber pressure of 1000 psia and the other with HE X-12 operating at 2500 psia. The N-5 propellant, because of its low burn rate, takes a double web (0.023 in. each) to make the grain thick enough to be handled conveniently. The grain would be in the form of a slab (0.155 × 0.125 inch by 0.046 inch thick) supported on both ends or suspended from the head dome. Two edges and one end would have to be inhibited to control the burning surface and maintain a neutral thrust-time relationship. Simultaneous ignition of the two sides will be a problem, in view of the extremely short burning time imposed.

High Energy X-12 operating at 2500 psia (at the mesa) is more amenable to the conventional design. An end burning grain of 0.136 in. diameter by 0.0602 in. long may be used instead of a slab. The grain can be supported by case-bonding which also eliminates the problem of inhibiting the periphery.

The high operating pressure incurred in the HE X-12 system does not affect the inert weight, as the minimum case thickness which can be conveniently fabricated is many times heavier than necessary. Aluminum alloy was chosen instead of steel to save weight. If the case is formed in one piece (thimble shape) the weakest place is probably at the juncture where the nozzle is attached to the case. An internal force of approximately 45 lb must be resisted by the adhesive bond in shear. Assuming a shear strength of a room-temperature-cured epoxy adhesive is 2000 psi, the bonded area is 0.022 in^2 or roughly the whole cylindrical length of the case. It may be visualized that the case be made in two halves with the cylindrical part tapered for easy mating (see Fig. 3-1). The nozzle is formed in the phenolic asbestos which fills the end dome.

For the motor with N-5 propellant, the operating pressures may be only 800 to 1000 psia. The force on the nozzle plug is only 10 to 12 lb. Assuming the same strength for the adhesive, the corresponding bonding area is around 0.005 – 0.006 in^2 or 16 mils of the cylindrical length. If a phenolic plate of 30 mil thickness is used as nozzle closure (see Fig. 3-2), the edge of the plate will provide sufficient area for bonding. The elliptical dome, therefore, is not necessary for the nozzle end.

The weight breakdowns for the two systems are as follows:

	N-5 System		HE X-12 System
Case – cylinder	8.0×10^{-5}		6.5×10^{-5}
dome(s)	1.6	(2)	3.4
nozzle plate	2.6		2.0
dome potting	1.0		-
adhesive	-		1.0
Total Case	13.2×10^{-5} lb		12.9×10^{-5} lb
Propellant	5.0		5.0
Inhibitor	2.0		0
Igniter	3.0		3.0
Total Weight	23.2×10^{-5} lb		20.9×10^{-5} lb
	or 0.105 gm		or .095 gm

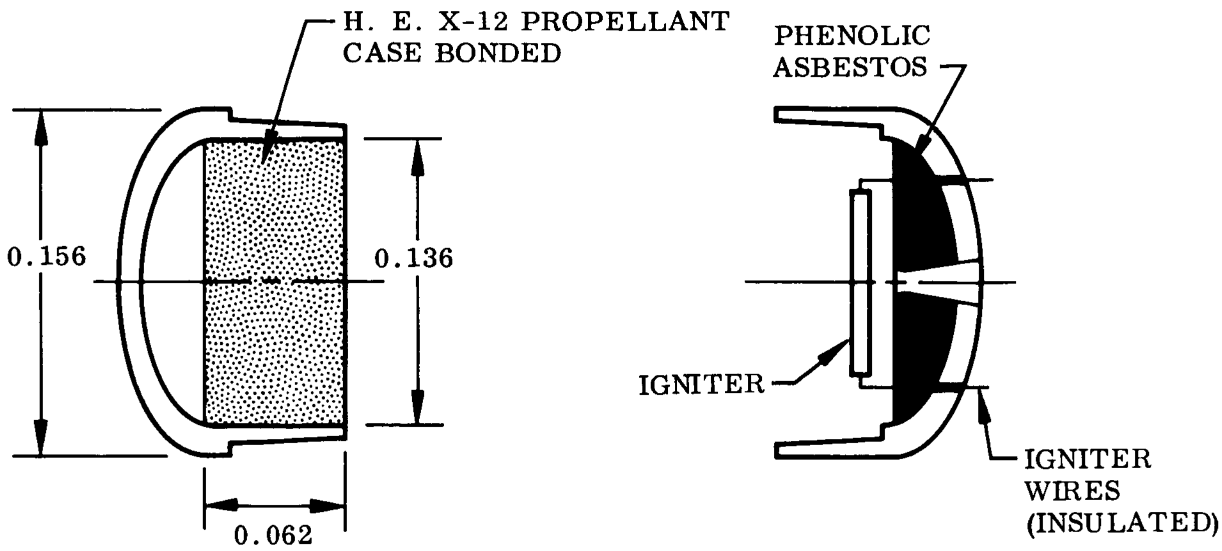

Fig. 3-1 Conceptual Drawing of RIG Motor With H. E. X-12 Propellant

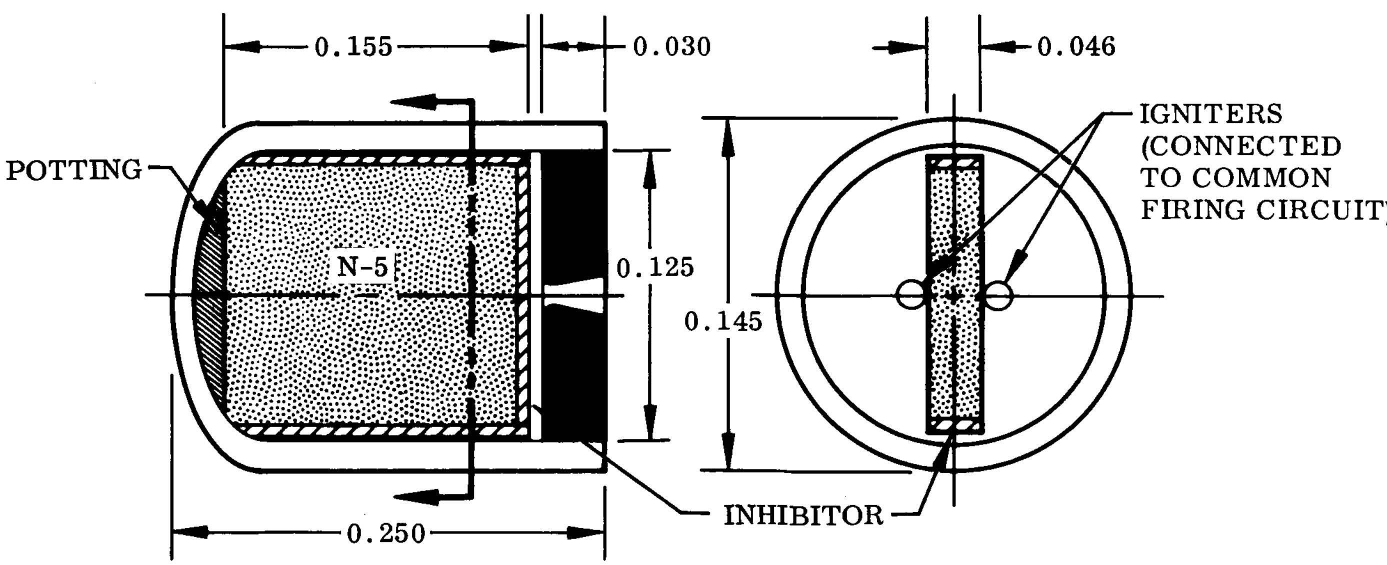

Fig. 3-2 Conceptual Drawing of RIG Motor with N-5 Propellant

The weight figures above may be optimistic if produced by the ordnance industry since the latter is not set up for miniaturization. Control of the various component weights to the calculated magnitude is beyond the capability of the measuring equipment generally used in production. Unless the item is "precision-made" these weights are expected to deviate from these estimates by several hundred percent. In view of the large number to be manufactured the production techniques will most likely be geared to low cost. In this event, weight control and quality control will be costly if not difficult.

3.3.4 Producibility

Some aspects of producibility have been discussed earlier in this section. The subliming solid motors, the hybrid hydrogen monopropellant system and the Repetitive Impulse Generator were each subjected to a production design analysis and producibility-cost evaluation. Designs were synthetically created from the basic concepts of the latter two systems. The existing design of the low temperature subliming solid motor was used for comparison. The three system hardware designs were compared for ease of processing, assembly, inspection and testing. Product repeatability and cost were also compared.

All systems were found capable of implementation into hardware.

3.4 ADVANCED CONCEPTS

3.4.1 High Specific Impulse Solid and Hybrid System

Screening. One approach to improving specific impulse of the solid and hybrid LTRCS, the superheated subliming solid system, has been described in earlier sections of both this report and the Phase I report. In the system described, a specific impulse of 205 lbf-sec/lbm could be attained at 2000°F. As noted in Section 2, this considerably improved the weight status of the subliming solid systems, but not sufficiently to displace the leading competitive systems. A still greater specific impulse is required for the relatively high total impulses of the Phase I missions.

These greater specific impulse values must be obtained at still higher temperatures which require greater amounts of power if from an auxiliary source. The greater power, in turn, entails higher system weights. With an internal heat source, such as a chemical heat of reaction, the weight of the power system can be reduced to that needed for sublimation or dissociation. Accordingly, reactions which could yield a significant increase in performance, to 285-300 lbf-sec/lbm or greater, were sought.

Of prime interest were those reactions which might prove hypergolic. Since a majority of the known hypergolic reactions involve fluorine or its compounds, attention centered on the reactions of fluorides and hydrides. To establish a molecular weight criterion for accepting or discarding a given reaction, an operating temperature of 3000°K was arbitrarily selected. This corresponded to a product molecular weight of 31 at specific impulse of 285 lbf-sec/ lbm. Higher values of reaction temperature could support higher molecular weights, and vice versa.

Two types of reactions were considered initially, bipropellants and hybrids. Since the hydrides generally decompose upon heating, rather than vaporize, a metallic or nonmetallic residue is left. The latter must also react with fluorine or its compound or be removed in some other way from the reaction zone. Therefore, even a bipropellant hydride-fluoride reaction reduces to a pseudo-hybrid classification. For the bipropellant reaction the potentially useful solid hydrides and fluorides were limited to those providing vapors by volatilization or decomposition at temperatures below 655°C. Review of handbook values (Ref. 2) narrowed the field of interest to those compounds shown in Table 3-5. Organic compounds may form polymeric products at high temperatures and were therefore excluded from the survey.

Table 3-5

POTENTIALLY USEFUL INORGANIC HYDRIDES AND FLUORIDES

Hydrides	Melting Pt, °C	Boiling Pt, °C	Fluorides	Melting Pt, °C	Boiling Pt, °C
*As_2H_2	d 200	-	NH_4HF_2	125.6	-
BeH_2	d 125	-	NH_4F	sublimes	-
$B_{10}H_{14}$	99.5	213	SbF_3	293	319 sublimes
CeH_3	ign	-	GeF_2	d > 350	sublimes
CsH	d	-	HfF_4	sublimes	-
*$(H_2P_4)_3$	ign 160	d	IF_7	5.5	4.5 (subl)
PbH_2	d	-	IrF_6	44.4	53
Pd_2H	d	-	MoF_6	17.5	35
KH	d	-	NbF_5	72-73	236
MgH_2	d 280 (vac)	-	OsF_6	32.1	45.9
			PdF_2	volatile	d. red heat
			ReF_4	124.5	d 500
			ReF_6	18.8	47.6
			RuF_5	101	250
			TaF_5	96.8	229.5
			TeF_4	subl.	>97
			TIF	327	655
			UF_6	64.5-64.8	56.2
			VF_5	-	111.2
			VF_4	d 325	–

d - decomposes
* - free energy of formation data not immediately available

The free energy of reaction (ΔF) between the various hydrides and fluorides was then determined for those combinations in which data were available. Both one-to-one stoichiometry and hydride-rich combinations were considered in order to "average down" the product molecular weights. The latter is possible with the light hydrides. In order for the reaction to be thermodynamically feasible, the change in free energy should be negative or, at most, a few kilocalories positive.

The results of potential bipropellant combinations at 300°K and 2500°K are shown in Table 3-6. Those combinations which are boxed meet both the free energy and product molecular weight criteria.

The hydrides of cerium, cesium, lead and palladium all yield average molecular weights above 31. The same is true for potassium hydride, except possibly a combination with the ammonium fluorides. Magnesium hydride, in 3-to-1 or greater mole ratio with germanium difluoride or vanadium tetrafluoride, would satisfy the criteria. Other fluorides qualify at high magnesium hydride/fluoride levels. Decaborane meets the criteria with all fluorides for which data are available and at all hydride/fluoride ratios of one or greater. Beryllium hydride presents somewhat fewer potentially useful combinations, all at hydride/fluoride ratios of two and higher.

From the foregoing, further search for bipropellant combinations should be centered on magnesium and beryllium hydrides, and decaborane if a "bipropellant" reaction is contemplated.

The number of potentially useful hybrid combinations should be considerably greater, since a volatile or decomposing hydride is not a prerequisite and an initially liquid or gaseous fluoride can be used. The choices are not limited to Table 3-5. Some hybrid combinations of gaseous fluoride and solid hydrides are given in Table 3-7. Data for some gaseous diborane-solid fluoride reactions are shown in Table 3-8.

Table 3-6

SUMMARY OF POTENTIAL BIPROPELLANT REACTIONS

	NH_4F	NH_4HF_2	SbF_3	GeF_2	HfF_4	IF_7	IrF_6	MoF_6	NbF_5	OsF_6	PdF_2	ReF_4	ReF_6	RuF_5	TaF_5	TeF_4	TlF	UF_6	VF_4	VF_5
BeH_2	-46 Δ	-82 Δ	X	X	X	X	X	X	X	X	X	X	X	X	X	X	X	X	X	X
2 BeH_2			X	-103 / - 86	X	X	X	X	X	X	X	X	X	X	X	X	X	X	-163 / - 95	-220 Δ
3 BeH_2			-191 / -167		X	X	X	X	X	X	-188 / -160	X	X	X	X	X	X	X		
4 BeH_2					-111 / - 52	X	X	-345 / -265	-311 / -205	X		X	X	-346 / -235	X	-337 / -282	-154 / -107	X		
5 BeH_2						-670 ?	X			X		-351 / -272	X		-315			X		
$B_{10}H_{14}$	-58 Δ	-76 Δ	-116 / -544	- 69 / -477	+4.8 / -414	-489 Δ	-485 / -915	-203 / -639	-182 / -572	-409 / -813	-126 / -530	-207 / -615	-329 / -615	-217 / -602	-158	-221 / -644	- 77 / -451	-107 / -549	-103 / -498	Δ
2 M_gH_2	-114 Δ	-166 Δ	X	X	X	X	X	X	X	X	X	X	X	X	X	X	X	X	X	X
3 M_gH_2			X	-194 Δ	X	X	X	X	X	X	X	X	X	X	X	X	X	X	-298 Δ	X
4 M_gH_2			X		X	X	X	X	X	X	-285 Δ	X	X	X	X	X	X	X		-449
5 M_gH_2			-344 Δ		X	X	X	-536 Δ	-480 Δ	X		X	X	-515 Δ	X	-184 Δ	X	X		
10 KH	Δ	Δ	X	X	X	X	X	X	X	X	X	X	X	X	X	X	X	X	X	X
CeH_3	X	X	X	X	X	X	X	X	X	X	X	X	X	X	X	X	X	X	X	X
CsH	X	X	X	X	X	X	X	X	X	X	X	X	X	X	X	X	X	X	X	X
PbH_2	X	X	X	X	X	X	X	X	X	X	X	X	X	X	X	X	X	X	X	X
Pd_2H	X	X	X	X	X	X	X	X	X	X	X	X	X	X	X	X	X	X	X	X

LEGEND:

Δ No thermodynamic data
X Too high molecular weight

Acceptable Combination, Kcal: $\boxed{\begin{matrix}\Delta F_{300K} \\ \Delta F_{2500K}\end{matrix}}$

Gen. Equations:

$$AMF_X + BNHy \rightleftarrows \frac{AX}{y} NFy + \left(B - \frac{AX}{y}\right) N + AM + \frac{BY}{2} H_2$$

or

$$AMF_X + BNH_y \rightleftarrows BNFy + (AX - BY) HF + AM + \left(BY - \frac{AX}{2}\right) H_2$$

Tables 3-6, 3-7 and 3-8 provide a basis for investigation in greater depth of the more promising reactions. Equilibrium calculations for certain of these combinations are described in the following paragraphs.

Table 3-7

SOME HYBRID SYSTEMS – GASEOUS FLUORIDES VS. SOLID HYDRIDES

	F_2	F_2O	ClF_3
BeH_2	-234 -330	-305 -314	X
2 BeH_2			-358 -349
$B_{10}H_{14}$	-227 -577	-233 -784	-318 -642

Table 3-8

SOME HYBRID SYSTEMS – GASEOUS HYDRIDE VS. SOLID FLUORIDES

	NH_4F	GeF_2	SbF_3	ReF_4	TeF_4	VF_5	RuF_5	NbF_5
B_2H_6	-30 Δ	-42. -187	X	X	X	-158 Δ	X	X
2 B_2H_6			-109 -383	-200 -452	-214 -483		-210 -442	-175 -412

Legend: Δ – No thermodynamic data

X – Too high molecular weight

$\boxed{\begin{matrix}\Delta F_{300K} \\ \Delta F_{2500K}\end{matrix}}$ – Acceptable combination, Kcal

Equilibria. Free energy calculations indicate whether a reaction is thermodynamically possible. Additional equilibrium calculations must then be made to determine reaction temperature, molecular weight, heat capacity ratio (γ), and specific impulse. The calculation process is iterative. First, a reaction temperature is assumed. Then mass balance and equilibrium equations are formed. From the derived tentative equilibrium concentrations the heat generated and absorbed by the system are computed. If these are equal, or approximately so, the assumed temperature was correct. If not, the assumed temperature must be adjusted and the process repeated.

Most of the promising combinations in Tables 3-6 through 3-8 are not amenable to computation by available propellant programs. In view of the short time available, slide-rule calculations were used in lieu of computer program modifications. While laborious, it was felt that the former method was more certain of yielding useful results in the time allotted.

The results of the equilibrium calculations are shown in Table 3-9. To simplify the computation, the total pressure was arbitrarily selected to equal the sum of the number of moles of reaction products. For this situation, the equilibrium constants calculated from pressures and moles are equal. Three of the reactions are estimated to provide chamber temperatures in excess of 3500°K and vacuum specific impulses in excess of 315 lbf-sec/lbm.

In general, the reaction heat can be increased by decreasing the hydride/fluoride ratio. This, however, increases the average molecular weight. A molecular weight increase can be tolerated in certain of the decaborane bipropellant and hybrid reactions due to the low molecular weight of the hydride.

From the list of Table 3-9,one reaction was chosen for further study by virtue of its high specific impulse and the fact that the reactants were initially in a condensed state. This was the reaction of beryllium hydride and iodine heptafluoride.

Table 3-9

SELECTED REACTION EQUILIBRIUM PARAMETERS

	P (= Σn), (atm)	Est. Chamber Temperature (°K)	Isp (ϵ = 100)
Bipropellant (pseudo-hybrid)			
5 BeH_2+IF_7	13.0	4100	321
3 MgH_2+GeF_2	7.0	900-1000	134
5 MgH_2+MoF_6	11.3	2300-2400	201
$B_{10}H_{14}+IF_7$	17.6	<1800	188
Hybrid			
BeH_2+F_2	3.16	<4600	369
$B_{10}H_{14}+F_2$	16.8	1500	273
$B_{10}H_{14}+5F_2$	17.8	3500-3600	316
2 $B_2H_6+TeF_4$	11.0	<<1800	-

Iodine heptafluoride is a colorless solid which sublimes with a vapor pressure of 760 mmHg at 4.5°C. The vapor pressure equation is:

$$\log p_{IF_7} = 8.6604 - 1602.6/_T.$$

Under slight pressure the solid melts at 5-6°C. The latent heat of vaporization is 7330 cal/mole or approximately 51 BTU/lb. (Ref. 3). From the standpoint of power requirement, this compares quite favorably with a value of 743 BTU/lb for methyl carbamate, a presently employed subliming solid propellant.

Beryllium hydride decomposes between 125 and 250°C. Additional information is given in the discussion of kinetics which follows. A summary of the equilibrium reaction parameters for the 5 BeH_2 - IF_7 system is given in Table 3-10.

Table 3-10

REACTION PRODUCTS OF BERYLLIUM HYDRIDE AND IODINE HEPTAFLUORIDE

Reactants: 5 BeH_2 + IF_7

T = 4100°K

P = Σn = 13.03 atm = 192 psi

Products	n	q	nq	(H_t-H_{298})	$n(H_t-H_{298})$	MW	n(MW)	$C_p°$	$n\ C_p°$
BeF_2	1.605	-265.3	-425	54.64	87.9	47.0	75.5	14.82	23.80
BeF	2.920	-131.0	-383	33.56	98.0	28.0	81.8	9.23	26.95
Be	0.358	0	0	97.40	34.8	9.0	3.2	5.44	1.95
BeI	0.121	- 63.3	- 7.7	34.44	4.2	135.9	16.4	9.30	1.12
H_2	2.945	0	0	31.25	92.1	2.1	6.1	9.39	27.60
H	3.220	+ 55.4	+178	18.89	60.8	1.0	3.25	4.97	16.00
HI	0.062	- 1.72	- 0.1	32.60	2.0	127.9	7.9	9.26	0.60
HF	0.888	- 66.9	- 59.2	30.77	27.3	20.0	17.8	8.98	8.00
I	0.879	+ 20.2	+ 17.7	19.62	17.3	126.9	111.3	5.43	4.77
F	0.029	+ 20.5	+ 0.6	19.16	0.5	19.0	0.55	4.98	0.10
	13.027		-678.7		424.9		323.8		110.89

Reactants

	n	q	nq
BeH_2	5	- 4.8	- 24.0 - 229 -(253) -425.7
IF_7	1	- 229	

Aver MW = 24.9

Aver C_p = 8.50

Isp = 321 lbf-sec/lbm (ϵ = 100)

γ = 1.305

The equilibrium characteristics indicate that the system would be highly energetic, approaching the hydrogen-fluorine system in operating temperature. The equilibrium characteristics, however, give no indication of the rate of reaction. The possibility of hypergolicity is discussed in the following paragraphs.

Reaction Kinetics. In order to evaluate conditions for a hypergolic reaction to occur in a low-thrust system, some information on the rate of reaction is required. However, the number of systems for which rate constant measurements have been made at very high temperatures is small. Generally, several man years of effort are required to determine the rate constant for a specific high temperature reaction.

One of the most promising systems identified in the thermodynamic study of hydride-fluoride reactions has been that of beryllium hydride and iodine heptafluoride. By comparison with similar systems there is some basis for anticipating a hypergolic reaction in this case. For example, potassium hydride reacts energetically with iodine pentafluoride (Ref. 4). Also, in an abstract of U.S. Patent No. 3,147,710, a hypergolic reaction between fluorine and beryllium hydride is claimed.

Whether a reaction is hypergolic, or not, is chiefly dependent on whether the reactant concentrations and rate of reaction are sufficiently high to generate heat at a rate more than sufficient to offset heat losses to the substrate or gas. The temperature of the system reaches a "runaway" condition. Ignition and sustained combustion follow. The kinetics and exact mechanism by which beryllium hydride and iodine heptafluoride may react can only be speculative at this point. The controlling mechanism will probably vary as the temperature rises, particularly since the range of interest lies from 298° to 4100°K. At least two zones of interest can be postulated, initiation or "triggering" of the reaction and sustaining the reaction at elevated temperature.

It is unlikely that the initiation step will involve all eleven atoms originally present in the hydride and fluoride, since these are relatively unstable molecules. The rate-controlling step of a reaction usually involves only two or three reacting entities. For the fluorine source the following equilibria will exist at 25°C:

$$IF_7 \rightleftarrows IF_5 + F_2 \tag{3.1}$$

$$IF_5 \rightleftarrows IF + 2\ F_2 \tag{3.2}$$

$$IF \rightleftarrows 1/2\ I_2 + 1/2\ F_2 \tag{3.3}$$

The vapor pressure of iodine heptafluoride at 298°K is 2.63 atm (Ref. 1, p. 179). From thermodynamic data (Ref. 5) the equilibrium pressures are estimated to be as shown in Table 3-11. The extent of dissociation at this temperature is quite small, but the fluorine concentrations are significant if a chain mechanism is involved. No data were found on forward or reverse rates in Reactions (1), (2), and (3), but they are presumed to be rapid. Because of the much larger concentration of IF_7, it is possible that this may be chemisorbed by the surface and react with beryllium hydride or beryllium directly, without requiring a shift in the gas-phase fluorine equilibrium.

Beryllium hydride dissociation occurs in the 125°–250°C range (Ref. 6) and is said to occur irreversibly (Ref. 7). The vapor pressure of the hydride is unknown, but is probably negligibly small. Therefore, the fuel will be considered to be either dissociated hydrogen in the presence of solid beryllium (bipropellant fuel source) or solid hydride (hybrid fuel source).

In this system, both the "bipropellant" and hybrid concepts share common features. The first "bipropellant" step must involve the dissociation of beryllium hydride to provide hydrogen:

$$BeH_2 \rightarrow Be + H_2 \tag{3.4}$$

or

$$BeH_2 \rightleftarrows \frac{1}{2}(Be - BeH_2) + \frac{1}{2} H_2 \tag{3.5}$$

Table 3-11

CALCULATED PARTIAL PRESSURES OF IF_7 AND ITS COMPONENTS AT 298° K

Species	P, atm
IF_7	2.63
IF_5	7.82×10^{-7}
IF	3.63×10^{-111}
I	1.35×10^{-134}
I_2	7.81×10^{-244}
F	1.30×10^{-14}
F_2	7.82×10^{-7}

Dissociation is said to proceed via Reaction (4) (References 7 and 8), although Reaction (5) cannot be discarded in the present case, since the decomposition propagates from the Be-BeH_2 interface.

After dissociation, the fluorine and hydrogen species may react with each other and with beryllium as shown below:

$$BeH_2 \rightarrow Be + H_2$$

$$BeH_2 \rightleftharpoons BeH + H$$

$$IF_7 \rightleftharpoons F_2 + IF_5$$

$$IF_5 \rightleftharpoons 2F_2 + IF$$

$$IF \rightleftharpoons 1/2F_2 + 1/2I_2$$

$$F_2 + H_2 \rightleftharpoons 2HF$$

$$F_2 \rightleftharpoons 2F$$

$$H_2 \rightleftharpoons 2H$$

$$BeH + F \rightleftharpoons BeF + H$$

$$Be + F_2 \rightleftharpoons BeF_2$$

$$Be + 2HF \rightleftharpoons BeF_2 + H_2$$

The reactions shown are by no means a complete set. Other reactions, such as those involving iodine, also contribute, but the contributions are probably small and would further complicate the diagram. Direct reaction between beryllium or its hydride and IF_7 or IF_5 cannot be discounted, but the controlling step would involve fewer atoms.

A literature survey was made to find appropriate rate constants and activation energies, if previously determined. A compilation of the findings is given in Table 3-12.

Table 3-12

AVAILABLE KINETIC INFORMATION FOR THE BeH_2-IF_7 SYSTEM

$$\begin{bmatrix} X & = & \text{mole fraction} \\ n & = & \text{moles} \\ C & = & \text{moles/liter} \end{bmatrix}$$

Reaction	Controlling Rate Expression	k	Temp Range °C	Source
(3.4) $Be\,H_2 \rightarrow Be + H_2$	$\frac{-d\,X_{BeH_2}}{dt} = k\,X_{BeH_2}\,X_{Be}$	1.80×10^{10} (exp - 25,000/RT) (mole fraction)$^{-1}$ min^{-1}	200–250	Ref. 7
(3.6) $Be + F_2 \rightarrow BeF_2$	$\frac{-d\,n_{F_2}}{dt} = \frac{k^{1/2}}{2\,t^{1/2}}$	7.96×10^{-15} (exp 800/RT) (moles F_2)^2 cm^{-4} min^{-1}	125–525	Ref. 9
		2.98×10^{-11} (exp -8000/RT) (moles F_2)^2 cm^{-4} min^{-1}	525–775	Ref. 9
(3.7) $H_2 + F_2 \rightarrow 2\,HF$	$\frac{-d\,C_{F_2}}{dt} = k\,C_{F_2}$	$3.80 \times 10^{11}\,T^{1/2}$ (exp -25,500/RT)* sec^{-1}	110	Ref. 10
(3.8) $BeH + F \rightarrow H + BeF$	$\frac{-d\,C_{BeH}}{dt} = k\,C_{BeH}\,C_F$	$2.5 \times 10^8\,T^{0.69}$ (exp - 2400/RT) liters mole^{-1} sec^{-1}	700–5700	Ref. 11

*k estimated in Appendix G.

In view of the scarcity of data, use of the rate expressions was not limited to the original temperature ranges.

For a hypergolic reaction to occur the initial rate of reaction and heat generation must be sufficiently high. If the hydride temperature were only 25° C, the initial rate of hydrogen formation would be only 6.4×10^{-13} mole/liter-sec. If the oxidant were $[F_2]$ at 7.82×10^{-7} atm (Table 3-11), the hydrogen would disappear at 5.1×10^{-13} mole/liter-sec. These are very slow compared to the initial infinite rate of Reaction (6). Reaction (8) is proposed for a gas phase and the rate constant is a theoretical value. If it can also be applied to the exchange of hydrogen and fluorine between solid beryllium phases, a rate of 1.7×10^{-4} moles/liter-sec at 25° C can be calculated by assuming the [Be H] concentration equal to the solid density. The fluorine supply may be exhausted locally by Reactions (6), and perhaps (8), and the rate of resupply may control the overall rate until a surface barrier of solid beryllium fluoride has formed. The latter would serve to both restrict hydrogen evolution and access of fluorine to beryllium. If we assume that the fluorine equilibria shift rapidly, another point of concern then is whether the beryllium fluoride volatilizes sufficiently rapidly to avoid choking off the reaction. This would require that the heat of beryllium fluoride formation exceed the sum of the fusion, vaporization and sensible heats required to raise the fluoride to the boiling point, plus heat losses to substrate and gas phase. The heat of formation is 241 kcal/mole; the sensible and phase change heats total 67 kcal/mole. A maximum of 174 kcal/mole is then left for heat losses. (This is a conservative estimate since concurrent gas phase reactions may also contribute heat). Hence the configuration of propellant and system may be crucial to propagation of the reaction, but the outlook for beryllium fluoride volatilization is encouraging.

Assuming successful fluoride volatilization, the overall rate may then be controlled by the rate of hydride decomposition. As the temperature of the hydride rises, the rate of hydrogen evolution increases. At 227° C (500° K) the initial hydrogen evolution rate has increased to 1.8×10^{-5} moles/liter-sec, but hydrogen could be consumed in Reaction (7) at at least 2.3×10^{-5} moles/liter-sec. The latter rate is probably low, inasmuch as the $[F_2]$ concentration at 298° K was used. Hence, the rate of beryllium hydride dissociation will probably control the overall rate if the fuel is preheated to 500° K, or if it is heated to that temperature by reaction heat.

To summarize, purely theoretical analysis of reported reaction rates for certain components of the BeH_2-IF_7 system suggests that the reaction could be hypergolic under the proper conditions. If the hydride and fluoride are both cold, the rates of Reactions (4) and (7) are probably too slow to initiate reaction. This does not preclude a surface absorption by IF_7, of which nothing is presently known. The gas-solid reaction (6) is initially infinitely fast and highly exothermic, and slows due to formation of a product BeF_2 layer. The rate at this stage may be limited by fluorine access to the surface. With the proper configuration there should be enough heat from reaction (6) to volatilize the product BeF_2. (This cannot presently be established due to the lack of thermal data for BeH_2). As the solid and adjacent gas phase are heated, Reactions (4) and (7) will increase rapidly, and the rate will be controlled by Reaction (4). This in turn will be controlled by the rate at which the heat pulse penetrates the hydride. Other (unreported) reactions may also occur but these should contribute to the potential hypergolicity.

System Thermal Analysis. Theoretically, it should be possible to predict the performance of a rocket motor using the preceding chemical system, as long as all of the reaction kinetics are known. The resulting mathematical complexity, which would be required for a space-time solution for the thermodynamic coordinates, generally precludes any rigorous solution. A simpler approach is to choose one gas-phase reaction which appears to be rate-controlling and apply this to the equations governing the flow of the reactants in a combustion chamber. This will allow calculation of the temperature, pressure, and molecular weight as a function of position, which in turn will provide an indication of whether or not the reaction will go to completion and the required chamber length to effect ignition. A serious shortcoming to this approach is the neglect of axial conduction which, in the case of large temperature gradients, leads to calculated lengths that are larger than the actual case. A second approach is to assume that the reactants are thoroughly mixed with a mean temperature and molecular weight. This allows calculation of the transient response for the system at the expense of the space-dependent nature of the temperature and molecular weight. Such an assumption is only truly valid for the case where the residence time is much larger than the time for complete reaction. This will generally result in the predicted performance being something less than the actual.

The two mathematical models described above have been presented in Appendix H along with their analogues.

Structural Materials. The materials problems associated with a reaction of hydrides and fluorides in the temperature range of 5000 to 7000°F are difficult to rationalize. Few materials are solid at these temperatures and the reactants are extremely corrosive. The highest melting materials which can be obtained are carbide ceramics, such as hafnium and tantalum carbides which melt at about 7050°F. These materials, unfortunately, have a poor corrosion resistance, and poor thermal shock resistance. Other ceramics have lower melting points. From this, it is indicated that the approach must be taken that the design of the system and the combustion chamber/ nozzle must be such that the material will never quite reach the reaction temperature. With short duty cycles, and a chamber/ nozzle design that radiates heat fairly rapidly, this may be possible. For a detail design, the heat balance will have to be rigorously calculated. With this approach, the use of pressed and sintered refractory metals is considered feasible. Tungsten melts at 6170°F and molybdenum melts at 4730°F.

It is considered feasible, with some development, to press and sinter and machine these materials and their alloys into the small chambers and nozzles required. The specific metal and/ or alloy (rhenium is a valuable alloying agent) would depend on more detailed requirements. These metals are claimed to have resistance to hydrofluoric acid and molten alkali metals, so they may show some resistance to the reactants.

Coatings for these metals are available to increase corrosion resistance, and it may be possible to metallize them with an alloy similar to Hastelloy N, which was specifically developed for resistance to molten fluoride salts.

Weight Comparison. The weight advantage of increasing the specific impulse to approximately 300 lbf-sec/ lbm is shown in Table 3-13, in which the weights of the leading contenders (from Table 2.7) and the potential weight of the advanced BeH_2-IF_7 system are compared. Weight reductions result not only from the reduced amount of propellant required but also from accompanying fixed weight reductions.

Table 3-13

WEIGHT COMPARISON OF THE LEADING CONTENDERS AND THE ADVANCED BeH_2-IF_7 SYSTEM

Mission Requirement	Projected System Weights (lb)			
	Leading Contenders			Adv. System
ATS-4				
Attitude Control and Slewing	Ion Engines 16.0	Bipropellant Vapor 30		24.4
E-W Station-keeping	Colloid Ion Engine 8.8	Water Electrol-ysis 19.7		13.3
N-S Station-keeping	Water Elect. 32.3	Monopropellant Hydrazine 35.	Repetitive Impulse Generator 39	24.3
Station Acquisition	Bipropellant Liquid 40-42	Colloid Ion Engine 58	Repetitive Impulse Generator 63	48.3
Voyager				
Attitude Control	Monopropellant Hydrazine 8.5	Bipropellant Vapor 10.5	Bipropellant Liquid 10.5	6.3
Evasive Maneuver	Pressurized Cold Gas 3.3	Monopropellant Hydrazine 4	Subliming Solid 5.4	1.6
ATM				
Attitude Control and Slewing	Gyro and Mag-netic Torque 182	Bipropellant Vapor 225	Water Elec-trolysis 248	213.5
Mom Discharge	Magnetic Torque 22	Ion Engine 32.3	Colloid Ion Engine 39.9	213.5
EVA	Bipropellant Vapor 12	Bipropellant Liquid 13	Monopropellant Hydrazine 16	11.5

The potential reductions in weight are impressive. From the present situation, in which solid and hybrid systems are competitive in only two of the nine requirements, the position of these systems is improved to the point where they are competitive weightwise in eight of the nine requirements.

3.4.2 Very Low-Thrust Systems

Another area requiring LTRCS is in the thrust regime of 10^{-6} to 10^{-9} lbf. There appears to be a developing need for thrusts of this type on navigational satellites to operate at high duty cycles and counter effects such as atmospheric drag. Little development is known to be underway in this area at present but Lockheed Missiles & Space Company (LMSC) has conducted several tests. The only known solid or hybrid systems are discussed in the following paragraphs.

Subliming Ammonium Compounds. A valveless design (Fig. 3-3) provides the advantages of subliming solid units already developed and qualified. For thrust at or near 3×10^{-8} lbf, ammonium halides offer the combination of properties required for propellant. In particular, ammonium chloride provides 100 micron propellant chamber pressure at an operating temperature of 250°F, exhausting through a 10-mil orifice with $C_F = 0.2$. An electronic temperature controller maintains proper power usage for the propellant heater. Other than on-off signals to the temperature controller, no valve or pressure regulation is necessary. With power off, the propellant cools below 75°F and produces less than 1×10^{-9} lbf thrust. If operation at other temperatures should be desired for system integration, propellants such as benzoic acid (higher temperature) or biphenyl (lower temperature) could be substituted.

Vaporizing Metal. The high vapor pressure of zinc suggests its use as a propellant for thrust requirements in the 10^{-9} to 10^{-5} lbf range where rapid response is not required, and where a relatively high duty cycle is desired. Power requirements for such a propulsion system are low, comparable to subliming ammonia compounds. Thrust level is adjusted by varying surface area and temperature (vapor pressure) in the 300 to 500°F range.

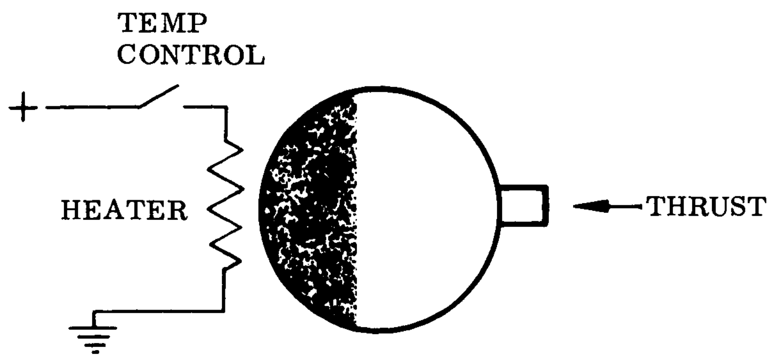

Fig. 3-3 Valveless Design

A laboratory device (Fig. 3-4) was constructed at LMSC by wrapping a glass-insulated resistance wire about a 2-inch diameter zinc disc weighing 121 grams. This was enclosed in a glass-wool pad on all but the front face. The assembly was placed in a short Dewar flask for further isolation. The Dewar was mounted so that the front face of the disc was directed toward the receptor paddle of an indirect thrust-measuring balance. A thermocouple was inserted in a shallow hole on the disc surface. The heating wire was connected to a power supply. The system was pumped down to 0.40 ± 0.15 micron.

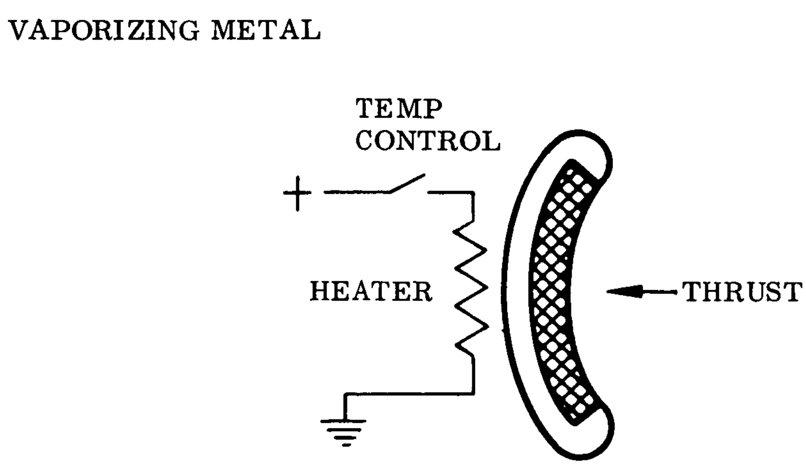

Fig. 3-4 Laboratory Metal Vaporizing Device

In this low thrust range there is a definite thermal effect on the measurement balance. Compensation was effected by measuring the apparent thrust of an aluminum disc and subtracting this from the observed thrust of the zinc disc. Over the thrust range of 4×10^{-7} to 3×10^{-5} lbf, the measured zinc thrust was reasonably close to the theoretical values calculated from vapor pressure data.

Section 4
PROGRAMMING POTENTIAL

Experience in the tradeoff studies indicated that in order to make an objective comparison of low-thrust systems, some of which are fully developed while others are only conceptually designed, the selection must be based on weight and, to some extent, reliability. Cost can only be roughly estimated for advanced systems, since development expense is often unpredictable. State-of-development is no criterion since the advanced systems are admittedly underdeveloped. Producibility can provide only an arbitrary comparison of existing and advanced systems, but it can serve as a basis for discarding advanced system designs which are appreciably more difficult to produce than existent systems. The size of the minimum pulse bit was eliminated since all systems met the requirements of the Phase I missions, insofar as the latter are presently known.

The fourth task, as originally planned, was to establish the feasibility of programming the system selection process described in Section 2. It was concluded that programming was feasible but unessential, since the only two parameters (weight and reliability) found valid for advanced planning purposes can be displayed on a two-dimensional plot.

Section 5
REFERENCES

1. Lockheed Missiles & Space Co., Mission and Low-Thrust Solid and Hybrid Reaction System Definition, LMSC-A847751, 15 Feb 1967

2. Handbook of Chemistry and Physics, 45th Edition

3. J. W. Mellor, A Comprehensive Treatise on Inorganic and Theoretical Chemistry, Vol. II, Supp. I, p. 179

4. J. W. Mellor, A Comprehensive Treatise on Inorganic and Theoretical Chemistry, Vol. II, p. 114, 1961

5. Dow Chemical Company, JANAF Thermochemical Tables, 1963 and later

6. C. R. Tipton, Jr., Editor, Reactor Handbook, 2nd Ed., Vol. I Materials

7. North American Aviation, Stability of a Light Metal Hydride (U), NAA-SR-8533, 1963 (C)

8 North American Aviation, Mechanisms of Light-Metal Hydride Reactions (U), ROD-R-6193, 1965 (C)

9. P.M. O'Donnell, NASA-TN-D-3992 Kinetics of the Fluorination of Beryllium, 1967

10. J. Phys. Chem 67, 2156-9, 1963

11. S. W. Mayer, J. B. Szabo, L. Schieler, and H. S. Johnston, WSCI 65-24, 1965

Appendix A
DEFINITION OF LOW THRUST REACTION CONTROL SYSTEM CHARACTERISTICS

The selection of a low thrust reaction control system (LTRCS) to satisfy mission performance and installation requirements requires a careful review of LTRCS characteristics to assist in matching the performance and design criteria. The fundamental limits of fabrication feasibility, the heat producing processes (where applicable) and the operational efficiency factors have been examined and compared with demonstrated performance. The results of this evaluation are presented in Table 1-1 of this report. The following paragraphs describe work performed in this evaluation for the pressurized cold gas, vaporizing liquid, monopropellant hot gas hydrazine, monopropellant cold gas, bipropellant liquid and bipropellant vapor systems.

A.1 PRESSURIZED COLD GAS SYSTEMS

Cold gas systems which are commonly employed may use hydrogen, helium, carbon tetrafluoride (Freon 14), or nitrogen. Cold gas systems are well developed and relatively simple although high pressure storage creates some problems. Since nitrogen is the most commonly used gas, it was selected for this analysis. The gas, typically stored at a pressure of 3000 psia, is regulated to the desired working pressure and routed to the thrust nozzles through solenoid actuated shutoff valves. The initial step in the evaluation of fundamental limits for low thrust systems involves an examination of the basic thrust formula:

$$F_n = A_t P_c C_f$$

where

F_n = net thrust

A_t = throat area

P_c = chamber pressure

C_f = nozzle thrust coefficient

From Table 1-1 the upper limit of thrust capability for nitrogen is noted to be greater than 10 lbf, an upper limit to the area of interest for this study. Since this thrust level has been repeatedly demonstrated on the LMSC Agena spacecraft and since this configuration does not constitute an upper limit for design capability, no analysis of the upper thrust limit was performed. The minimum thrust level of 1×10^{-3} lbf was established from a practical feasibility for drilling a small throat for the nozzle with a No. 80 drill (0.0135 in. diameter). This provides a throat area (A_t) of 0.154×10^{-3} in.^{2}. It is further assumed that the lowest reasonable pressure to which a pressure regulator can be expected to provide accurate and reliable operation is in the region of (P_c) = 4–5 psia. A nozzle thrust coefficient (C_f) of 1.66 is obtained from nozzle performance tables using the ratio of specific heats for nitrogen of 1.4, a nozzle expansion ratio of 15 with an infinite pressure ratio across the nozzle.

$$F_n = A_t P_c C_f$$

$$1 \times 10^{-3} \approx (0.154 \times 10^{-3})(4.0)(1.66)$$

The nearest experience to this low value is reported in Ref. A-1 at a thrust level of 0.002 lbf. Throat diameters less than 0.010 in. are considered to be unsatisfactory due to the high potential for partial or complete blockage by contaminants. Regulation of the gas pressure to values less than 4–5 psia introduces an accuracy problem due to frictional loads in the moving parts.

The specific impulse of a propellant is dependent on temperature, pressure, molecular weight and ratio of specific heats. Based on nitrogen at 70° F, 4 psia and using a nozzle expansion ratio of 15, the specific impulse of 60 lbf sec/lbm is derived and agrees with data reported in Refs. A-2 and A-3.

The minimum impulse bit which can be delivered as a function of command control may be defined as the product of the minimum thrust level and the minimum time interval for opening and closing the thrust chamber valve. The minimum time interval for valve actuation is primarily a function of development experience. For this application, an actuation time of 10 milliseconds from start of opening through full open to complete closure is consistent with existing hardware. The specific impulse associated with the minimum impulse bit is assumed to be 60 lbf-sec/lbm. This implicitly assumes that nozzle efficiency factors are characteristic of continuum flow and that no reaction occurs during expansion.

A.2 VAPORIZED LIQUID SYSTEMS

Vaporized liquid systems have been considered for use in LTRCS; however, no systems are known to have been flown. Candidate propellants for a vaporized liquid system have been limited to water and ammonia. The use of ammonia is preferred due to its better storage characteristics (low freezing point and high vapor pressure) in a spacecraft environment. Storage of the propellant is accomplished in a positive expulsion tank at a pressure level 50 to 100 psi above the vapor pressure associated with its thermal environment (vapor pressure is 150 psia at 77° F). The gas is regulated to the desired working pressure. The evaluation of fundamental limits for maximum thrust, minimum thrust and minimum impulse bit is identical to that presented in the preceding discussion of pressurized cold gas systems and results in maximum thrust levels greater than 10 lbf, minimum thrust levels of 1×10^{-3} lbf and minimum impulse bits of 7.5×10^{-6} as noted in Table 1-1. The specific impulse for vaporized ammonia can be computed to reach 100 sec at 70° F. However, due to the need to add heat to the vapor after expansion through the pressure regulator and due to the further tendency to condense during expansion through the nozzle, a delivered specific impulse of 85 lbf-sec/lbm is estimated to be realized for both the steady state condition and the minimum impulse bit condition.

A.3 MONOPROPELLANT HOT GAS SYSTEMS

The application of monopropellant hydrazine LTRCS to satisfy mission requirements has recently become attractive to vehicle and systems engineers as a result of the development of the new catalyst, Shell 405. Monopropellant hydrogen peroxide has been utilized successfully in both manned and unmanned spacecraft. However, the storage limitations for hydrogen peroxide and the higher specific impulse of hydrazine have resulted in the selection of hydrazine for most new applications. Storage of the propellant is accomplished in a positive expulsion tank. The propellant is discharged through the pressure regulator to the propellant distribution manifold. The assignment of thrust level limits, minimum impulse bit and specific impulse noted in Table 1-1 was accomplished based on test data noted in Refs. A-3 and A-4. Since thrust levels substantially above 10 lbf have been demonstrated, no analysis of the upper limit was conducted. The minimum thrust level and minimum impulse bit were based on current technology due to the complex relationship that exists between catalyst, chamber pressure and the propellant flow rate. The specific impulse associated with very-low thrusts is degraded to 190 sec or less due to operation at very-low pressures where incomplete decomposition is favored. A further reduction to 140 sec occurs when the impulse bits are reduced to the minimum possible with rapid valve actuation.

A.4 MONOPROPELLANT COLD GAS SYSTEMS

Monopropellant cold gas systems are attractive for LTRCS applications since the primary propellant storage is in liquid form while the thrust nozzles operate on gas generated from the stored liquid. Although either hydrogen peroxide or hydrazine propellants appear feasible, only hydrazine has been selected for use. This system is characterized bythe storage of a limited quantity of gas, generated from the liquid, until thrustor operation lowers the accumulator pressure below a preset level. The most efficient operation of the system is dependent upon minimizing the cooling of decomposed hydrazine stored in the accumulator. The assignment of thrust level limits, minimum impulse bit and specific impulse, noted in Table 1-1, was accomplished using information obtained from Ref. A-3. The upper thrust level limit was not investigated since operation at over 10 lbf is limited only by the gas supply. The minimum thrust level of 0.5×10^{-3} lbf was estimated based on a design analysis which included consideration of the nozzle throat diameter, gas storage pressure, and gas temperature. The anticipated decay of temperature of the decomposed hydrazine is also responsible for the relatively low delivered specific impulse of 110 lbf-sec/lbm which is well below the level noted for monopropellant hot gas systems. However, since no chemical reaction process takes place between the accumulator and the thrust nozzle, the specific impulse is not reduced when operating at the minimum impulse bit of 0.3×10^{-3} lb/sec.

A.5 BIPROPELLANT LIQUID SYSTEMS

Bipropellant liquid systems have been used extensively at thrust levels of 1 lbf or more for reaction control systems. These applications normally use hypergolic propellants since the use of a separate ignition system degrades the overall system reliability. Experimental bipropellant rockets have been built and successfully tested at thrust levels down to 0.1 lbf, but at lower thrusts orifice plugging and extreme sensitivity to fabrication limits for alignment of injectors is encountered. At relatively low thrusts, specific impulse at steady state is less than delivered performance at thrust levels above 10 lbf due to the thrust chamber size effect on combustion kinetics. A delivered specific impulse of 300 lbf-sec/lbm is considered to be maximum for bipropellant liquid systems operating at less than 1 lbf. Operating at the minimum impulse bit of 1×10^{-3} lb-sec the delivered specific impulse is estimated to be further reduced to 150 lbf-sec/lbm due to thermal losses induced by the transient start and stop portions of each short pulse. The losses become significant parts of the overall pulse performance.

A.6 BIPROPELLANT VAPOR SYSTEMS

Bipropellant vapor rockets have been built and tested at thrust levels of 10×10^{-3} lbf and should be feasible at thrust levels down to 1×10^{-3} lbf. Hypergolic, cryogenic or semicryogenic propellants are best suited for this application since high confidence in the quality of vapor results when used in most environments. The delivered specific impulse for steady state operation has been demonstrated to be $\approx$ 350 lbf-sec/lbm. However, the use of vapor induces a performance sensitivity to mixture ratio which will result from minor changes in the regulated feed pressure. Due to the thermal losses induced by the transient start and stop portions of a single short pulse, a lower delivered specific impulseof $\approx$230 lbf-sec/lbm is estimated to occur.

A.7 REFERENCES

A-1 "Electrical Propulsion for Control of Stationary Satellites," AIAA Preprint 3009, Mar 1963

A-2 Hughes Aircraft Company, Spacecraft Attitude Control Gas Systems Analysis, HAC-SSD-70172R, Apr 1967

A-3 "A Review of Microrocket Technology – 10^{-6} to 1 lbf Thrust," AIAA Preprint 65-620, Jun 1965

A-4 Hamilton Standard, Mini-Thrust System, Interim Development Report, Report SLS 6521, (not dated)

Appendix B
PHASE I MISSION REQUIREMENTS

B.1 ATS-4

From Ref. 1 (p. 3-10) the minimum required torque in attitude control is twice the disturbing torque. Assuming a value of 4.5×10^{-4} ft-lb for the disturbing torque, a minimum correction torque of 9×10^{-4} ft-lb is calculated. This corresponds to a minimum thrust of 30×10^{-6} lb. The maximum duty cycle can be no more than 50 percent, or there would be a net gain in angular velocity. However, at 30×10^{-6} lb and 833 lb-sec per thruster, the total on-time is 2.77×10^{7} sec. This corresponds to a 44 percent duty cycle, within limits.

The maximum thrust is derived from the minimum pulse bit of about 10^{-2} lb-sec (Ref. 1, p. 3-12). If the minimum firing time is 15 millisec, the upper thrust limit is 0.7 lbf.

The maximum impulse requirement for slewing is 2.6×10^{-2} lb-sec (Ref. 1, Table 3-6). This must be performed in less than 30 min and the thrust level must only exceed 1.4×10^{-5} lbf. This is below the minimum attitude control level above and can be performed by the attitude control thruster. A slewing impulse requirement of 180 lb-sec was neglected relative to the much larger attitude-control requirement.

The minimum thrust level for east-west station-keeping is determined by the sum of the solar pressure and triaxiality effects. This corresponds to 49×10^{-6} lbf or, for an 1800-lb vehicle, 2.72×10^{-8} g acceleration. If applied continuously in the appropriate direction, a total impulse of 3060 lbf-sec is required. The use of a matching continuous low thrust involves some loss of effective impulse due to directional changes over an extended period. Higher thrusts for shorter duty cycles avoid this inefficiency. Thrusts of 232×10^{-6} lb and higher were calculated to avoid effective impulse loss.

The north-south station-keeping function arises principally from solar and lunar gravitational forces, and the propulsion system was required to be effective for only one year. A total impulse of 5420 lb-sec was required at thrust levels of 1.27×10^{-3} lb or higher to avoid any directional impulse loss. This corresponded to duty cycles of 13-1/2 percent or lower.

Station attainment is likely to require makeup of velocity deficits of 100–200 ft/sec. Reference 6 in LMSC-A847751 gives the following acceleration requirements and periods in which to be accomplished:

	Acceleration	
Velocity Deficit	Long. Shift (60 deg)	Long. Shift (120 deg)
100 ft/sec	3.3 μg (11 days)	1.7 μg (22 days)
200 ft/sec	13.2 μg (5 days)	6.6 μg (11 days)

For an 1800 lb satellite, the extremes correspond to limits of 3 to 24 mlbf thrust. From Formula (1) in Ref. 1, limits of 3 to 11 mlbf are calculated. The highest limit of 24 mlbf was chosen for this study. This corresponds to a total impulse of 10,300 lb-sec.

B.2 VOYAGER

The evasive maneuver requires 34.2 lb-sec total impulse. The separation could take place over a 2-day period without impairing the mission (Ref. B-1). This would correspond to a thrust level $\geqq 2 \times 10^{-4}$ lbf.

The attitude control function was originally planned to require 0.044 lbf thrust (Ref. 1, p. 3-26). A subsequently published study (Ref. B-2) of a Voyager-type mission suggests a maximum thrust requirement of 340 lb-sec over a 5-hr period for roll calibration. This corresponds to a thrust of 0.019 lbf. This value was chosen instead of 0.044 lbf in order to afford the maximum opportunity for application of low-thrust systems.

B.3 ATM

The limits of thrust required for attitude control are described in Ref. 1 (p. 3-30). The upper limit of 4.2 lbf is set by the roll control requirement. The lower limit of 0.016 lbf is set by the slewing requirement. The lower limit for attitude control is 2.4×10^{-3} lbf for each axis or 5800 lb-sec for a 28-day mission. An equal amount of impulse was arbitrarily assigned for slewing.

B.4 EVA

The thrust level and total impulse required for Extra Vehicular Activities (EVA) were set at 1 lbf and 2500 lb-sec in Ref. 1 (P. 3-36).

B.5 REFERENCES

B-1 B. Ellis, LMSC Private Communication

B-2 Hughes Aircraft Company, HAC-SSD 70172R, April 1967

Appendix C
VAPOR AND LIQUID SYSTEM WEIGHTS

One of the principal criteria employed in the selection of a reaction control system is overall system weight. System weights have been estimated, based on existing components that are compatible with the environmental operational, and performance requirements. The following paragraphs describe working bases for the pressurized cold gas, vaporizing liquid, monopropellant hot-gas hydrazine, monopropellant cold-gas, bipropellant liquid, and bipropellant vapor systems.

C.1 PRESSURIZED COLD GAS SYSTEMS

System weights for pressurized cold gas LTRCS vary principally as a function of the stored total impulse. This is due to the relationship of the relatively low specific impulse (60 sec) which necessitates the storage of a large mass of gas when compared with the weights for low thrust nozzles and their associated shutoff valves. The pressurized cold gas LTRCS schematic presented in Fig. C-1 is representative of the components required and their general arrangement.

C.2 VAPORIZING LIQUID SYSTEMS

System weights for vaporized liquid LTRCS vary principally as a function of the stored total impulse. This is due to the relationship of the specific impulse (≈ 85 sec), which necessitates the storage of a large mass of liquid, compared with weights for low thrust nozzles and their associated shutoff valves. The vaporized liquid LTRCS schematic presented in Fig. C-2 is representative of the components required and their general arrangement.

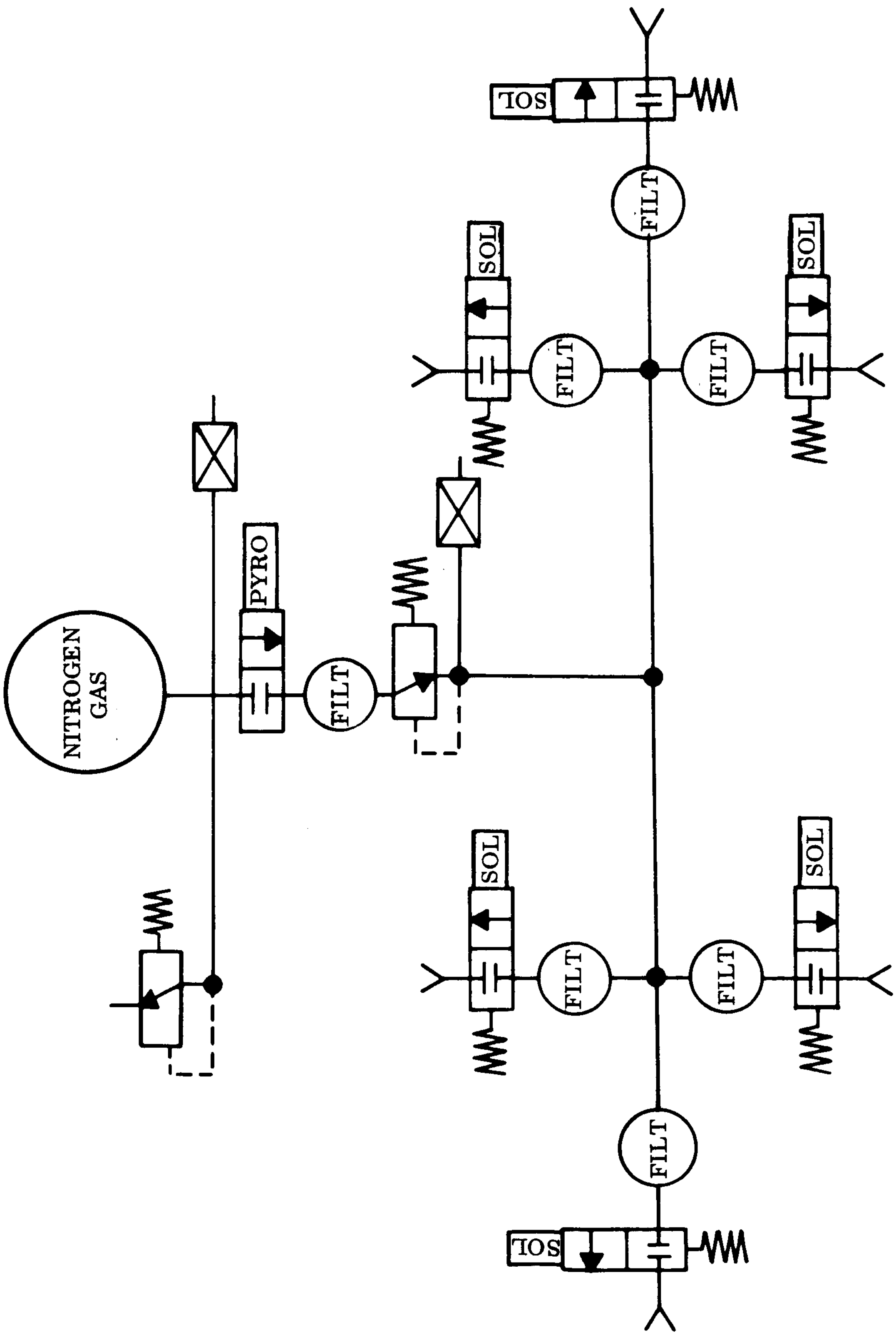

Fig. C-1 Pressurized Cold Gas System

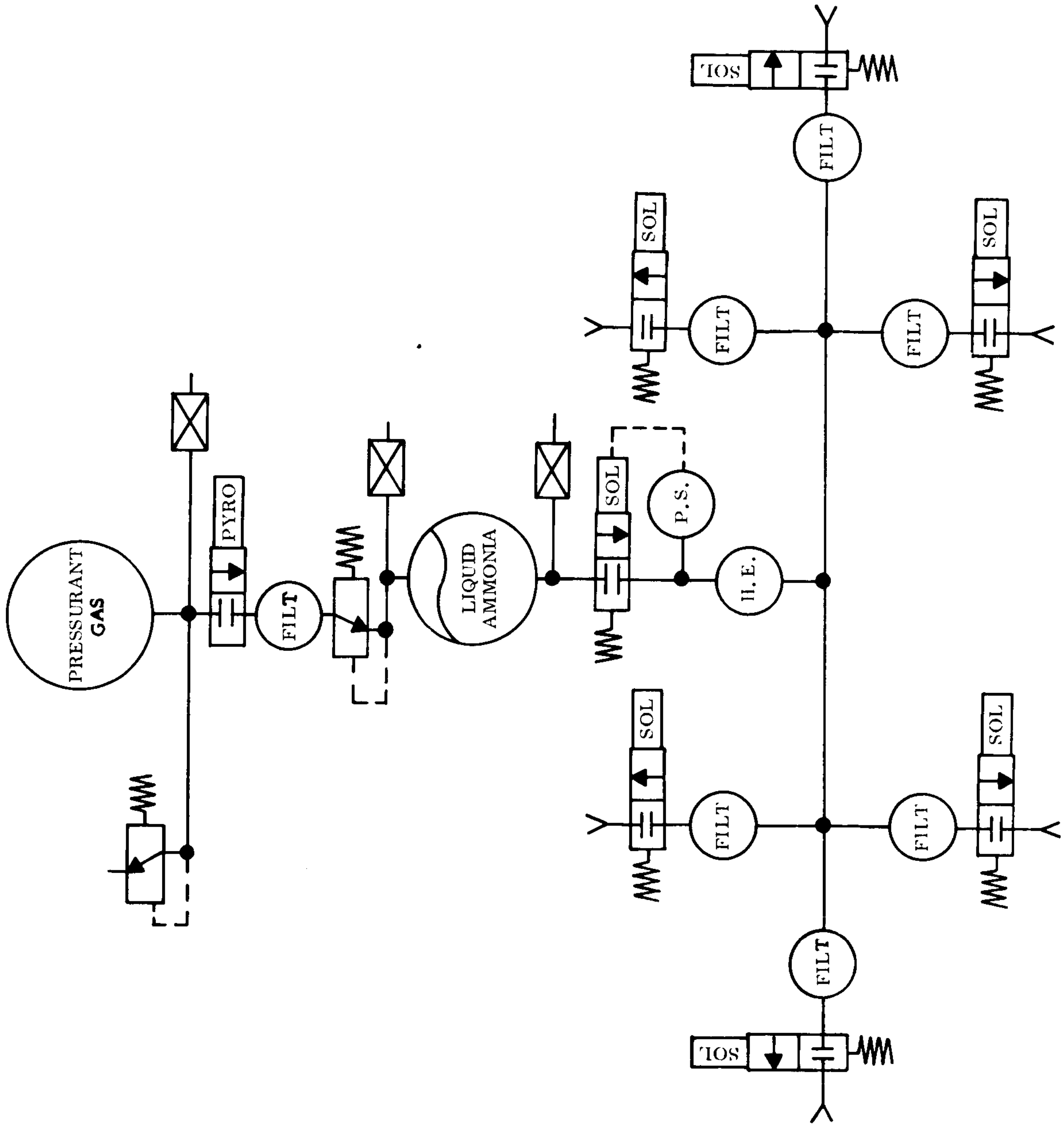

Fig. C-2 Vaporized Liquid System

C.3 MONOPROPELLANT HOT-GAS HYDRAZINE SYSTEMS

System weights for monopropellant hydrazine LTRCS are less than weights for pressurized cold gas and vaporized liquid systems due to the higher delivered specific impulse. The system schematic for monopropellant hot-gas, presented in Fig. C-3, is representative of the components required and their general arrangement.

C.4 MONOPROPELLANT COLD-GAS SYSTEMS

The general arrangement of components for the monopropellant cold-gas system closely parallels the arrangement of components for the monopropellant hot-gas system. The notable differences are the use of an accumulator or plenum chamber with the cold-gas system (Fig. C-4), and the use of a single catalyst reactor on the cold-gas system in lieu of catalyst reactors on each thrust nozzle for the hot-gas system. The lower delivered specific impulse of the monopropellant cold-gas system results in higher overall system weights.

C.5 BIPROPELLANT LIQUID/VAPOR SYSTEMS

Bipropellant liquid rockets have been extensively developed for attitude control applications requiring thrust levels above 1 lbf. At lower thrust levels, the problems of manufacturing small propellant injectors and preventing their contamination in operation may be resolved by vaporizing the liquid before injection into the thrust chamber. General arrangements for each of these systems are presented in Figs. C-5 and C-6. Typically, propellants for bipropellant liquid systems, such as nitrogen tetroxide with Aerozine-50, are in the earth-storable class. The bipropellant vapor systems would use fluorine with methane or hydrogen. The influence on system weights of the higher specific impulse is noticeable when compared with monopropellant systems.

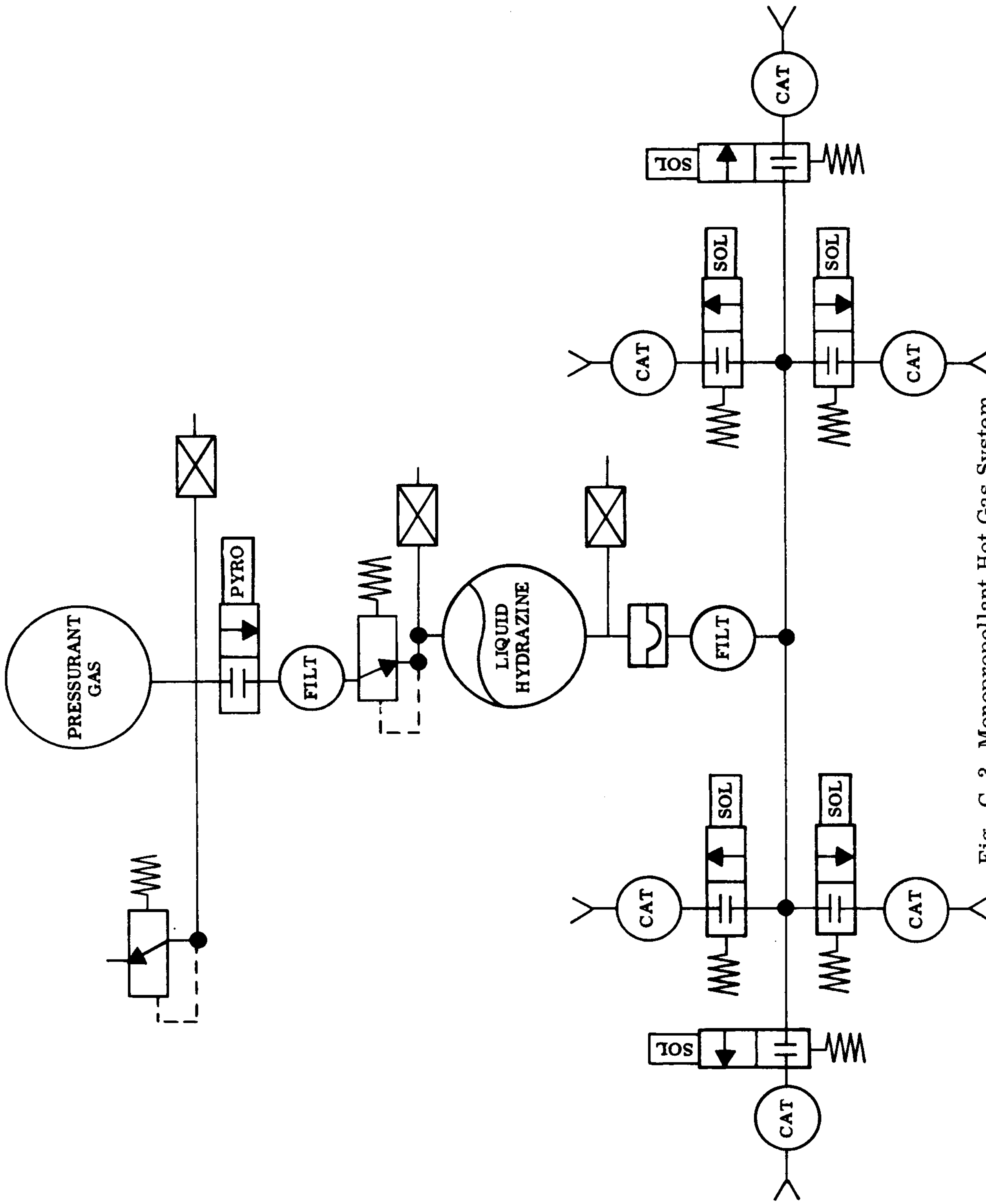

Fig. C-3 Monopropellant Hot Gas System

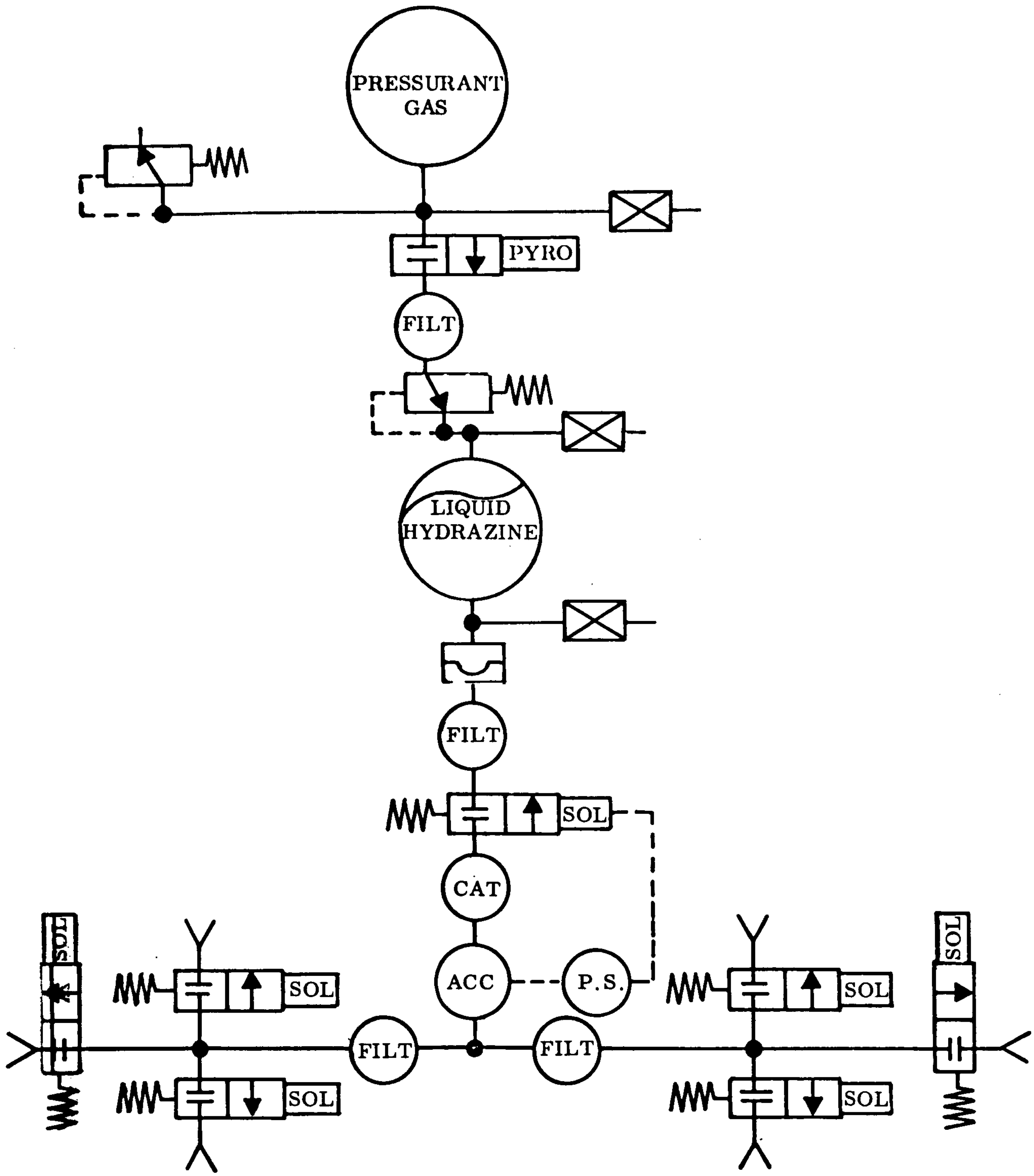

Fig. C-4 Monopropellant Cold Gas System

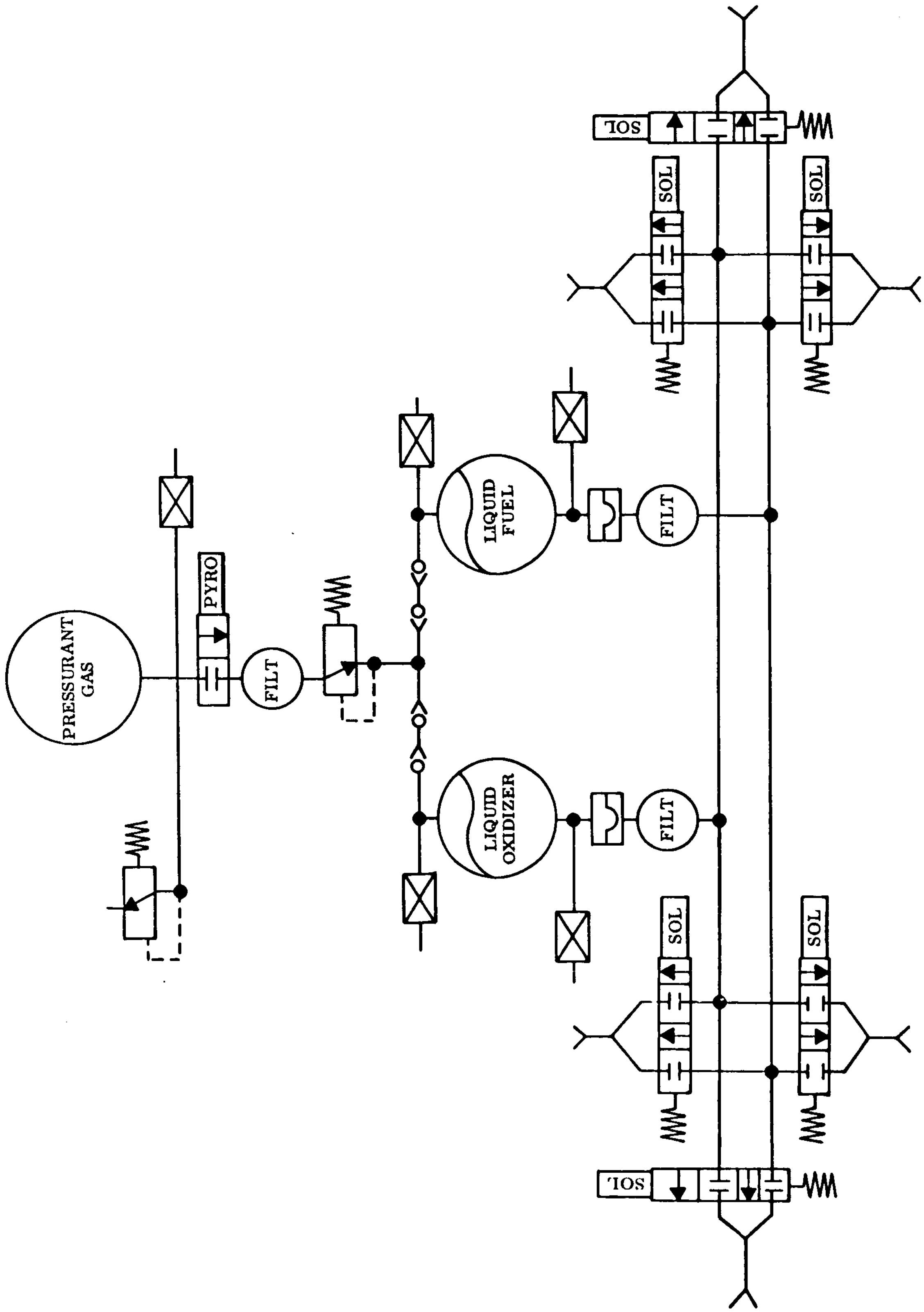

Fig. C-5 Bipropellant (Liquid) System

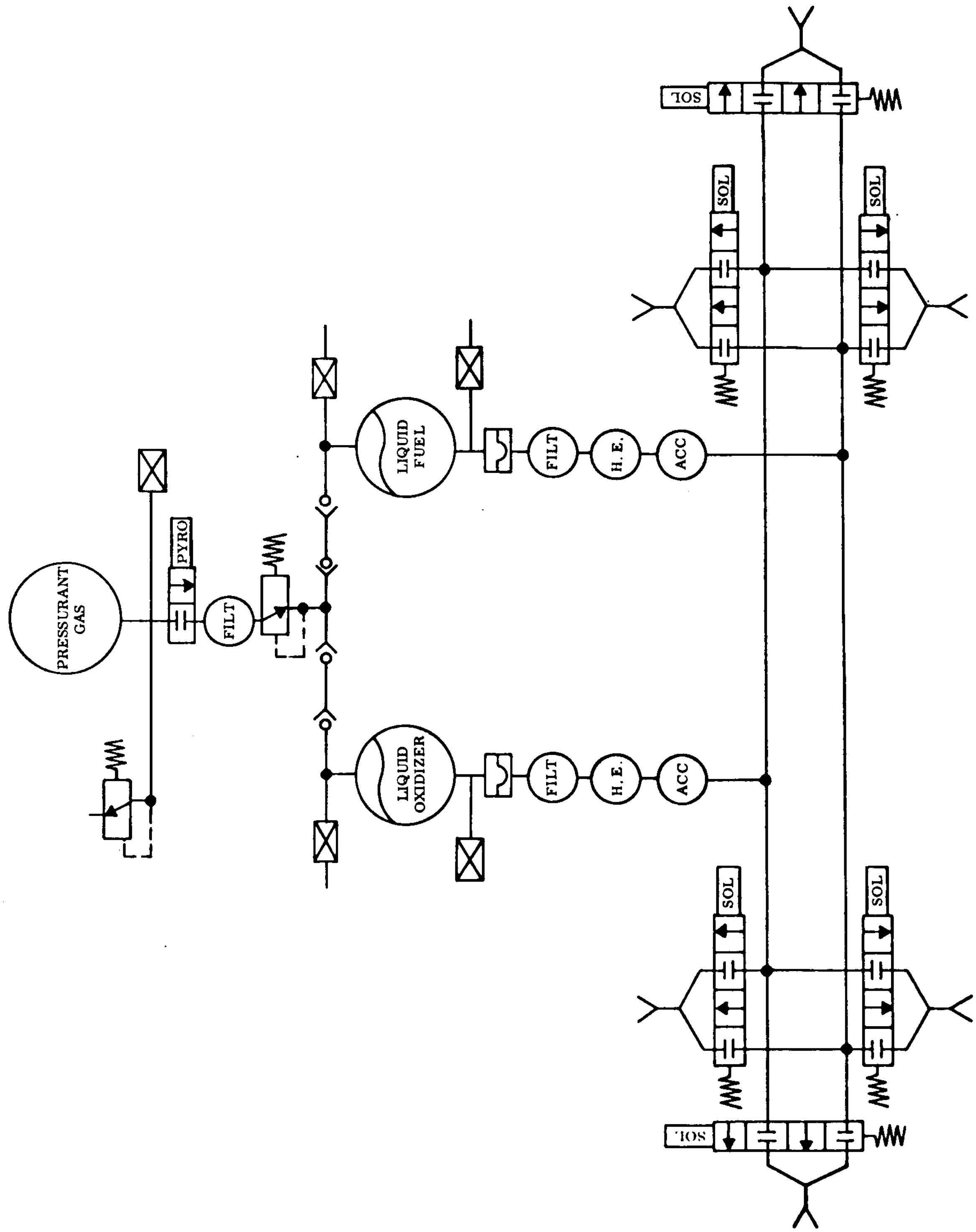

Fig. C-6 Bipropellant (Vapor) System

C.6 STUDY RESULTS

Estimates of component weights for high/low thrust levels and high/low total impulse capacities were obtained from a review of existing systems. The components such as shutoff valves, pressure regulators feed lines, filters and thrust nozzles were assigned weights consistent with the fixed thrust level (minimum thrust or maximum thrust) while tankage and propellant weights were varied in accordance with total impulse requirements and the delivered specific impulse. From this data the variation of system weight as a function of thrust level and total impulse were plotted in Figs. C-7 through C-12). These curves were compared with data from Refs. C-1 and C-2 and found to be in excellent agreement.

Separate plots were prepared to illustrate the influence of operation at steady state conditions and operation at minimum impulse bit conditions. Particular attention was given to the preparation of estimates for total impulse quantities less than 1000 lb-sec and this data is presented in Figs. C-8 and C-10.

This study illustrates the significant influence of specific impulse on overall system weights where the total impulse exceeds 1000 lb-sec. Where the total impulse is less than 1000 lb-sec the basic system is sensitive to the number and size of the individual components and thus will necessitate further consideration for each mission or application encountered.

C.7 REFERENCES

C-1 Hughes Aircraft Company, Spacecraft Attitude Control – Gas Systems Analysis, HAC-SSD-70172R Apr 1967

C-2 "Electrical Propulsion for Control of Stationary Satellites," AIAA Preprint 3009, Mar 1963

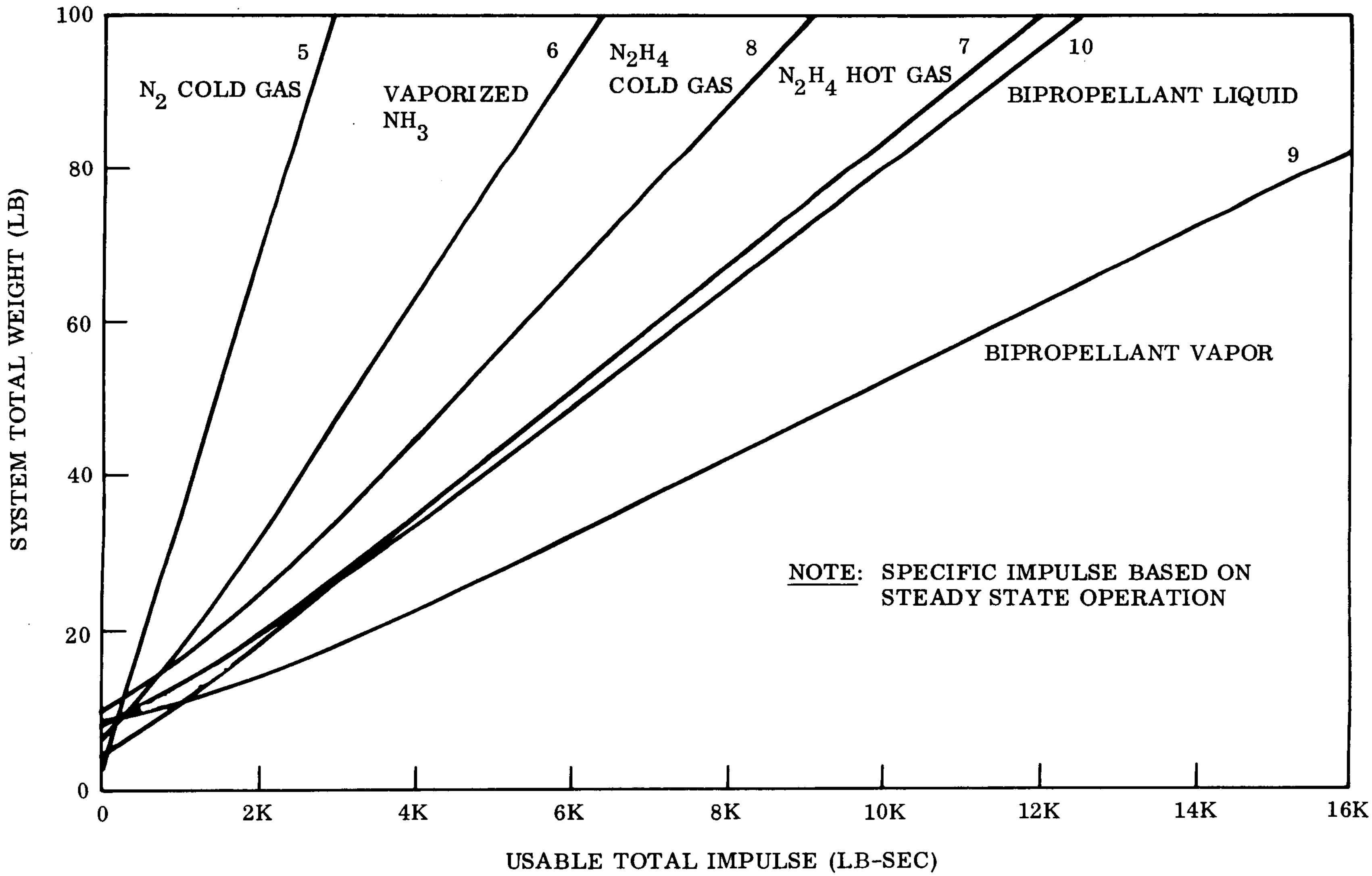

Fig. C-7 System Comparison Minimum Thrust Configuration

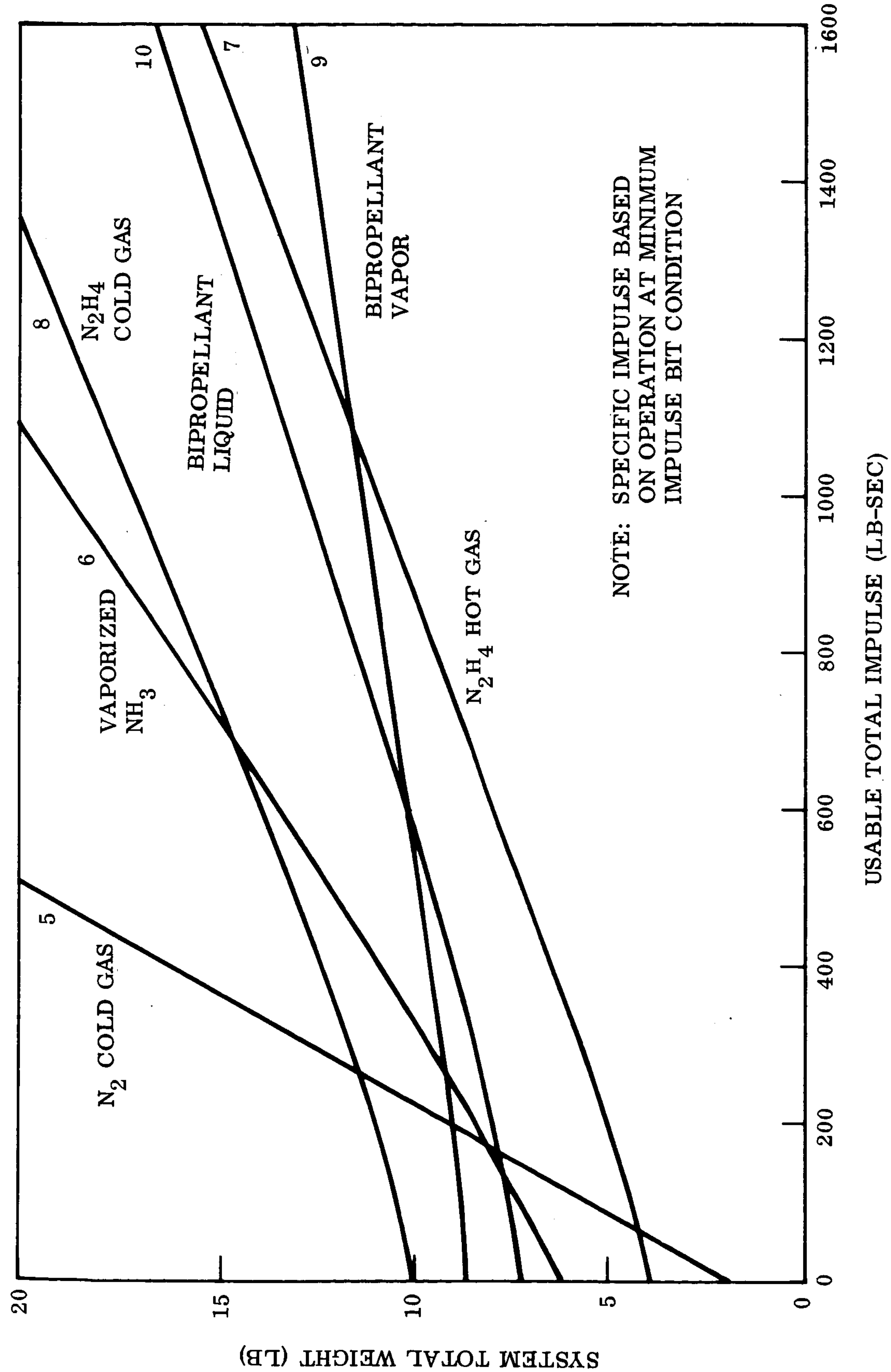

Fig. C-8 System Comparison Minimum Thrust Configuration

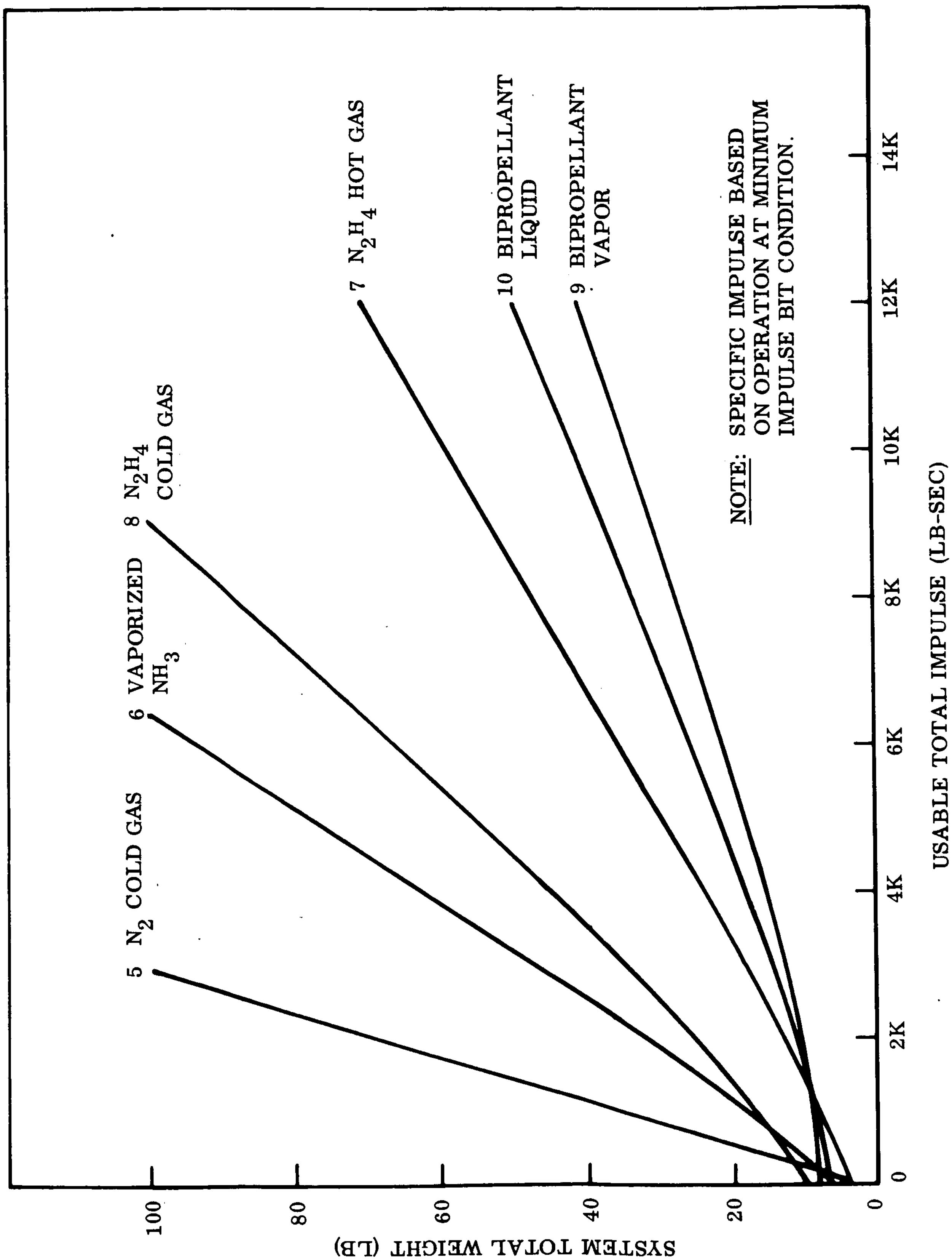

Fig. C-9 System Comparison Minimum Thrust Configuration

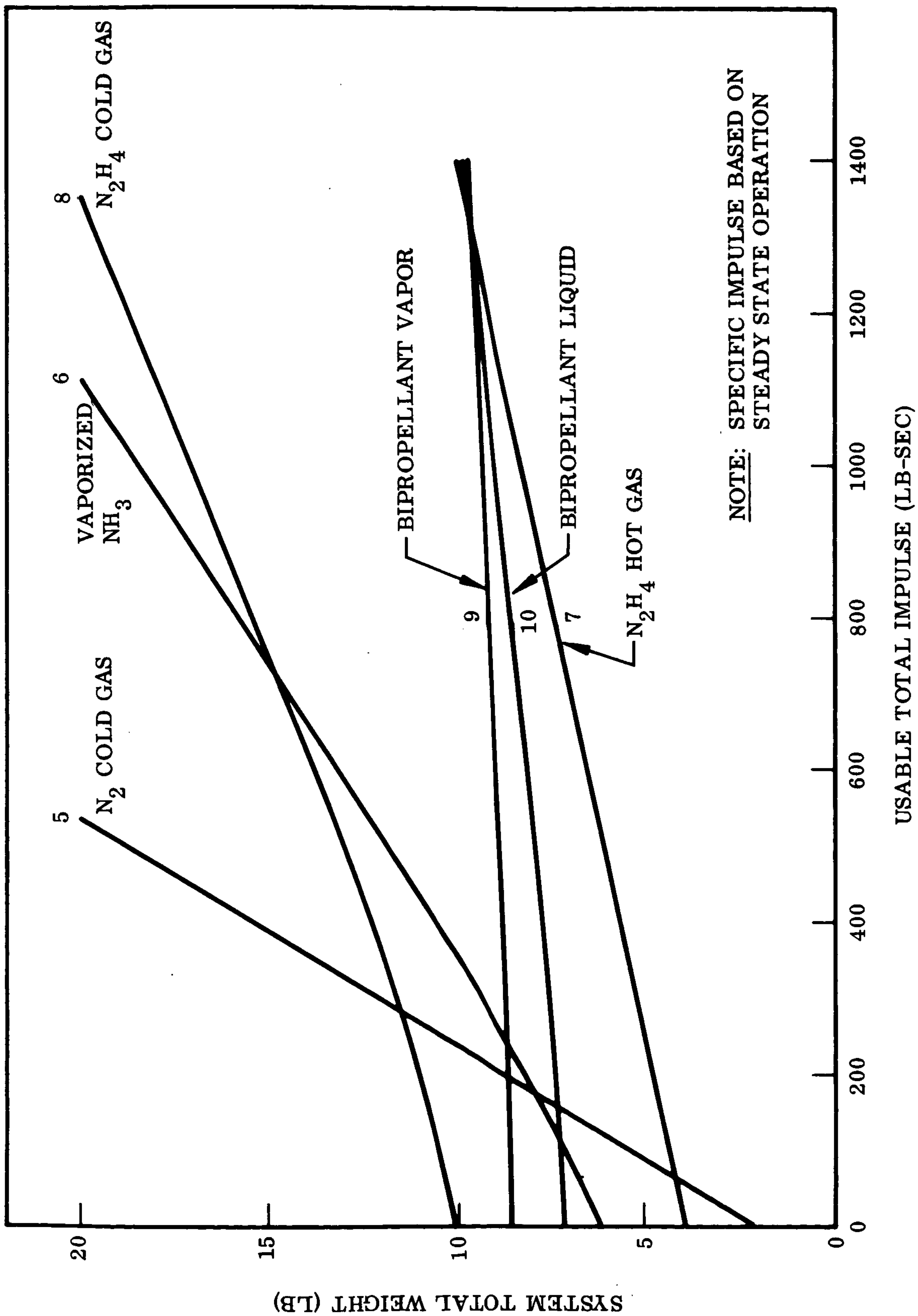

Fig. C-10 System Comparison Minimum Thrust Configuration

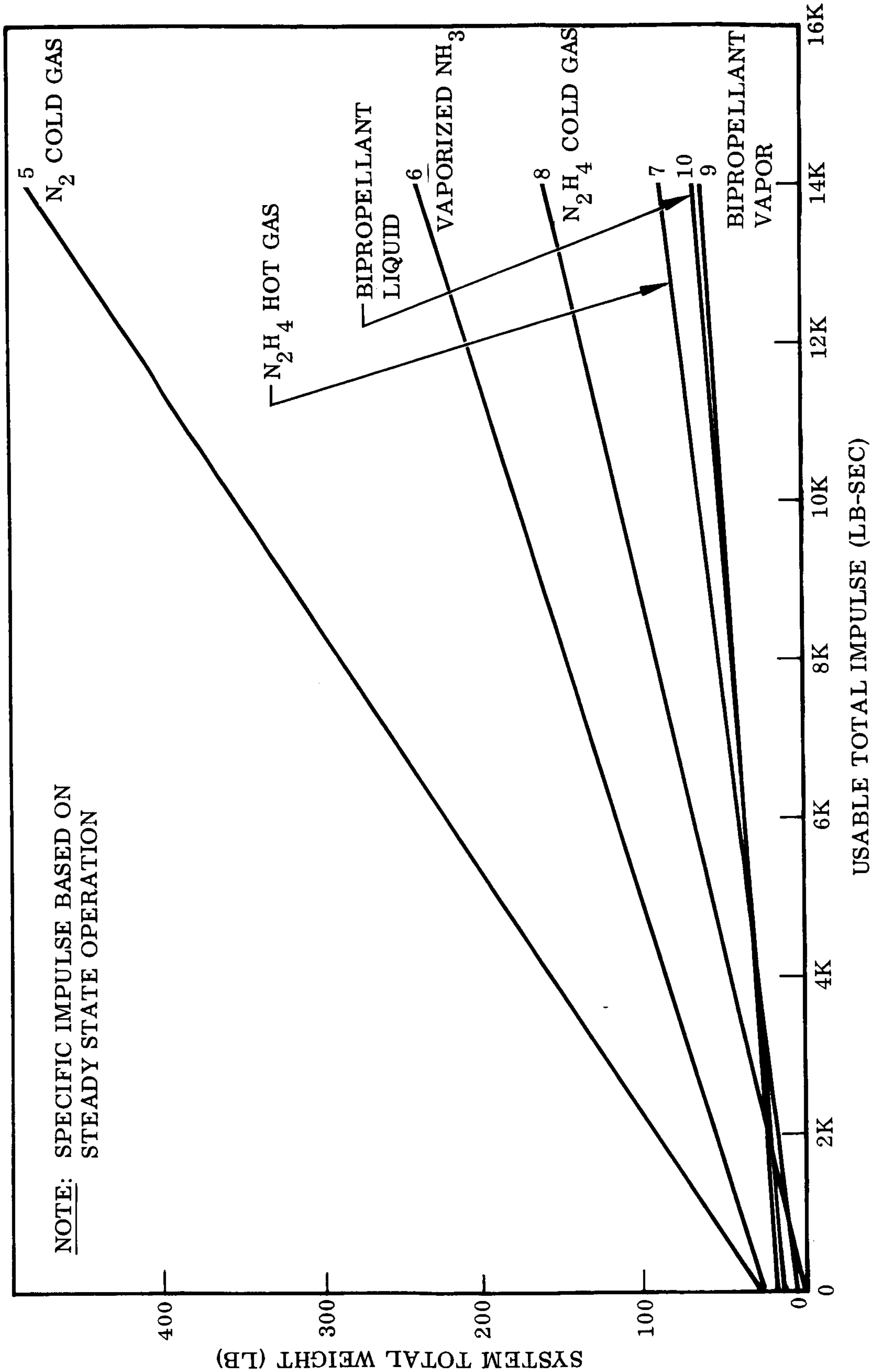

Fig. C-11 System Comparison Maximum Thrust Configuration

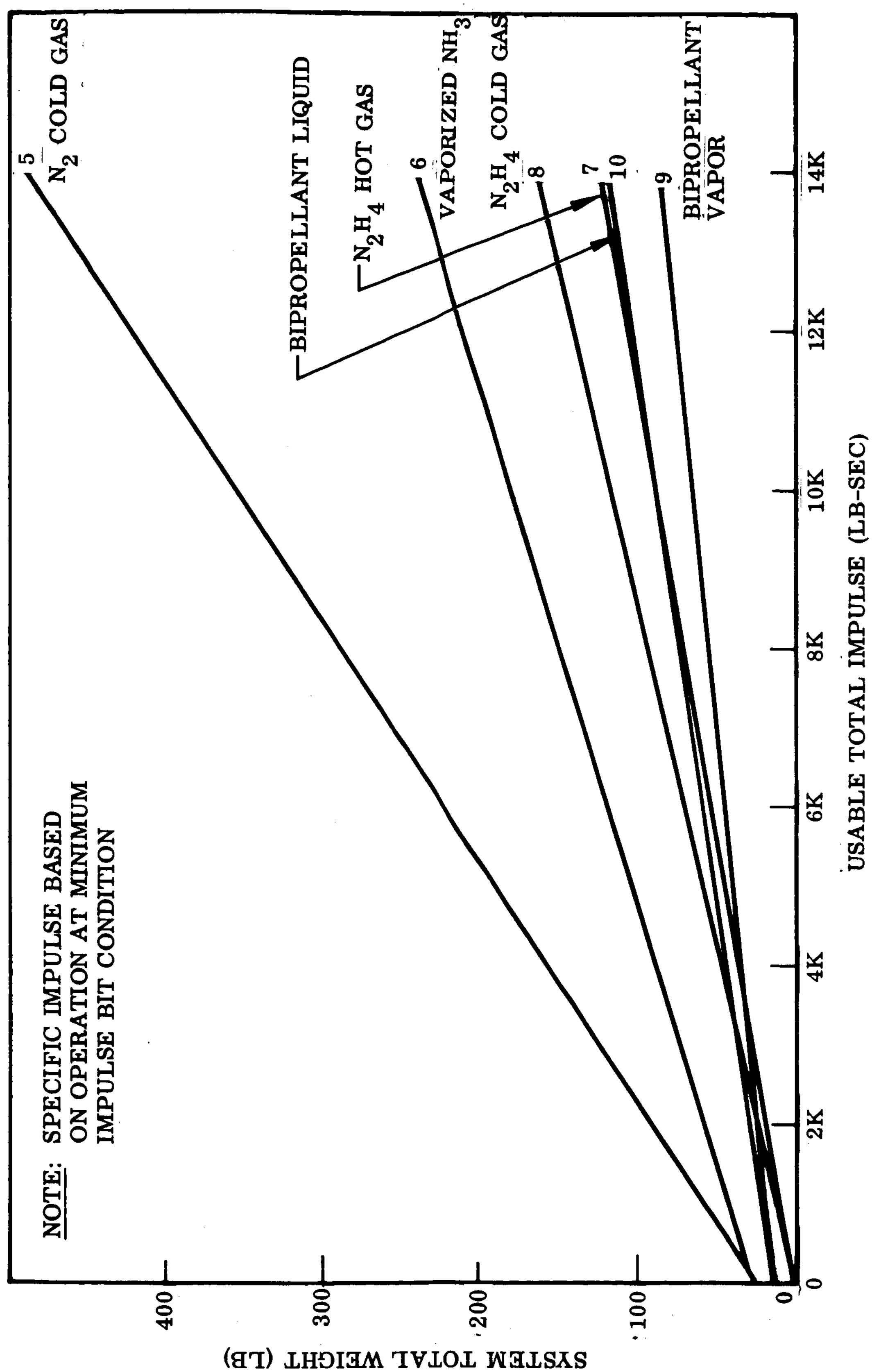

Fig. C-12 System Comparison Maximum Thrust Configuration

C.8 SYMBOLS

Pressure regulator valve .... 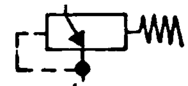

Pressure relief valve .... 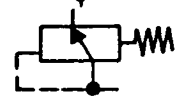

Shutoff valve manual (fill or vent) .... 

Shutoff valve, pyrotechnic actuated (normally closed)................ 

Shutoff valve, solenoid actuated (normally closed) .... 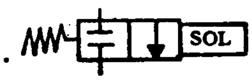

Rupture disc .... 

Check valve .... 

Filter .... 

Heat exchanger .... 

Catalyst .... 

Accumulator .... 

Line joint .... 

Bypass .... 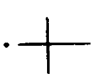

Thruster.. 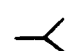

Appendix D
ELECTRICAL SYSTEM WEIGHTS

The electrical system weights are estimated by summing the various items making up the system. These are:

- Propellant and tankage
- Valves and feed lines
- Power conditioning circuitry
- Power source (solar cell panels)
- Supporting structure

Wherever possible, weight parameters based on existing flight or prototype hardware are used. When weight estimates involve scaling down from existing systems, the parameters are adjusted to account for the fixed minimum weights associated with the irreducible size of certain components and their packaging. Based on prior experience, parameters were weighted to account for relative simplicity or complexity of the system and whether the system is compact or distributed throughout the spacecraft.

Propellant weight is calculated from the total impulse required and the specific impulse of the candidate thruster. A fixed percentage is added to this weight to account for tankage.

Valve and feed line weights are based on part count and weight of actual hardware.

Power conditioning weight is estimated using a specific weight of 0.02 lbm/w plus an additional fixed weight of the order of 1 lbm. Additional weight of switching equipment is included where multiple thrusters operate from a central power conditioning unit.

Power source weight is computed using a specific weight of 0.27 lbm/w for the solar panels.

Power requirements are determined by the specific characteristics of the thruster. In all cases involving multiple thrusters except the thermal storage resistojet, no more than one thruster is assumed to operate at any time.

Structural weights are estimated on the basis of weight, simplicity, and compactness of the system.

D.1 WATER ELECTROLYSIS

The weight parameters and power requirements are chosen to be compatible with the characteristics of an existing sytem of 30,000 lbf-sec total impulse, developed by Hughes Aircraft Co.

D.2 AMMONIA RESISTOJET

For most missions studied, a fast-heatup concept, in which power is supplied only during thrusting periods, was best-suited. However, one mission required a thermal-storage type in which heat for short periods at relatively high thrust is stored as sensible heat of a massive heater body.

The power requirements are determined from a 10- to 20-w radiation loss plus the heat required to raise the propellant temperature in the case of the fast-heatup type, or a constant input of 30 w per thruster for the thermal storage type.

D.4 ION ENGINE

System weights are based on weights of components developed by Hughes Research Laboratories and Electro-Optical Systems for comparable missions. A central power conditioning unit is employed where multiple thrusters are required.

D.5 COLLOID

The colloid thruster develops thrust by acceleration of massive colloidal ions. It operates efficiently over a specific impulse range of 400 to 1500 lbf-sec/lbm in its present state of development. Since higher specific impulse allows reduction of propellant weight at the expense of higher power requirement, an optimization for each mission is possible. The weight estimates include such optimization, with system weight parameters based on components developed by TRW.

D.6 PULSED PLASMA

The weights quoted are those of a system developed by Grumman/Fairchild-Hiller.

D.7 PENNING DISCHARGE

The weight estimates employ weight parameters based on a prototype system developed at NASA, Lewis Research Center.

Appendix E
PASSIVE SYSTEM WEIGHTS

A preliminary survey of the capability of passive systems to meet the several attitude control requirements eliminated many of the systems for the reasons indicated in Table E-1. Surviving combinations are indicated by + signs.

Table E-1

MISSION APPLICABLE ATTITUDE CONTROL SYSTEMS
(Preliminary Survey)

Attitude Control System \ Mission	ATS-4 (2 Years)	ATM (23 Days)	Voyager Transfer (6 Months)	Voyager Orbit (Elliptical) (6 Months)
Gravity-Gradient	+	Inaccurate (also not local vert.)	Negligible gravity field	Highly elliptical orbit
Gravity-Gradient/ Passive CMG	+	Inaccurate (also not local vert.)	Negligible gravity field	Highly elliptical orbit
Active Control-Moment Gyros	+	+	+	+
Magnetic Torquers	2 axes only; no maneuvers	Inaccurate	Negligible magnetic field	Magnetic field unknown
Magnetic Torquer/ Momentum Wheel	2 axes only; no maneuvers	Inaccurate	Negligible magnetic field	Magnetic field unknown

The field was narrowed further by elimination of the gravity gradient systems for ATS-4 attitude control. The gravity gradient restoring torques are:

$$\text{pitch} \quad T_{ygg} = 3\omega_o^2 (I_x - I_z)\,\theta$$

$$\text{roll} \quad T_{xgg} = 3\omega_o^2 (I_y - I_z)\,\phi$$

The disturbance torques due to solar pressures are given in Table 3-5 of Ref. 1.

	Disturbance Torque (10^{-6} ft-lb)	
	Pitch	Roll
Total symmetric array	145	85
Total offset array	145	310

Stabilization to at least ±0.3 deg is required. To achieve restoring torques equal to the disturbance torques at 0.3 deg requires inertia differences shown below:

	Inertia Differences (slug-ft^2)	
	$I_x - I_y$	$I_y - I_z$
Symmetric Array	174×10^4	102×10^4
Offset Array	174×10^4	372×10^4

Inertias of the order of 2×10^6 slug-ft^2 are required. With 100-ft booms, tip masses of 200 slugs or approximately 6000 lb are required. A gravity gradient system is therefore impractical. Furthermore, gravity gradient systems do not permit orientation and tracking.

The active control moment gyros (CMG) are the only remaining passive contenders. Individual mission weight assignments follow.

E.1 ATS-4

Four scissored single gimbal CMGs (2 each for stabilization and slewing) were as follows, with H = 25 ft-lb-sec each:

Each CMG:	Rotor	2.5 lb	(12,800 rpm)
	Torquer	3.8 lb	(0.078 w average power; provides 1/4 rad/sec maximum gimbal rate)
	Misc. hardware	12.3 lb	
	System wt	18.6 lb	
	Power wt	8.4 lb	(31 w at 0.27 lbm/w)
		27.0 lb	

E.2 ATM

Three double gimbal CMGs with H = 100 ft-lb-sec each were as follows:

Each CMG:	Rotor	6.5 lb	(14,000 rpm)
	Torquers (2)	16.4 lb	(0.63 w average power; provides 1/4 rad/sec maximum gimbal rate)
	Misc. hardware	20.1 lb	
	System wt	43.0 lb	
	Power wt	10.3 lb	(38 w at 0.27 lbm/w)
		53.3 lb	

E.3 VOYAGER

Three single gimbal CMGs with H = 3 ft-lb-sec each are as follows:

Each CMG:	System wt	15.5 lb	(11,600 rpm)
	Power wt	1.9 lb	(7 w, at 0.27 lbm/w)
		17.4 lb	

The only remaining application of passive control systems to the given missions was that of momentum discharge on ATM by a magnetic torquer. The weight of this torquer was estimated to be 20 lb and the weight of an associated timer 2 lb. The required magnet weight is 1000 lb/ft-lb at the orbital altitude. The torque is determined as follows:

Given

i = inclination angle = 28.5 deg

γ = angle between earth's magnetic dipole and spin axis = 11 deg

η = orbit position angle

T_B = torque about body

M_B = magnetic moment of magnet

$T_{B/o}$ = transformation from orbital to body axis system

H_o = magnetic field

$$H_{xo} = \frac{M_\epsilon}{r^3} \cos \eta \sin i$$

$$H_{yo} = -\frac{M_\epsilon}{r^3} \cos i$$

$$H_{zo} = \frac{2M_\epsilon}{r^3} \sin \eta \sin i$$

Assuming body axes and orbit axes coincide,

$$T_B \cong M_B \times H_o$$

It can be shown that for

$$M_y = M_z = 0 \Rightarrow \quad I_x = 0$$

$$I_y = -\frac{2M_\epsilon}{r^3}\sin i \int_{t_2}^{t_3} M_x \sin \eta \, dt$$

$$I_z = -\frac{M_\epsilon}{r^3}\cos i \int_{t_1}^{t_2} M_x \, dt$$

$$M_x = \begin{cases} M_x \; ; \; \text{for} \; , \; 0 < \eta < 2\pi & \text{(for z axis discharge)} \\ M_x \,\mathrm{Sgn}\sin\eta \; ; \; \text{for} \; , \; 2\pi < \eta < 4\pi & \text{(for y axis discharge)} \end{cases}$$

$\therefore$ every other orbit

$$I_{y_{\substack{\text{per orbit} \\ \text{(every other)}}}} = -\frac{2M_\epsilon}{r^3}\sin i \, M_x \left(\frac{4}{\omega_o}\right)$$

$$I_{y_{\substack{\text{per orbit} \\ \text{(every other)}}}} = -\frac{4M_\epsilon}{\pi r^3} M_x T_o \sin i$$

$$I_{z_{\substack{\text{per orbit} \\ \text{(every other)}}}} = -\frac{M_\epsilon}{r^3} M_x T_o \cos i$$

For the mission

$$I_y = +\frac{2M_\epsilon M_x P_o \sin i}{\pi r^3}$$

$$I_z = + \frac{M_\epsilon M_x P_o \cos i}{2r^3}$$

where

P_o = mission period

The larger value for M_x comes from the I_y equation since I_y and I_z are equal.

$$M_x = \frac{\pi r^3 I_y}{2M_\epsilon P_o \sin i}$$

but

$$I_y = T_y P_o$$

where

T_y = equivalent constant disturbance torque

$$M_x = \frac{\pi r^3 T_y}{2M_\epsilon \sin i}$$

$$T_M = M_x \frac{M_\epsilon}{r^3} = \frac{\pi T_y}{2 \sin i}$$

$$M_x \sim \text{lb-ft/orsted}$$

$$\frac{M_\epsilon}{r^3} \sim \text{orsted}$$

$\therefore$ T_m = required torque of magnet in ft-lb

$$W = \frac{1000\ \text{lb}}{\text{ft-lb}} \left(\frac{\pi}{2} \frac{T_y}{\sin i} \right) = 19.8\ \text{lb} \qquad \text{for} \quad \begin{aligned} i &= 28° \\ T_y &= 6 \times 10^{-3}\ \text{ft-lb} \end{aligned}$$

Appendix F
COMPONENT RELIABILITIES

In order to derive the reliabilities it is necessary that several assumptions be made:

- That any element of the system is assigned a reliability numeric which represents the best available index of its performance as of the current period 1967−70.
- That any component used which may be novel in its application, but exists as actual hardware is assigned a reliability numeric applicable to its actual present use.
- That any class of component is assigned a reliability/failure rate which is the value ascribed to its genus, i.e., check valve vs. fill valve, both fall into the generic category of high reliability valves.
- That components such as tanks and monolithic devices such as baffles or accelerators are almost infinitely reliable when designed to proper safety factors, adequately tested, and not subjected to extremes of stress.
- That the probability of a chemical change not taking place given the required conditions is almost infinitely small.

All components were product-ruled to find the primary reliability values, as all of the systems appear to be in series with respect to the operation of their components; that is, all must operate or the system fails. Where alternate configurations to any one system are postulated, the redundancies included are incorporated into the system to achieve the more reliable final numeric.

The rationale accompanying this report explains the method by which the reliability values for 1975 and 1980 are evolved, and from an intensive study of the available literature referenced, as well as the USAF index of reliable components, appears to be completely defensible and in fact a conservative method. The period in question over which reliability improvement may be noted is actually 4 yr, but for the sake of conservatism, 5 yr has been used.

From a study of all of the numbers evolved and tabulated it may be discerned that all of the systems under review are quite closely related with respect to reliability, or probability of survival in functioning condition in a space environment. While this may not prove true under actual space simulation tests or flights, this result is to be expected in a reliability predictive assessment, due to the similarity of hardware used in many of the systems. It follows then that reliability cannot be used as a decision tool to choose candidates, or a candidate, to develop or produce.

F.1 RATIONALE

Bases for the results shown in Table 2-6 were:

- All probability of survival P_S values assume 50 percent confidence level (in absence of test data)
- State-of-the-art improvement suggests an improvement for systems of no less than:

$$R_{1975} = \sqrt{R_{1970}} \quad , \quad R_{1980} = \sqrt{R_{1975}}$$

(MTBF doubles every five years)

These are from trends reported in failure rate improvement for aerospace hardware (Refs. F-1 and F-2).

F.2 COMPONENT RELIABILITIES

F.2.1 Subliming Solid Reaction Control System

	R_{1yr}
Structure s/s	.9999
Pressure Controller	.9997
Control and TLM	.9995
Power Cond. and Regn.	.9995
Thermal s/s	.9999
Propellant s/s	.9999
	.9984

F.2.2 Superheated Subliming Solid RCS

	R_{1yr}
Superheated nozzle may degrade R by .002, although the resistojet heater is rated at 0.99999.	
	.9964 – 0.9983

F.2.3 Hybrid Hydrogen Monopropellant System

	R_{1yr}
Self-regulating valve	.99996
Self-regulating valve	.99996
Gas/water tank	.9999
Injector	.99999
Solenoid valve	.9996
Gas/solids tank	.9999
Solids Separation Screen	.99999
	.9993

F.2.4 Repetitive Impulse Generator

	R_{1yr}
Pulse generator	.9997
Switching mechanism	.99987
Motor	.99995
	.9995

F.2.5 Cold Gas System A

	R_{1yr}
Nitrogen Tank	.9999
Relief valve	.9996
Fill/drain valve	.9996
Pyro valve	.9996
Filter (3)	.99997
Regulator	.99995
Nozzles (6)	.99994
	.9987

F.2.6 Cold Gas System B

	R_{1yr}		
Same as above except			
Pyro valve	.9993	Active redundancy	.99925
Regulator	.99995		
	.9991		

F.2.7 Vaporized Liquid Ammonia System

		R_{1yr}
Helium tank		.99999
Relief valve		.9996
Inlet Regulator	Active redundance	.99999
Burst disc		.99999
Heat exchanger		.99999
Nozzles (6)		.99994
		.9995

F.2.8 Monopropellant Hydrazine A

	R_{1yr}
Helium tank	.99999
Relief valve	.9996
Control valve	.9996
Filter (3)	.99997
Fill valve	.9996
N_2H_4 tank	.99999
Nozzles (2)	.99994
	.9987

F.2.9 Monopropellant Hydrazine B

	R_{1yr}
Same except Control valve active redundance	
	.9991

F.2.10 Monopropellant Cold Gas Generator A

	R_{1yr}
Helium tank	.99999
Fill valve	.9996
Control valve (2)	.9992
Filter (4)	.99996
N_2H_4 tank	.99999
Gas generator	.99993
Decompression N_2H_4 tank	.99999
Release valve	.9996
Nozzles (6)	.99994
	.9982

F.2.11 Monopropellant Cold Gas Generator B

	R_{1yr}
Same as above except Control valve (2) active redundance	
	.9990

F.2.12 Bipropellant Vapor

	R_{1yr}
Helium tank	.99999
Oxygen tank	.99999

Fuel tank	.99999
Control valve	.9996
Check valve (2)	.9992
Fill valve (3)	.9988
Heat exchanger (2)	.99998
Filter (3)	.99997
Nozzle (6)	.99994
	.9975

F.2.13 Bipropellant Liquid A

	R_{1yr}
Helium tank	.99999
Fill valve (3)	.9988
Control valve	.9996
Relief valve (2)	.9992
Check valve (2)	.9992
Oxygen tank	.99999
Fuel tank	.99999
Filters (3)	.99997
Nozzle (6)	.99994
	.9967

F.2.14 Bipropellant Liquid B

	R_{1yr}
Same as A version except:	
Control valve (active redundancy	
Check valve (active redundancy	
	.9979

F.2.15 Water Electrolysis System

	R_{1yr}
Electrolysis cell	.999995
Zero G venting device	.999995
Fill valve	.9996
Relief valve	.9996
Burst diaphragm	.999999
Power supply solar cells	.99995
Relay	.99999
Pressure switch	.99999
Start valve	.99995
Filter	.99999
Regulator	.99995
Nozzle	.99999
Igniter	.99997
	.9990

F.2.16 Ammonia Resistojet

	R_{1yr}
Propellant tank	.99999
Valves (2)	.99992
Vaporizer and phase separator	.9994
Pressure regulator	.99995
Control & TLM	.9995
Power conditioning and regulation	.9995
Heater	.99995
Thermal element	.99999
Nozzle	.99999
	.9982

F.2.17 Cesium Contact Ion Engine

	R_{1yr}
Propellant feed	.99999
Vaporizer	.9994
Valve	.99996
Heater	.99995
Control and TLM	.9995
Power conditioning and regulation	.9995
Acceleration/deceleration electrodes	.99999
Ionizer	.99999
Neutralizer	.99999
	.9983

F.2.18 Electron Bombardment Ion Engine

	R_{1yr}
Propellant feed	.99999
Vaporizer	.9994
Valve	.99996
Control and TLM	.9995
Conditioning and regulation	.9995
Neutralizer	.99999
Acceleration/deceleration electrodes	.99999
Cathode	.99999
	.9982

F.2.19 Colloidal Ion Engine

	R_{1yr}
Propellant feed	.99999
Valve	.9996
Colloid generator	.99999
Acceleration/deceleration electrodes	.99999
Neutralizer	.99999
Propellant flow control	.9996
Control and TLM	.9995
Power conditioning and regulation	.9995
	.9982

F.2.20 Pulsed Plasma Engine

	R_{1yr}
Propellant feed	.99999
Acceleration/deceleration electrodes	.99999
Control and TLM	.9995
Power conditioning and regulation	.9995
Capacitor	.99999
Trigger circuit	.9996
	.9986

F.3 REFERENCES

F-1 RADC Failure Rate Data, 1958 Vs. Autonetics Minute Man Failure Rate Data, 1963

F-2 Naval Ordnance Laboratories (FARADA), 1967 (Accepted Sources by DOD, NASA)

Appendix G
HYDROGEN-FLUORINE REACTION KINETICS

The rate of the hydrogen-fluorine reaction is given by Ref. G-1

$$\frac{d(HF)}{dt} = k(F_2) \tag{G.1}$$

The lack of dependence on hydrogen concentration is noteworthy. A single value of $k = 0.022\ \text{sec}^{-1}$ at 110° C is given. Apparently, no energy of activation for the reaction was determined (although an energy of activation (ΔE_a) of 16.7 kcal is cited later (Ref. G-2) for the oxygen-inhibited reaction of hydrogen and fluorine). From Ref. G-3 the calculated ΔE_a = 50 kcal and the observed ΔE_a > 25 kcal for the molecular H_2 - F_2 reaction. The former is in reasonable agreement with values of 45 - 50 kcal quoted (Ref. G-4) for the other halogen-hydrogen reactions.

An alternate to the molecular reaction mechanism involves a chain of atomic reactions:

$$1/2\ F_2 \rightarrow F \tag{G.2}$$

$$F + H_2 \rightarrow HF + H \tag{G.3}$$

$$H + F_2 \rightarrow HF + F \tag{G.4}$$

Activation energies for the components of this chain have been determined or estimated individually. For reaction (G-2), ΔE_a = 18.5 kcal (Ref. G-2, p. 415). The ΔE_a for (G-3) and (G-4) are estimated to be 5 kcal and 2 kcal, respectively (Ref. G-5). The sum of this alternate path is only 25.5 kcal, assuming the recombination activation energies to be zero. The atom chain path is therefore the favored path, relative to the much higher ΔE_a for the molecular reaction.

The modified form of the Arrhenius equation used for the rate constant k is therefore,

$$k = AT^{1/2} \exp[-25,500/RT] \tag{G.5}$$

where A is the frequency factor for the first-order reaction, $R = 1.987$ cal mole^{-1} deg K^{-1}, and T is the absolute temperature, °K.

From the value of k at 110°C, equation (G-6) is calculated:

$$\frac{d(HF)}{dt} = 3.80 \times 10^{11}\, T^{1/2} \exp[-25,500/RT] \tag{G.6}$$

G.1 REFERENCES

G-1 J. Phys. Chem. 67, 2156–9 (1963)

G-2 J. Phys. Chem. 69, 408–15 (1965)

G-3 S. Glasstone, K. J. Laidler and H. Eyring, The Theory of Rate Processes, McGraw-Hill Book Co., Inc., New York (1941), p. 236.

G-4 K. J. Laidler, Chemical Kinetics, McGraw-Hill Book Co., Inc., New York (1950), p. 217

G-5 J. Amer. Chem. Soc. 86, 2115–19 (1964)

Appendix H
ANALYSIS OF HYPERGOLIC IGNITION FOR A GASEOUS OXIDIZER-FUEL SYSTEM

The prediction of ignition for a flowing stream of completely mixed gases which can undergo a chemical reaction is rather difficult. Several simplifying assumptions are necessary to make solution of this problem practical. The approach taken in the present instance is to determine the temperature as a function of combustion chamber duct length, assuming that there is no axial heat conduction in the reacting gases.

Determination of the thermodynamic coordinates requires simultaneous solution of the equations of state, continuity, energy, and momentum. The formal analytical description of such a system of equations is facilitated by using the influence coefficients of the independent variables of heat loss, internal heat generation, frictional loss and change in molecular weight. A glossary of terms used is given at the conclusion of this appendix.

H.1 GENERAL ARRANGEMENT

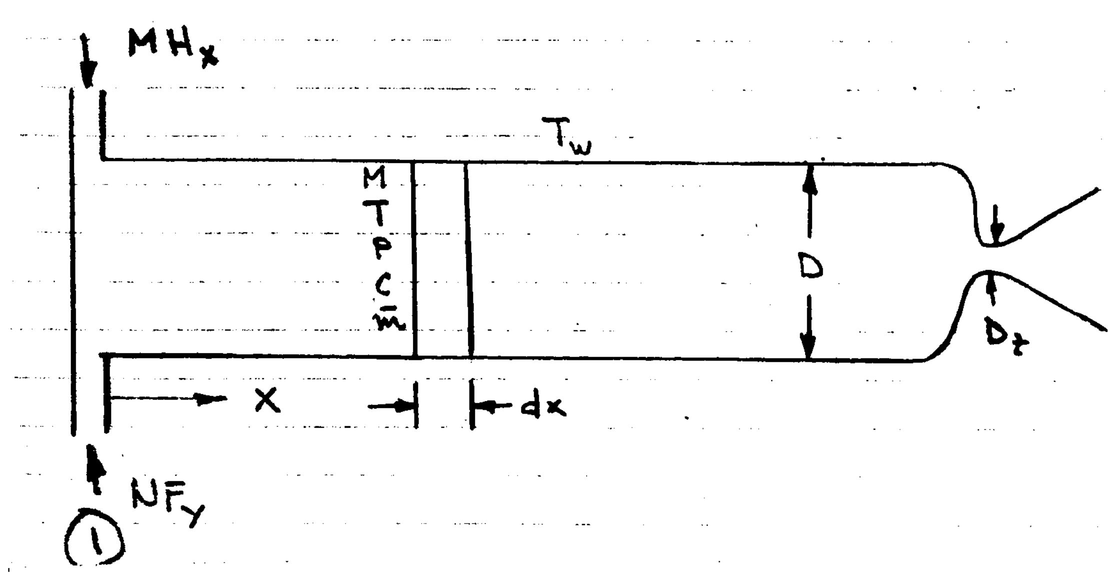

H.2 SYSTEM OF EQUATIONS

$$\frac{dT}{T} = \frac{1-\gamma M^2}{1-M^2}\,\frac{1}{c_p T}\,(dQ + dH) - \frac{\gamma(\gamma-1)M^4}{1-M^2}\,\frac{4f}{D}\,dx + \frac{(\gamma-1)M^2}{1-M^2}\,\frac{d\bar{m}}{\bar{m}}$$

$$\frac{dp}{p} = -\frac{\gamma M^2}{1-M^2}\,\frac{1}{c_p T}\,(dQ + dH) - \frac{\gamma M^2\left[1+(\gamma-1)M^2\right]}{2(1-M^2)}\,\frac{4f}{D}\,dx + \frac{\gamma M^2}{1-M^2}\,\frac{d\bar{m}}{\bar{m}}$$

Determination of specific heat loss

$$dQ' = c_p \rho A\, dx\, dT \qquad \text{(H.1)}$$

$$\text{define} \quad dQ \equiv \frac{dQ'}{\rho A\, dx} = c_p\, dT \qquad \text{(H.2)}$$

From heat transfer relationship

$$dT = -\frac{4}{D_c}\, st\,(T - T_w)\, dx$$

$$\therefore \quad dQ = -\frac{4\, c_p\, st}{D_c}\,(T - T_w)\, dx \qquad \text{(H.3)}$$

where

$$st = \frac{0.019}{Re^{0.2}\, P_r^{2/3}} \qquad \text{(H.4)}$$

Determination of internal energy generation

$$dH = \Delta H \, dc$$

Assuming a second order reaction

$$\frac{dc}{dt} = k(a-c)(a-b)$$

or

$$dc = k(a-c)(a-b)\left(\frac{dt}{dx}\right)dx$$

since

$$\frac{dx}{dt} = V$$

$$dc = \frac{k}{V}(a-c)(a-b)\,dx \qquad \text{(H.5)}$$

hence

$$dH = \Delta H \, k(a-c)(b-c)\,dx \qquad \text{(H.6)}$$

where

$$k = A e^{-\frac{\Delta H_a}{RT}} \qquad \text{(H.7)}$$

Determination of velocity from continuity equation

$$V = \frac{\dot{m}}{\rho A_{cs}}$$

since

$$\rho = \frac{\bar{m} P}{R T}$$

$$V = G \frac{R T}{\bar{m} P} \tag{H.8}$$

Determination of Mach Number

$$M = \frac{V}{c} = \frac{G}{\rho \sqrt{\gamma g_c R T}}$$

$$M = \frac{G}{\sqrt{\gamma g_c P/\rho}} \tag{H.9}$$

Determination of Molecular Weight

It is assumed that a linear relationship exists between the molecular weight of the reactants and the products

$$\therefore \quad \bar{m} = \frac{c}{a} \bar{m}_p + \left(1 - \frac{c}{a}\right) \bar{m}_r \tag{H.10}$$

$$d\bar{m} = \frac{\bar{m}_p - \bar{m}_r}{a} dc \tag{H.11}$$

The system of equations represented by Eqs. (H.1) through (H.11) allows prediction of the temperature and pressure as a function of combustion chamber length.

Considerable simplification is possible by choosing conditions for which the change in pressure is negligible. In all instances it can be assumed that the chamber flow area to throat area will be on the order of 5 or larger which results in a negligible change in chamber pressure with length. Associated with an area ratio of 5 or greater is a

The preceding analysis has been for the case of a long thin combustion chamber where the ignition process is definitely space dependent. A second approach is to assume that the combustion chamber is short and squat with an L/D on the order of 1. For this case, the assumption of complete mixing is possible and one can take into account the transient response of the system. This is only strictly valid where the residance time , τ . is much larger than the time for complete reaction. This will, in general, not be true during ignition but the only alternative is a space, time solution for the thermodynamic coordinates.

H.4 GENERAL ARRANGEMENT

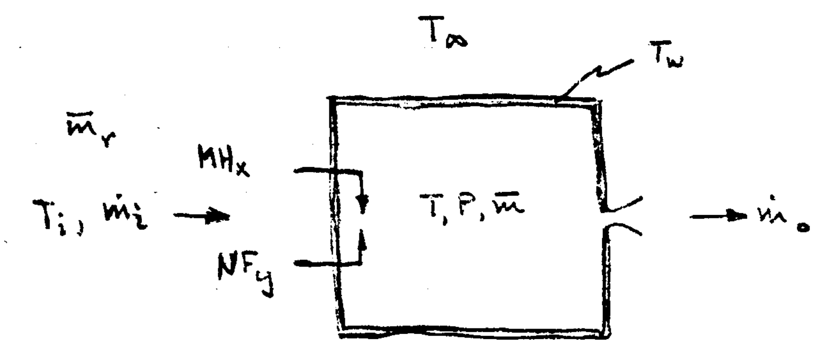

H.5 SYSTEM OF EQUATIONS

Energy equation

$$T\,d\rho + \rho\,dT = \left[\frac{q}{c_v} + \frac{\gamma}{V_c}\left(T_i \dot{m}_i - T \dot{m}_o\right)\right] dt \qquad \text{(H.13)}$$

Continuity equation

$$d\rho = \frac{1}{V_c}\left(\dot{m}_i - \dot{m}_o\right) dt \qquad \text{(H.14)}$$

a chamber exit Maoh number of approximately 0.1 or less. It may also be assumed that the influence of friction is negligible.

Equation (H.1) becomes

$$T - T_1 = \int_0^x \left[\frac{\Delta H\, k}{c_p V} (a-c)(b-c) - \frac{4\, St}{D_c} (T - T_w) \right] dx . \quad \text{(H.12)}$$

Since ignition is essentially a two-dimensional event with the thermodynamic coordinates functions of both time and position until steady state conditions are attained, a few basic assumptions are necessary to simplify the solution for the ignition length. The most important assumption is the effective chamber pressure at which ignition is assumed to occur. This pressure will range between ambient and the eventual steady state value. The pressure to be used in the solution will be that attained for steady state flow of the unreacted substance assuming a constant propellant inlet mass rate.

H.3 ANALOGUE

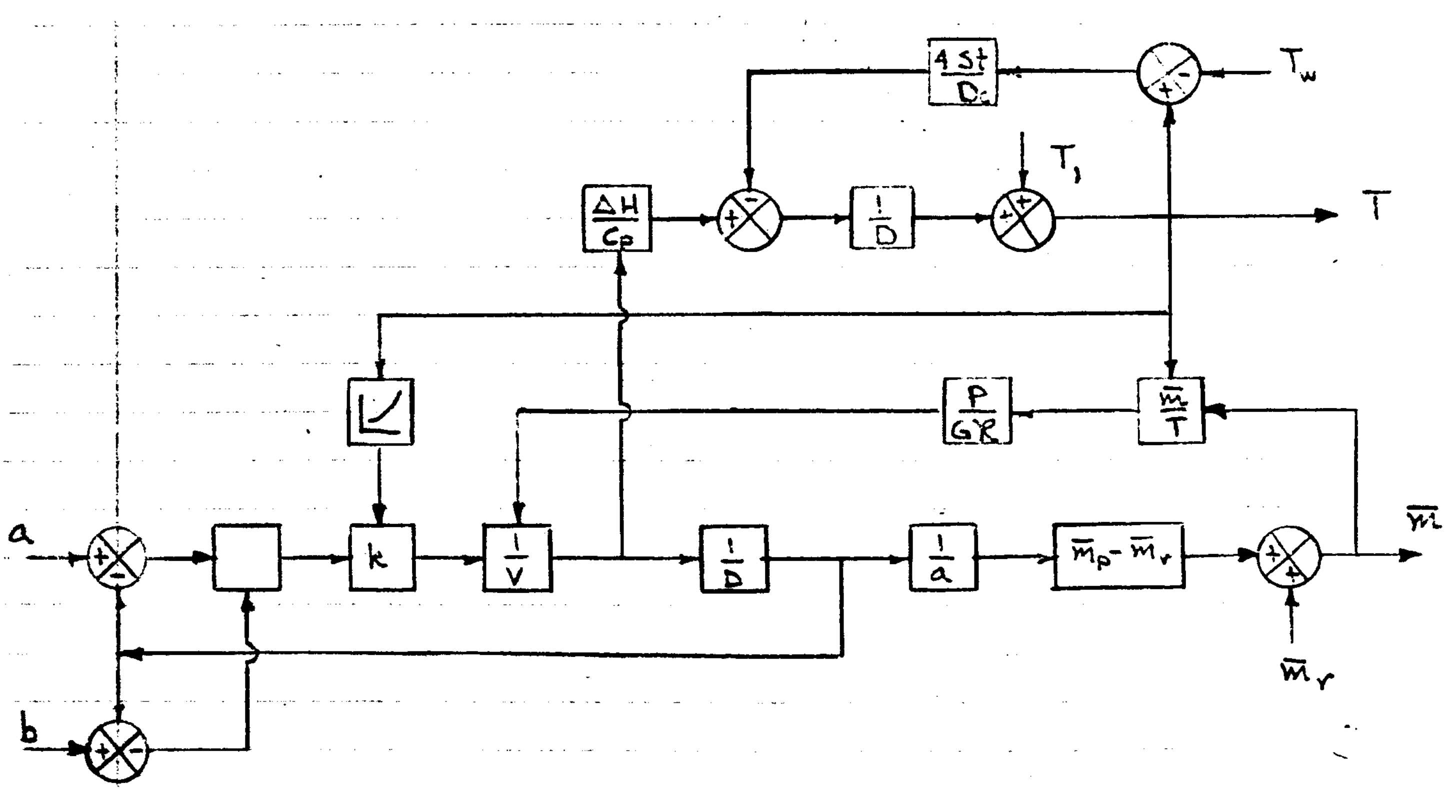

Equation of state

$$\frac{dP}{P} - \frac{d\rho}{\rho} - \frac{dT}{T} + \frac{d\bar{m}}{\bar{m}} = 0 \qquad \text{(H.15)}$$

Calculation of molecular weight

$$\bar{m} = \left(1 - \frac{c}{b}\right) \bar{m}_r + \frac{c}{b} \bar{m}_p \qquad \text{(H.16)}$$

$$d\bar{m} = \frac{\bar{m}_p - \bar{m}_r}{b} \, dc \qquad \text{(H.17)}$$

From the rate equation for a second order reaction

$$\frac{dc}{d\tau} = k(a-c)(b-c) \qquad \text{(H.18)}$$

where k is given by Eq. (H.7)

The residence time, τ, is given by

$$\frac{dx}{dt} = V = \frac{\dot{m}}{\rho A_{cs}}$$

$$\int_0^{\tau} dt = \frac{A_{cs}}{\dot{m}} \int_0^L \rho(x)\, dx$$

since

$$\dot{m} = c_w P A_t$$

$$\tau = \frac{A_{cs} L}{A_t} \frac{1}{c_w P} \frac{1}{L} \int_0^L \rho(x)\, dx$$

$$= \frac{L^\star}{c_w P} \rho = \frac{L^\star c^\star}{c_D g_c} \frac{\bar{m}}{\mathcal{R} T}$$

since

$$c^\star = \sqrt{\frac{g_c \mathcal{R} T}{\bar{m}}} \; \gamma^{-1/2} \left(\frac{\gamma+1}{2} \right)^{\frac{\gamma+1}{2(\gamma-1)}}$$

$$\therefore \quad \tau = \frac{L^\star}{C_D} \sqrt{\frac{\mathcal{R}}{g_c \gamma}} \left(\frac{\gamma+1}{2} \right)^{\frac{\gamma+1}{2(\gamma-1)}} \sqrt{\frac{\bar{m}}{T}} = \frac{6.93 \, L^\star}{C_D \, \Omega(\gamma)} \sqrt{\frac{\bar{m}}{T}}$$

Letting

$$E = L^\star \sqrt{\frac{\mathcal{R}}{g_c \gamma}} \left(\frac{\gamma+1}{2} \right)^{\frac{\gamma+1}{2(\gamma-1)}}$$

$$\tau = E \sqrt{\frac{\bar{m}}{T}} \tag{H.19}$$

$$d\tau = \frac{E}{2} \sqrt{\frac{\bar{m}}{T}} \left(\frac{d\bar{m}}{\bar{m}} - \frac{dT}{T} \right)$$

$$= \frac{\tau}{2} \left(\frac{d\bar{m}}{\bar{m}} - \frac{dT}{T} \right) \tag{H.20}$$

solving for dc from Eq. (H.18) and substituting for $d\tau$ gives

$$dc = k(a-c)(b-c) \frac{\tau}{2} \left(\frac{d\bar{m}}{\bar{m}} - \frac{dT}{T} \right) \tag{H.21}$$

substituting Eq. (H.21) into (H.17)

$$d\bar{m} = \frac{\bar{m}_p - \bar{m}_v}{b} \; k(a-c)(b-c) \frac{\tau}{2}\left(\frac{d\bar{m}}{\bar{m}} - \frac{dT}{T}\right) \tag{H.22}$$

letting

$$B = \left(\frac{\bar{m}_p - \bar{m}_v}{2}\right) k \; (a-c) \left(1 - \frac{c}{b}\right) \tau$$

$$\therefore \quad \frac{d\bar{m}}{\bar{m}} = \frac{B}{B-\bar{m}} \; \frac{dT}{T} \tag{H.23}$$

Substituting Eq. (H.23) into (H.15) gives three equations and three unknowns.

Equations of state

$$\frac{dP}{P} - \frac{d\rho}{\rho} + \left(\frac{B}{B-\bar{m}} - 1\right) \frac{dT}{T} = 0 \tag{H.24}$$

solution of Eq. (H.13), (H.14), and (H.24)

$$D \equiv \begin{vmatrix} 0 & T & \rho \\ 0 & 1 & 0 \\ \frac{1}{P} & -\frac{1}{\rho} & \left(\frac{B}{B-\bar{m}} - 1\right)\frac{1}{T} \end{vmatrix} = -\frac{\rho}{P}$$

solution for dT

$$dT = -\frac{P}{\rho} \begin{vmatrix} 0 & T & \frac{q}{V_c c_v} + \frac{r}{V_c}(T_i \dot{m}_i - T\dot{m}_o) \\ 0 & 1 & \frac{1}{V_c}(\dot{m}_i - \dot{m}_o) \\ \frac{1}{P} & -\frac{1}{\rho} & 0 \end{vmatrix} dt$$

$$dT = \frac{1}{\rho V_c}\left[\frac{q}{c_v} + r\,(T_i \dot{m}_i - T\dot{m}_o) - T\,(\dot{m}_i - \dot{m}_o)\right] dt \qquad \text{(H.25)}$$

solution for dP

$$dP = -\frac{P}{\rho V_c}\begin{vmatrix} \frac{q}{c_v} + r(T_i \dot{m}_i - T\dot{m}_o) & T & \rho \\ (\dot{m}_i - \dot{m}_o) & 1 & 0 \\ 0 & -\frac{1}{\rho} & \left(\frac{B}{B-\bar{m}} - 1\right)\frac{1}{T} \end{vmatrix}$$

$$dP = -\frac{P}{\rho V_c}\left\{\left[\frac{q}{c_v} + r(T_i \dot{m}_i - T\dot{m}_o)\right]\left(\frac{B}{B-\bar{m}} - 1\right)\frac{1}{T} - (\dot{m}_i - \dot{m}_o)\frac{B}{B-\bar{m}}\right\} dt$$

(H.26)

$$d\rho = \frac{1}{V_c}\,(\dot{m}_i - \dot{m}_o)\,dt \qquad \text{(H.27)}$$

Calculation of heat rate

$$q = q_{reac} - q_{loss} = \frac{c}{b}\,\dot{m}_i\,\Delta H - hA\,(T - T_w) \qquad \text{(H.28)}$$

$$T_w = T_{w_i} + \frac{1}{(c_p m)_e}\int\left[hA\,(T - T_w) - h_o A_o\,(T_w - T_\infty)\right] dt \qquad \text{(H.29)}$$

Calculation of nozzle mass rate

$$\dot{m}_o = c_w A_t P = 0.1443\, c_D\, \Omega(r)\, A_t \sqrt{\frac{\bar{m}}{T}}\; P \qquad \text{(H.30)}$$

Calculation at degree of reaction

$$\frac{dc}{dt} = k(a-c)(b-c)$$

integrating between limits

$$k\int_0^{\tau} dt = \int_0^{c} \frac{dc}{(a-c)(b-c)} = \left[\frac{1}{a-b} \ln \frac{a-c}{b-c}\right]_0^{c}$$

or

$$k\tau = \frac{1}{a-b} \ln \frac{b}{a} \frac{a-c}{b-c}$$

solving for c/b

$$\frac{c}{b} = \frac{1-e^{-k\tau(a-b)}}{1-\frac{b}{a}e^{-k\tau(a-b)}} \qquad \text{(H.31)}$$

Solution for the thermodynamic coordinates requires solution of the system of equations tabulated below:

$$T = \frac{1}{V_c}\int \frac{1}{\rho}\left[\frac{q}{c_v} + r(T_i \dot{m}_i - T\dot{m}_o) - T(\dot{m}_i - \dot{m}_o)\right] dt$$

$$P = \frac{R}{V_c}\int \frac{1}{\bar{m}}\left\{\left(1-\frac{B}{B-\bar{m}}\right)\left[\frac{q}{c_v} + r(T_i\dot{m}_i - T\dot{m}_o)\right] + (\dot{m}_i - \dot{m}_o)T\frac{B}{B-\bar{m}}\right\} dt$$

$$\rho = \frac{1}{V_c}\int (\dot{m}_i - \dot{m}_o)\, dt$$

$$q = \frac{c}{b}\dot{m}_i \Delta H - hA(T-T_w)$$

$$T_{w} = T_{w_i} + \frac{1}{(c_p m)_c} \int \left[hA(T - T_w) - h_o A_o (T_w - T_\infty) \right] dt$$

$$\dot{m}_o = 0.1443\, C_D\, \Omega(\gamma)\, A_t\, P \sqrt{\frac{\bar{m}}{T}}$$

$$\tau = \frac{6.93\, L^{*}}{C_D\, \Omega(\gamma)} \sqrt{\frac{\bar{m}}{T}}$$

$$k = A\, e^{-\frac{\Delta H_a}{RT}}$$

$$\frac{c}{b} = \frac{1 - e^{-k\tau(a-b)}}{1 - \frac{b}{a} e^{-k\tau(a-b)}}$$

$$\bar{m} = \left(1 - \frac{c}{b}\right) \bar{m}_r + \frac{c}{b} \bar{m}_p$$

$$B = \left(\frac{\bar{m}_p - \bar{m}_r}{2}\right) k (a-c) \left(1 - \frac{c}{b}\right) \tau$$

$\dot{m}_i$ & T_i assumed constant

H.6 SYSTEM ANALOG

Figure H-1 and H-2 show the system analog and the solution.

Solution of the analogue shown in Fig. H-2 would allow estimation of the transient response for a bipropellant gas system. An obvious shortcoming, as mentioned previously, is the assumption of a uniform chamber gas temperature during the transient startup period. This will result in the calculated performance being somewhat less than the actual performance in terms of response time and specific impulse.

H.7 APPENDIX H GLOSSARY

Term	Meaning
a	constant in eqs. 5 and 18
A	area or frequency factor
b	constant in eqs. 5 and 18
c	concentration
c_D	discharge coefficient
c_p	specific heat at constant pressure
c_v	specific heat at constant volume
c_w	flow coefficient
c*	characteristic velocity
D	diameter
I/D	integration operator
f	friction factor
g_c	conversion in Newton's law of motion
G	mass flux
h	heat transfer coefficient
H	internal energy generation
ΔH	heat of reaction
ΔHa	heat of activation
I	inversion

Term	Meaning
k	rate constant
L	length
$\dot{m}$	mass rate
$\overline{m}$	molecular weight
M	Mach number
P	pressure
Pr	Prandll number
q	Heat rate
Q	heat loss
R	universal gas constant
Re	Reynolds number
St	Stanton number
t	time
T	temperature
V	velocity
V_c	chamber volume
x	distance

Greek

γ	ratio of specific heats
$\Omega(\gamma)$	function specific heat ratio
ρ	density
τ	residence time

Term	Meaning
Subscripts	
c	chamber
cs	cross-section
i	in and initial
o	out, outside
p	products
r	reactants
t	throat
w	wall

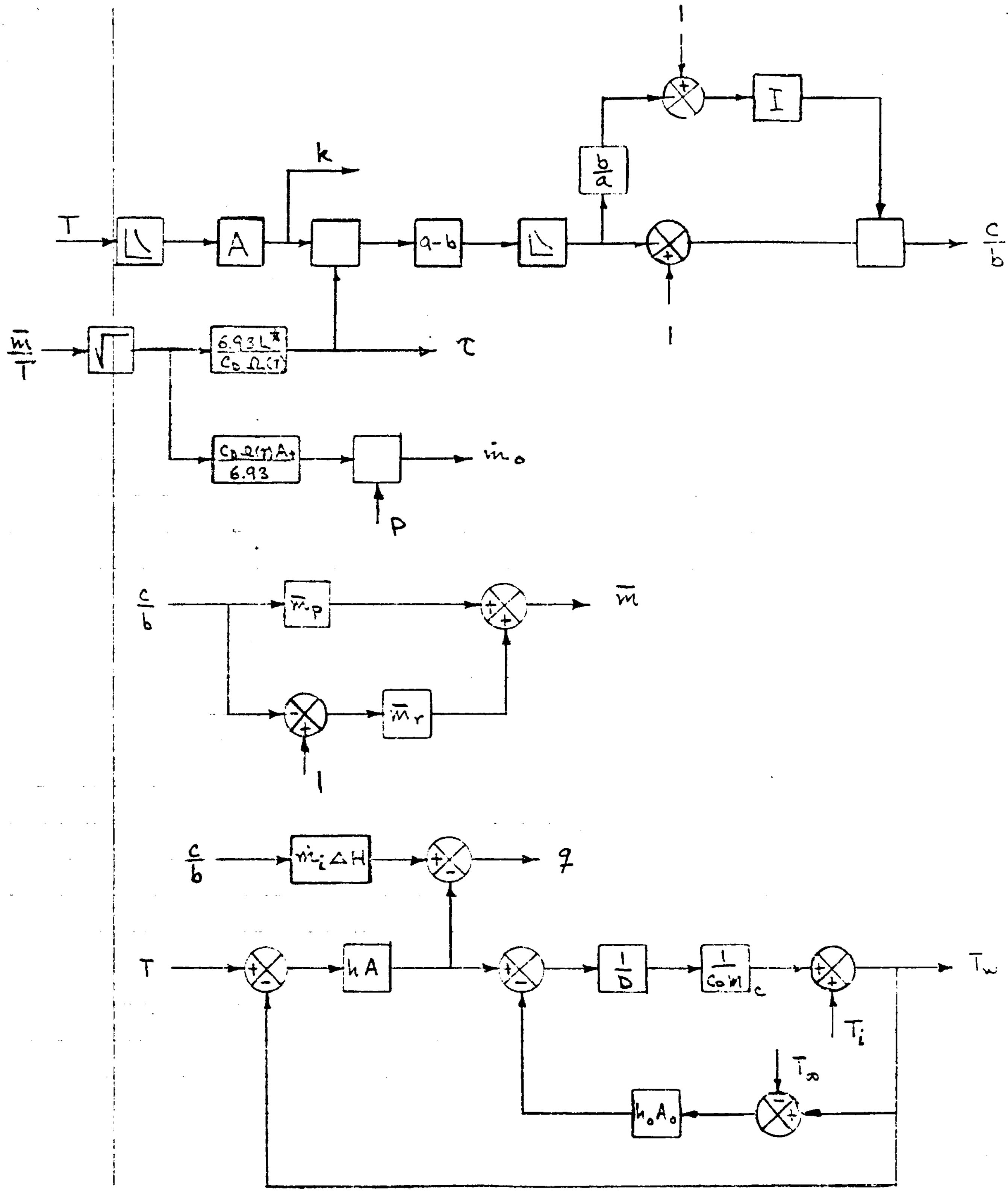

Fig. H-1 System Analog

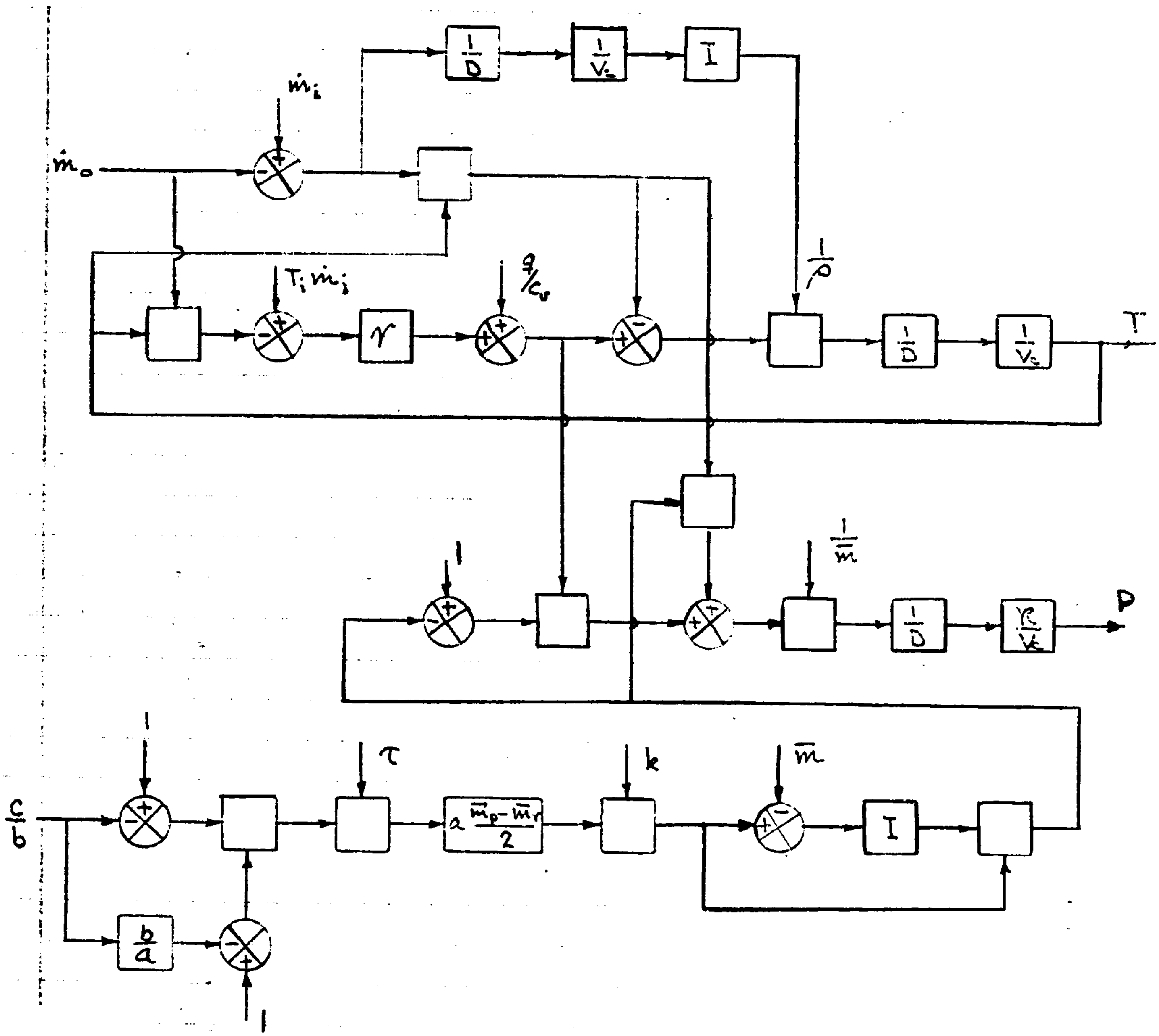

Fig. H-2 Solution to System Analog

X68-18062

Lockheed
MISSILES
& SPACE
COMPANY

In reply refer to:
LMSC/677083

June 24, 1968

TO:

Distribution

Subject: Errata Sheet for LMSC 685070, Final Report, "Low-Thrust Solid and Hybrid Propulsion Systems (Phase II)" NAS 7-573

Please correct the following typographical errors in Table 3-9, page 3-28.

	P, atm	T, °K	Isp
BeH_2+F_2	>3.16	>4600	>369

Thank you.

Very truly yours,

A. M. McGory, Jr.

A. M. McGory, Jr.
R&D Contracts